CAND1 CATALYZES THE REDISTRIBUTION OF SCF COMPLEXES TO PROMOTE MITOTIC PROGRESSION

&

ELUCIDATING FOLR-1 FUNCTION IN NEURONAL SIGNALING IN *CAENORHABDITIS ELEGANS*

by

FATHIMA ZAHRA ABDUL NAWAZ

(Under the Direction of EDWARD T. KIPREOS)

ABSTRACT

SCF (Skp1-Cullin-F-box) ubiquitin ligases regulate diverse cellular processes including multiple aspects of the cell cycle, transcription, signal transduction, apoptosis, angiogenesis, and cell migration. There are 69 human F-box proteins that function as substrate receptors (SRs) for SCF complexes. The binding of each F-box protein to the core SCF complex produces a unique E3 that targets different subsets of substrates that regulate different cellular pathways. The CAND1 protein is a SR exchange factor for SCF complexes. CAND1 strips off adaptor–SR complexes from the SCF core complex and allows new adapter–SRs to bind to create new active SCF complexes. We have analyzed the SR proteins present in SCF complexes throughout the cell cycle and found systematic changes in SR association with SCF complexes during mitosis. The differences in SCF complexes occur even when the SRs are constitutively present throughout the cell cycle. We show that CAND1 is required to reorganize the diversity of SCF complexes during

mitosis. CAND1 is required for the removal of multiple SRs from SCF complexes during mitosis and promoting the integration of a specific SR, FBXW11/β-TrCP2, into SCF complexes. Inactivating CAND1/2 causes mitotic arrest that often leads to cell death, and these mitotic defects have been observed in human cells, including HeLa, U2OS, and normal hTERT-derived fibroblasts. These results highlight a novel mechanism by which SCF complexes can undergo large-scale reorganization through a CAND1-dependent process.

Folate (vitamin B_9) is an essential nutrient that is required for one-carbon metabolism. Emerging evidence indicates that vertebrate folate receptors have functions that do not rely on one-carbon metabolism. We have discovered a novel role for the C. elegans protein FOLR1 in neuronal signaling. We have identified that FOLR-1 expresses in the adult C. elegans NSM neurons, localizing in the two major processes. We also identify GON-2, a calcium channel protein that is required for calcium entry into the NSM neuron upon its activation by adding folate, physically interact with the FOLR-1 protein, and co-localize in the same NSM processes, suggesting a direct mechanism through which FOLR-1 promotes calcium entry during neuronal activation.

INDEX WORDS: CAND1; SCF; MITOSIS; FOLR1; GON-2; NSM; SIGNALING; CANCER.

CAND1 CATALYZES THE REDISTRIBUTION OF SCF COMPLEXES TO PROMOTE MITOTIC PROGRESSION

&

ELUCIDATING FOLR-1 FUNCTION IN NEURONAL SIGNALING IN *CAENORHABDITIS ELEGANS*

by

FATHIMA ZAHRA ABDUL NAWAZ

BSc, University of Colombo, Sri Lanka, 2013

A Dissertation Submitted to the Graduate Faculty of The University of Georgia in Partial Fulfillment of the Requirements for the Degree

DOCTOR OF PHILOSOPHY

ATHENS, GEORGIA

2021

CAND1 CATALYZES THE REDISTRIBUTION OF SCF COMPLEXES TO PROMOTE MITOTIC PROGRESSION

&

ELUCIDATING FOLR-1 FUNCTION IN NEURONAL SIGNALING IN *CAENORHABDITIS ELEGANS*

by

FATHIMA ZAHRA ABDUL NAWAZ

Major Professor:	Edward T. Kipreos
Committee:	Jacek Gaertig
	Scott Dougan
	Jonathan Eggenschwiler

Electronic Version Approved:

Ron Walcott
Vice Provost for Graduate Education and Dean of the Graduate School
The University of Georgia
December 2021

DEDICATION

TO MY PARENTS

for raising me to believe that anything is possible

TO MY HUSBAND

for making everything possible

TO MY DAUGHTER

for keeping my spirit up

ACKNOWLEDGEMENTS

I thank my major professor Dr. Edward T. Kipreos, whose intelligence, patience, advice, and assistance encouraged me through this program. His guidance has helped me hone my experimental, scientific reasoning and critical thinking skills and my ability to be an independent researcher. I would like to thank all my committee members for their advice over the years, keeping me on track in my graduate career and evaluating this dissertation.

I thank my husband, for his unconditional love, constant encouragement, patience, and his unwavering support throughout graduate school and for always being there for me. I would not have achieved any of this without you. I thank my parents for always believing me and letting me choose my own path and my sisters and brother for their endless support and encouragement.

I would like to thank the past and present members of the Kipreos lab for your friendship, and thoughtful discussions on my projects. Especially James Anderson and Riju Balachandran for being wonderful lab mates and for helping me with all my technical problems, Anusha Khan and Jonathan Stevenson for their technical assistance. Last but not least, my friends in Athens, for being our second family and always being there for us.

TABLE OF CONTENTS

Page

LIST OF TABLES

Page

LIST OF FIGURES

Page

CHAPTER 1

INTRODUCTION AND LITERATURE REVIEW

Protein degradation is an essential for the regulation of most cellular processes (Goldenberg et al., 2004; Liu et al., 2012; Wojcik and DeMartino, 2003). One of the major regulators of protein degradation is the cullin-RING ubiquitin ligases (CRLs). CRLs are protein complexes that recognize substrate proteins and attach a poly-Ub chain, which then acts as a signal for protein degradation by the proteasome (Kipreos et al., 1996; Mathias et al., 1996). The best-characterized CRL family member is the SCF (Skp1, Cullins, F-box proteins) ubiquitin ligase (Zheng et al., 2002b). CAND1 protein is a substrate receptor (SR) exchange factor for CRL complexes. CAND1 strips off adaptor–SR complexes from the SCF core complex and allows new adapter–SR to bind to create new active SCF complexes. In this dissertation, I present my findings that describe a novel mitotic regulatory mechanism and a novel *C. elegans* neuronal signaling pathway.

In Chapter 2, I will summarize the current literature on a potential signaling role for the folate receptor in cancer. In Chapter 3, I will present my discovery of a novel role for CAND1 in the reorganization of the diversity of SCF complexes during mitosis, and its significance for mitotic progression. In Chapter 4, I will describe the association of folate receptor FOLR-1 and the TRPM calcium channel GON-2 in NSM neurons in the nematode *Caenorhabditis elegans*, which suggests a novel role in neuronal signaling. Finally, in Chapter 5, I will summarize and discuss the implications of my discoveries and present future directions for the research.

In this chapter, I introduce and outline the relevant literature that provides background for the discoveries in this dissertation. To provide background for Chapter 3, I will provide a broad overview of the Cullin-RING E3 ubiquitin ligases (CRLs), their composition, regulation and how CRL complexes involve in regulating cellular processes. I will specifically discuss the subclass of CRL complexes called SCF complexes and their regulation. Because one of our major findings is the interaction of CAND1 with a specific substrate receptor (SR/F-box protein), β-TrCP2/FBXW11, I will discuss the relevance of FBXW11 in cell cycle progression.

Chapter 4 focuses on a novel folate dependent neuronal signaling pathway in *C. elegans.* As background for that chapter, I will provide an overview of folates and their role as a nutrient and a potential signaling molecule (with the latter reviewed in more detail in Chapter 2). I will also discuss the folate receptor, and the NSM neuron, and the Ca^{2+} channel GON-2, which functions with the folate receptor to promote calcium entry into the NSM neuron to mediate its activation.

The Ubiquitin-Proteasome pathway

Protein degradation plays a central role in regulating protein homeostasis in diverse cellular processes. The vast majority of proteins in the cell are degraded by the ubiquitin proteasome system (UPS) through a highly selective and regulated mechanism (Ciechanover, 1994; Rock et al., 1994). Ubiquitin (Ub) is a highly conserved 76 amino acid polypeptide that is expressed ubiquitously in all prokaryotes and eukaryotes, and is covalently attached to protein substrates with the help of three enzymes (E1, E2, and E3) (Ciechanover, 1994).

The Ub-activating enzyme E1, with the hydrolysis of one ATP; binds to Ub through a thiolester linkage and then transfers the Ub to the Ub-conjugating enzyme E2. The E2, bound to the activated Ub through a thiolester linkage, binds to a ubiquitin ligase E3. E3 enzymes bind substrate proteins that are to be ubiquitylated and facilitate the transfer of the Ub from the E2 to

the substrate protein (Kipreos, 2005). E3 ubiquitin ligases provide the specificity that attaches Ub to the intended substrate proteins. One reaction of the E1 to E3 cascade causes monoubiquitylation of the substrate, which does not target the protein to the proteasome, but instead causes changes in protein transport, localization, or function. Multiple runs of E2 addition of Ub form a poly-Ub chain on the substrate (Glickman and Ciechanover, 2002; Pickart, 2001). If the covalent linkage to the Ub residue occurs on lysine 48, then 4 Ub in a poly-Ub chain serves as a signal for degradation by the 26S proteasome (Thrower et al., 2000).

Cullin-RING Ubiquitin Ligases

Mammals have only two E1 enzymes, around 40 E2s, and over 600 different E3 enzymes (Valimberti et al., 2015; Zhao and Sun, 2013). The E3 enzymes selectively recognize specific protein substrates for degradation. The largest group of E3 ubiquitin ligase enzymes are the cullin-RING ubiquitin ligases (CRLs) that comprise over 200 members and are responsible for proteasome-mediated degradation of over 20% of the proteins in cells (Bulatov and Ciulli, 2015; Soucy et al., 2009).

CRLs are multi-subunit complexes that include a cullin a scaffold protein, a catalytic RING finger protein that is the physical link between the E2 and the E3 (Rbx1/Roc1 or Rbx2/Roc2), a substrate receptor (SR) protein that provides specificity by binding specific substrates; and one or more adaptor proteins that link the SR to the core CRL complex (Bosu and Kipreos, 2008; Zhao and Sun, 2013). In humans, eight cullin family members have been identified (CUL1, 2, 3, 4A, 4B, 5, 7, and 9) (Zheng *et al.*, 2002b). Each of the eight cullins shares an evolutionarily conserved cullin homology domain at the C-terminus.

CRLs are modular structures that utilize cullins as scaffold proteins that bind interchangeable adaptor-SR module to enable assembly of functionally diverse E3 ligase

complexes (Betsch et al., 2019). This diversity in the ligase complexes , which arises due to the many different SRs that binds the CRL complexes, allows CRLs to regulate multiple cellular processes including regulating multiple aspects of the cell cycle, transcription, signal transduction, DNA replication and repair, chromatin remodeling, cell differentiation, metabolism, cell migration, and developmental programming (Jang et al., 2018). Perturbation of CRL activity has been linked to severe developmental growth defects, and cancer (Betsch *et al.*, 2019). Therefore, CRLs have become a sought-after target for drug discovery and therapeutics for a variety of human diseases.

Structural studies have demonstrated that the RING H2 finger protein RBX1 is harbored in the C-terminal domain of all cullins, while RBX2 (a paralog of RBX1) preferentially associates with CUL5 (Duda et al., 2008; Zheng *et al.*, 2002b). RBX1 is a RING-type zinc finger, which consists of a N-terminal β-strand and a C-terminal core domain that coordinates three zinc ions (Zheng *et al.*, 2002b). RBX1 intercalates a long β-sheet into the C-terminus of CUL1 (unmodified with Nedd8) to form a single globular CRL unit, existing in a "closed" conformation, which is considered a rigid structure (Duda *et al.*, 2008). Neddylation of the C-terminal domain of cullin/RBX1/2 complex results in a change of conformation "opening" of the CRL complex. Upon neddylation of the cullin, the RING domain of RBX1 pops out of the closed structure to move relatively freely while tethered by the now exposed flexible β-sheet (Rusnac and Zheng, 2020). Freeing the Rbx1 RING domain allows the E2 bound to RBX1 to move closer to the anchored substrate (Duda *et al.*, 2008; Saha and Deshaies, 2008). This flexibility allows E2s bound to RBX1 to sequentially add Ub to the growing poly-Ub chain on the substrate.

Neddylation is a process where NEDD8, a Ub-like protein covalently attaches to cullins via a cascade of E1, E2, E3 enzymes that are specific for NEDD8, similar to the E1, E2, E3 cascade

for ubiquitylation. (Fig. 1.1) (Rusnac and Zheng, 2020). RBX1 binding to the CRL complex is required for neddylation. In *C. elegans*, RBX-1 mutants undergo embryonic arrest, suggesting that its function is essential. (Moore and Boyd, 2004; Sasagawa et al., 2003).

Post-translational modifications of CRL substrates

CRL E3 ligases recognize and bind substrates usually by interaction with a specific short linear sequence motif, termed the 'degron', that is present on the substrate. Polyubiquitylation of the substrate proteins facilitates their degradation. The majority of known substrates for CRL E3 ubiquitin ligases are recognized and bound in response to the post-translational modification of the substrate (Rusnac and Zheng, 2020). Degrons can be post-translationally modified by phosphorylation, acetylation, glycosylation, or hydroxylation (Nguyen and Businо, 2020). Phosphorylation of proteins is a major mechanism by which proteins are specified for degradation to regulate cell cycle progression (Bosu and Kipreos, 2008). Substrate phosphorylation is regulated by kinases and phosphorylation. Depending on the substrate, phosphorylation can induce their recognition by the E3 ligases that will target them for degradation or stabilize them (Skaar et al., 2013).

CRL regulation by the CSN complex and CAND1

Neddylation is a reversible process and the removal of NEDD8 (termed deneddylation) is catalyzed by an evolutionarily conserved eight subunit protein complexes, known as the COP9 signalosome (CSN).

The COP9 Signalosome (CSN) is associated with phosphorylation, deneddylation, and deubiquitylation, all of which can regulate CRL complexes. The CSN complex inhibits CRLs by deneddylating cullins preventing them from binding substrate proteins (Fig. 1.1). But while doing so, the CSN complex stabilizes the fully assembled CRL complex by inactivating the cullin (by

deneddylation) thus preventing the autoubiquitylation of SR proteins, which can lead to their degradation in the absence of a substrate. This protective mechanism to stabilize SR proteins in the absence of a substrate is conserved amongst various eukaryotes, from yeast to humans. Consistently, loss of CSN activity in vivo causes a decrease in CRL activity (Cope and Deshaies, 2003).

CAND1 (cullin-associated and neddylation-dissociated-1) is an evolutionarily conserved protein that binds CRL complexes, and is required for CRL activity in vivo (Bosu et al., 2010). CAND1 physically associates with CUL1 forming a complex, where CAND1 forms a "sinuous superhelical structure" partially coiling around CUL1-RBX1 in a head-to-tail pattern. Both the CUL1 N-terminus (where Skp1 binds) and the unneddylated C-terminus are required for CAND1 to associate with CUL1. Hence, the adapter Skp1 or neddylation dissociates CAND1 from CUL1(Liu et al., 2002; Zheng et al., 2002a). Similarly, CAND1 dissociates the adaptor Skp1 from the SCF complex while inhibiting the neddylation process (Liu *et al.*, 2002; Oshikawa et al., 2003; Zheng *et al.*, 2002a). Though in vitro studies have suggested that CAND1 acts as an inhibitor to the CRL complex, many studies conducted on model organisms have shown that CAND1 promotes CRL activity in vivo (Bosu *et al.*, 2010; Chuang et al., 2004; Feng et al., 2004).

Pierce et al used a fluorescence resonance energy transfer (FRET) assay on the interaction between F-box protein and CUL1-RBX1 in real time to follow SCF assembly and disassembly in the presence or absence of CAND1 (Pierce et al., 2013). They reported that addition of CAND1 to an unneddylated SCF complex increased the dissociation rate of Skp1-F-box protein while neddylation abolished that effect by blocking CAND1 association with CUL1. Conversely, the spontaneous dissociation of CAND1 from CUL1-RBX1 was extremely slow but

was accelerated by the addition of Skp1-F-box protein. Based on those observations they proposed that CAND1 mediates the exchange of SRs on the CUL1-RBX1scaffold. Notably, the reversible exchange of CAND1 and adaptor–SR does not appear to require an energy source such as ATP. To explain the process, they described a transient ternary complex consisting of CAND1, Skp1-SR and CUL1-RBX1, where both CAND1 and the Skp1-SR module can destabilize each other's association with CUL1-RBX1. Hence CAND1 was defined as a "substrate receptor exchange factor" (Pierce *et al.*, 2013).

In 2017, Reitsma et al. reported that there was a huge variation in the percentage of F-box proteins associated with CUL1, suggesting the existence of a non-equilibrium pool of SCF complexes. They further showed that nearly half of CUL1 assembles with CAND1, concluding that cellular concentrations of F-box proteins do not correlate with their percentage association with Cul1 (Reitsma et al., 2017). Recent reports by Liu et al have shown that CAND1 promotes the binding of DCN1, the NEDD8 ligase, to CUL1-RBX1, despite the fact that CAND1 inhibits the neddylation of cullins (Keuss et al., 2016; Kim et al., 2008). In the presence of F-box-Skp1 modules, CAND1-bound to CUL1 demonstrated a higher neddylation rate than free CUL1, due to the loading of DCN1 to CUL1 (Liu et al., 2018). Human cells have two CAND1 paralogs, CAND1 and CAND2 (Aoki et al., 2002). CAND2 is found to occupy less than 0.25% of endogenous CUL1 in HEK293T cells (Reitsma *et al.*, 2017).

The current model on SCF assembly and disassembly

CUL1 constantly cycles between neddylated and unneddylated states. Substrate bound to the SR stabilizes the SCF complex in the neddylated state (i.e., the active conformation), thus allowing continuous substrate ubiquitylation and degradation (Liu *et al.*, 2018; Olma and Dikic, 2013; Pierce *et al.*, 2013). In the absence of substrates, CSN catalyzes the deneddylation of Cul1,

and CAND1 binds the deneddylated SCF removing the F-box-Skp1 off the complex. DCN1 Nedd8 ligase, binds to the CAND1-CUL1-RBX1 complex, which facilitates immediate neddylation of Cul1 upon the removal of CAND11 by F-box-Skp1(Ji et al., 2016). Though the CAND1 mediated exchange of SR has been widely studied in vitro to develop this existing model, the role of CAND1 at different developmental stages in multiple eukaryotic organism levels is yet to be explored.

F-box proteins and cell cycle regulation

Key regulators such as cyclins and CDK inhibitors (CKI)s, drives the cell cycle. This progression is tightly regulated by the Ub-mediated proteolysis of those CDK regulators by ubiquitin ligases; mainly SCF complexes and the anaphase-promoting complex/cyclosome (APC/C) (Nakayama and Nakayama, 2005). The SCF complex is active throughout cell cycle. The following F-box proteins are well studied cell cycle regulators: S-phase kinase-associated protein 2 (Skp2); F-box and WD-40 domain protein 7 (FBXW7/Cdc4); and β-transducin repeat-containing protein (β-TrCP) (Nakayama and Nakayama, 2005; Zheng et al., 2016).

CKIs block cyclin–CDK kinase activity. Cip/Kip family CKIs (p21, p27, and p57) inhibit the G1-to-S transition and S phase progression by binding to CDK-cyclin complex in G1/S. The F-box protein Skp2 targets these negative regulators for degradation, and thereby promotes cell-cycle progression (Starostina and Kipreos, 2012). Skp2 expression is upregulated in many human cancers and is considered oncogenic (Bassermann et al., 2014). In contrast, the F-box protein FBXW7 is a tumor suppressor that targets positive regulators of the cell cycle, such as MYC, JUN, cyclin E, and Notch for degradation (Yeh et al., 2018). FBXW7 mainly functions in G1 and G2 phase and is often mutated in a subset of human cancers (Yeh *et al.*, 2018) The F-box β-TrCP2/FBXW11recognizes multiple cell-cycle EMI1/2, WEE1A, cyclin D1, MDM2, claspin,

BTG, REST, PLK4, and CEP68, while β -TrCP1/Fbxw1A joins regulating CDC25A/B and Bora. In addition, it targets multiple other substrates including β-catenin and IκB. Depending on the type of cancer, β-TrCP mutation or overexpression is observed (Lau et al., 2012).

Humans contain two β-TrCP paralogs, β-TrCP1/Fbxw1A and β-TrCP2/Fbwx11, and both are SRs of SCF complexes. Both β-TrCP1 and β-TrCP2 recognizes its substrate through the canonical DSGXXS, degron sequence where both serines are phosphorylated, thereby inducing their ubiquitylation and subsequent proteasomal degradation (Kim et al., 2015; Kipreos and Pagano, 2000). Despite having high similarity between β-TrCP1 and β-TrCP2, these proteins display a significant difference in subcellular localization, as β-TrCP1 is nuclear localized, while β-TrCP2 is cytosolic (Mangeat et al., 2009). Moreover, a protein-protein interaction study conducted utilizing tandem affinity purification and mass spectrometry (TAPMS) has revealed different substrates for both proteins (FBXW11 and BTRC were found to interact with 96 and 26 proteins, respectively, while twenty proteins (which overlaps between the 96 and 26 complexed with both FBXW11 and BTRC) (Kim *et al.*, 2015).

Folates – sources and absorption into cells

Folates are water-soluble B-vitamins consist of a pteridine ring joined by a methylene bridge to para-aminobenzoic acid (PABA), which is attached to glutamic acid residues by a peptide bond (Fig. 1.2) (Tam et al., 2012). Folates are a family of compounds that differ in their pteridine rings. The serum folate for systemic distribution in animals is 5-methy-tetrahydrafolate (5-methyl-THF) with a single glutamate (Zheng and Cantley, 2019). Once 5-methyl-THF is taken up by cells, it is converted to other folates and multiple Glu are added to allow the poly-Glu folates to be retained within cells (Zheng and Cantley, 2019).

Animals are unable to synthesize folates *de novo* and must obtain folates from their diet or from the microorganisms in their gut. The human colon microbiota represents a major source of folate and contributes more to host folate levels than folates obtained from diet (Liu et al., 2011). The gut microbiota predominantly makes and secretes folates in the form of 5-formyl-THF, 5,10-methenyl-THF, and 10-formyl-THF with up to 8 Glu residues, but the precise number of Glu residues is species specific (Sybesma et al., 2003). Polyglutamylated folates from the diet and microbiota folates in the gut are hydrolyzed into monoglutamates in the intestine prior to absorption by other cells and tissues (Imbard et al., 2013). Once monoglutamylated folates are taken up by cells, the folates are glutamylated with up to 9 glutamate residues, or longer (Beaudin and Stover, 2009). Polyglutamated folates accumulate in cells because they do not cross cellular membranes and are therefore retains in cells. Polyglutamylated folates also have a higher affinity for enzymes involved in one-carbon metabolism than their monoglutamate counterparts (Imbard *et al.*, 2013).

Folates in one-carbon metabolism

Folates have a canonical metabolic function in one-carbon metabolism, where they act as donors and receptors for one carbon unit. One-carbon metabolism (Fig. 1.3) functions in the synthesis of nucleotides (purines and deoxythymidylate monophosphate, dTMP), the amino acid methionine (which is required to generate the methyl-donor S-adenosyl methionine), and the interconversion of glycine and serine (Zheng and Cantley, 2019). Folate-mediated one-carbon metabolism is compartmentalized in the cell (Imbard *et al.*, 2013). The polyglutamated folates in the mitochondria and cytoplasm are two distinct pools that contribute activated cofactors with each other, but are not in equilibrium through folate exchange (Imbard *et al.*, 2013).

Folate is particularly important during periods of rapid cell division in proliferating cells when purine, dTMP, methionine synthesis, DNA replication, methylation, and repair are needed the most. For example, high amounts of folate prove beneficial for cell proliferation in embryonic neural tube closure, the proliferation of leucocytes, erythrocytes and enterocytes, and cancer progression (Beaudin and Stover, 2009; Liu *et al.*, 2011).

Folate supplementation in humans

Neural tube defects (NTDs) are severe birth defects arising from the failure of embryonic neural tube closure, causing brain and spine malformations in the newborn. To prevent NTDs, the United States and a few other countries mandate fortification of grains with folic acid, which has reduced NTD occurrence (Crott et al., 2008).However, the reduction in NTDs did not reduce proportionally to the amount of fortification. For example, United States and Chile had approximately 40% reduction in occurrence of NTDs, even though Chile mandated a 2-fold higher amount of folate fortification (Crider et al., 2011).

The human gut has a very efficient capacity to convert reduced dietary folates to 5-methy-THF but limited ability to reduce folic acid (Patanwala et al., 2014). Folic acid has only one glutamic residue and first needs to be reduced to the naturally bioactive form tetrahydrofolate (THF), through two reduction reactions catalyzed by dihydrofolate reductase (DHFR) (Fig. 1.3) (Imbard *et al.*, 2013). Therefore, large amounts of unmodified folic acid circulate in the portal vein (Patanwala *et al.*, 2014).

Folate transporters

Monoglutamylated folates are transported into mammalian cells and tissues by specialized membrane transport systems and receptors (Liu *et al.*, 2011). Mammals utilize three types of folate

transporters: the reduced folate carrier (RFC); the proton-coupled folate transporter (aka, SLC46A1); and folate receptors (FOLRs).

RFC

RFC (aka, the solute transport carrier SLC19A1) is ubiquitously expressed in mammalian cells and is required for the majority of folate transport into the majority of mammalian cells (Zhao et al., 2011). RFC is a low-affinity, but high-throughput transporter of the serum folate, 5-methyl-THF, and other reduced folates (Zhao *et al.*, 2011). RFC is an anion antiporter that uses a gradient of higher organic phosphate in the cell to transport folate into the cell while transporting phosphate linked to organic molecules out of the cell (Luteijn et al., 2019).

PCFT

PCFT (aka, SLC46A1) functions in the small intestine to absorb folate derived from food (Visentin et al., 2014). PCFT couples the transport of folates with protons (H^+) along the pH gradient from the lower pH environment of the lumen of the intestine to the higher pH within intestinal cells. PCFT also functions to release folate into cells after the endocytosis of folate receptors. After endocytosis, the folate receptor, bound to folate, becomes localized to endosomes, which become acidified. PCFT uses the higher proton concentration within the acidified endosomes to couple the transport of folate with protons into the cytoplasm (Zhao et al., 2009). Recent studies have also shown expression of PCFT in the placenta, choroid plexus (transporting folates into the cerebrospinal fluid), and kidney tubules (Geller et al., 2002; Umapathy et al., 2007; Williams et al., 2012). PCFT, works together with the Folate Receptor (discussed below) to mediate endocytosis and release of folates in the cell.

Folate Receptors

The folate receptors are high-affinity, low throughput transporters of folate (Zhao *et al.*, 2011). Each FOLR only binds one folate and brings the folate into cells via endocytosis of the FOLR–folate complex. The reliance on endocytosis to bring in a singly-bound folate ensures that this is a relatively slow, low-throughput transport mechanism. There are four FOLR1 genes that produce FOLR1, 2, 3, and 4 proteins (aka, folate receptors α, β, γ, and δ). Three of the FOLRs (FOLR1, 2, and 4) are linked to the plasma membrane by a carboxy terminus–glycosylphosphatidylinositol (GPI) anchor, while FOLR3 is secreted (Zhao *et al.*, 2011). In animals, non-canonical activity of folates (i.e.as a signaling molecule) has been linked to FOLR proteins. Below, we will describe the known functions of the four mammalian FOLR proteins in more detail.

FOLR1 has a restricted expression pattern in animals, and the majority of tissues do not express FOLR1. FOLR1 is expressed at the luminal (apical) surface of polarized epithelia, including proximal kidney tubules, type 1 and 2 pneumocytes in the lungs, choroid plexus, ovary, fallopian tube, uterus, cervix, epididymis, submandibular salivary gland, bronchial glands, and trophoblasts in the placenta (Elnakat and Ratnam, 2004). In several tissues, the polarized localization of FOLR1 corresponds to its role in the transcytosis of folates across cellular barriers. In the choroid plexus, FOLR1 transports folates from the basolateral to the apical membrane of the choroid plexus, where it is then transported in exosomes across the blood brain barrier (Grapp et al., 2013). In the placenta, FOLR1 transports folates from the mother to the fetus (Henderson et al., 1995). And, in the kidney, FOLR1 acts to reabsorb folates from pre-urine to transport it back into the body (Selhub et al., 1987).

FOLR2 is predominantly expressed in tissue-resident macrophages (Samaniego et al., 2020). FOLR2 is expressed in anti-inflammatory/regulatory M2 activated macrophages, but not

in pro-inflammatory M1 activated macrophages (Puig-Kroger et al., 2009). The role of FOLR2 expression in activated macrophages is not known.

FOLR3 lacks a GPI anchor and is secreted. FOLR3 is released into the bloodstream via secretory granules from neutrophil granulocytes (Holm and Hansen, 2020). FOLR3 is also expressed in monocytes (Sivapalaratnam et al., 2012). The purpose of FOLR3 secretion in both types of cells has not been clarified in the literature.

FOLR4 is unique among the FOLR proteins in that it is unable to bind folates because it lacks the folate-binding pocket in its protein structure (Bianchi et al., 2014; Kato et al., 2016). FOLR4, which is also known as Juno, is localized to the surface of mammalian eggs where it functions as the receptor for the Izumo protein on sperm (Bianchi *et al.*, 2014). The binding of FOLR4 and Izumo to each other is required to allow mammalian sperm to fertilize eggs. Because FOLR4 cannot bind folates, it provides a clear example of a well-defined FOLR cellular function that is mediated through a non-metabolic pathway, although in this case, also independent of folate binding. FOLR4 is also constitutively expressed on regulatory T cells, but its function in the T cells has not been reported (Jia et al., 2009).

***C. elegans* – a model system to study folate metabolism and signaling**

Caenorhabditis elegans is a nematode that was introduced as a model organism more than 40 years ago (Brenner, 1974). Since then, this roundworm has served as an invaluable tool to understand multiple aspects of developmental and cell biology (Wang and Sherwood, 2011). Many discoveries made in *C. elegans* have been shown to be conserved in higher eukaryotes and mammals.

The *C. elegans* diet consists of microbes that also includes the bacteria *E. coli* (Brenner, 1974), and hence the use of *C. elegans* to study folates in vivo has gained popularity. Like other

animals, *C. elegans* is unable to synthesize folate and acquires the metabolite through its diet (Nguyen and Clarke, 2012). *C. elegans* have orthologs of the human RFC (FOLT-1) and FOLR (FOLR-1) (Balamurugan et al., 2007; Chaudhari et al., 2016; Ortbauer et al., 2016). Our lab has recently discovered that bacterial folates, arising from *C. elegans* diet stimulate the proliferation of germ cells (Chaudhari *et al.*, 2016). Thus, *C. elegans* has been considered a promising model organism to study the effect of folates on metabolism and signaling.

***C. elegans* – a model system to study neuronal signaling**

Due to the substantial size and complexity associated with mammalian systems, as well as their long reproduction cycles, studies with invertebrate genetic model organisms like *C. elegans* can more rapidly identify pathways that are evolutionarily conserved. *C. elegans* are widely used to study neuronal signaling, the effect on behavioral responses to external stimuli, and to identify the receptors involved in signaling pathways and their sites of action within the system (Schafer, 2006). Importantly, *C. elegans* behaviors can generally be easily measured and quantified. *C. elegans* comes as two sexes; male and hermaphrodite, allowing genetic crosses and the obtaining homozygous progeny to be easily achieved (Brenner, 1974). The ability of adult hermaphrodites to self-fertilize allowing the passage of genetically identical animals within a week of time, provides a large source of subjects for analysis. Moreover, the *C. elegans* genome can be easily manipulated genetically using various gene editing techniques including cell specific RNAi knockdown, gene rescue and CRISPR (Dickinson and Goldstein, 2016; Esposito et al., 2007; Schade et al., 2005), while complex behaviors like thermotaxis, chemotaxis, aerotaxis and responses to mechanical and dietary stimuli can be evaluated (de Bono et al., 2002; Goodman, 2006).

***C. elegans* – NSM neuronal signaling**

Serotonin regulates the locomotion of *C. elegans* in response to its feeding state and feeding environment. Well-fed animals move slowly when encountering bacteria, but previously food-deprived animals slow their moving speed even more dramatically when encountering bacteria. Serotonin is required for this "enhanced slowing response" and worms with NSM neurons ablated show a small but significant defect in this behavior (Sawin et al., 2000)

tph-1, is a C. elegant orthologue of mammalian tryptophan hydroxylase (TPH)(Sze et al., 2000). TPH catalyzes the rate limiting step of the seretonin synthesis. A GFP tagged tph-1 (tph-1::GFP) is expressed in serotonergic neurons of C. elegans; and most of these neurons is observed by the L1 stage Expression of *tph-1* cDNA in NSM neurons but not in ADF neurons of *tph-1* mutant is sufficient to rescue the enhanced slowing response (Zhang et al., 2005). Both pieces of evidence suggest the "enhanced slowing response" in starved animals is promoted by serotonin from NSM neurons.

The NSM neurons are a pair of neurosecretory motor neurons have their cell bodies located in the pharyngeal subventral nerve cords just anterior to the nerve ring that synthesize and secrete serotonin, glutamate, and release neuropeptide-like proteins: NLP-13; NLP-18 and NLP-19 (Nathoo et al., 2001). One major process from each bipolar cell bifurcates near the cell body to two thick processes (Fig. 1.4). There is also a third, long, thin process that originates from the cell body. The first thick process turns within the nerve ring and continues its trajectory posteriorly within the dorsal nerve cord of the isthmus and the second thick process runs posteriorly within the subventral nerve cord of the isthmus, but both processes terminate before reaching the posterior bulb of the pharynx (Axang et al., 2008). Serotonin secreted from this pair of neurons can function as a neurotransmitter as well as a neurohormone, as these neurons have sensory endings in the

pharynx, the outside of pharynx and the pseudocoelom (a fluid-filled body cavity) (Chase and Koelle, 2007).

GON-2

GON-2 is a *C. elegans* transient receptor potential-M (TRPM) channel that is orthologous to the mammalian TRPM7 channel (Lambie et al., 2015). GON-2 is required for normal gonadogenesis, hence expressed in the gonad (Sun and Lambie, 1997). Gon-2 is also expressed in the intestine, where it is known to involve in the electrolyte homeostasis along with another TRPM channel GTL-1 (Teramoto et al., 2005).

Both channels are required for the proper absorption of trace metals such as Ni^{2+} and Mg^{2+} in the intestine (Teramoto et al., 2010). GON-2 is able to transport Ca^{2+} as well, and has a ten-fold higher permeability for Ca^{2+} than Mg^{2+}(Xing et al., 2008). GON-2 and GTL-1 are additionally required for proper defecation rhythms in the worm: the posterior body wall muscle contractions that induce defecation are maintained through inositol-1,4,5-triphosphate (IP3)-dependent Ca^{2+} oscillations in the intestine epithelium and evidence suggests that GON-2 and GTL-1 carry this calcium current (Kwan et al., 2008; Teramoto *et al.*, 2010; Xing *et al.*, 2008).

Mammalian TRPM7 is a constitutively active divalent cation channel with an enzymatically functional serine/threonine kinase domain (Nadler et al., 2001; Suzuki et al., 2018). The channel is inactivated by receptor-mediated activation of phosphatidylinositol 4,5-bisphosphate (PIP2) and high Mg^{2+} concentrations (Nadler *et al.*, 2001; Runnels et al., 2002). TRPM7 is identified be to involve in store-operated calcium entry (SOCE), in which the emptying of ER calcium stores causes influx of calcium across the plasma membrane (Faouzi et al., 2017). This process is regulated by the kinase activity of the TRPM7, which itself is activated by autophosphorylation of its kinase domain (Faouzi *et al.*, 2017).

References

Aoki, T., Okada, N., Wakamatsu, T., and Tamura, T.A. (2002). TBP-interacting protein 120B, which is induced in relation to myogenesis, binds to NOT3. Biochem Biophys Res Commun *296*, 1097-1103. 10.1016/s0006-291x(02)02031-4.

Axang, C., Rauthan, M., Hall, D.H., and Pilon, M. (2008). Developmental genetics of the C. elegans pharyngeal neurons NSML and NSMR. BMC Dev Biol *8*, 38. 10.1186/1471-213X-8-38.

Balamurugan, K., Ashokkumar, B., Moussaif, M., Sze, J.Y., and Said, H.M. (2007). Cloning and functional characterization of a folate transporter from the nematode Caenorhabditis elegans. American journal of physiology. Cell physiology *293*, C670-681. 10.1152/ajpcell.00516.2006.

Bassermann, F., Eichner, R., and Pagano, M. (2014). The ubiquitin proteasome system - implications for cell cycle control and the targeted treatment of cancer. Biochim Biophys Acta *1843*, 150-162. 10.1016/j.bbamcr.2013.02.028.

Beaudin, A.E., and Stover, P.J. (2009). Insights into metabolic mechanisms underlying folate-responsive neural tube defects: a minireview. Birth Defects Res A Clin Mol Teratol *85*, 274-284. 10.1002/bdra.20553.

Betsch, L., Boltz, V., Brioudes, F., Pontier, G., Girard, V., Savarin, J., Wipperman, B., Chambrier, P., Tissot, N., Benhamed, M., et al. (2019). TCTP and CSN4 control cell cycle progression and development by regulating CULLIN1 neddylation in plants and animals. PLoS Genet *15*, e1007899. 10.1371/journal.pgen.1007899.

Bianchi, E., Doe, B., Goulding, D., and Wright, G.J. (2014). Juno is the egg Izumo receptor and is essential for mammalian fertilization. Nature *508*, 483-487. 10.1038/nature13203.

Bosu, D.R., Feng, H., Min, K., Kim, Y., Wallenfang, M.R., and Kipreos, E.T. (2010). C. elegans CAND-1 regulates cullin neddylation, cell proliferation and morphogenesis in specific tissues. Dev Biol *346*, 113-126. 10.1016/j.ydbio.2010.07.020.

Bosu, D.R., and Kipreos, E.T. (2008). Cullin-RING ubiquitin ligases: global regulation and activation cycles. Cell Div *3*, 7. 10.1186/1747-1028-3-7.

Brenner, S. (1974). The genetics of Caenorhabditis elegans. Genetics *77*, 71-94. 10.1093/genetics/77.1.71.

Bulatov, E., and Ciulli, A. (2015). Targeting Cullin-RING E3 ubiquitin ligases for drug discovery: structure, assembly and small-molecule modulation. Biochem J *467*, 365-386. 10.1042/BJ20141450.

Chase, D.L., and Koelle, M.R. (2007). Biogenic amine neurotransmitters in C. elegans. WormBook, 1-15. 10.1895/wormbook.1.132.1.

Chaudhari, S.N., Mukherjee, M., Vagasi, A.S., Bi, G., Rahman, M.M., Nguyen, C.Q., Paul, L., Selhub, J., and Kipreos, E.T. (2016). Bacterial Folates Provide an Exogenous Signal for C. elegans Germline Stem Cell Proliferation. Dev Cell *38*, 33-46. 10.1016/j.devcel.2016.06.013.

Chuang, H.W., Zhang, W., and Gray, W.M. (2004). Arabidopsis ETA2, an apparent ortholog of the human cullin-interacting protein CAND1, is required for auxin responses mediated by the SCF(TIR1) ubiquitin ligase. Plant Cell *16*, 1883-1897. 10.1105/tpc.021923.

Ciechanover, A. (1994). The ubiquitin-proteasome proteolytic pathway. Cell *79*, 13-21. 10.1016/0092-8674(94)90396-4.

Cope, G.A., and Deshaies, R.J. (2003). COP9 signalosome: a multifunctional regulator of SCF and other cullin-based ubiquitin ligases. Cell *114*, 663-671. 10.1016/s0092-8674(03)00722-0.

Crider, K.S., Bailey, L.B., and Berry, R.J. (2011). Folic acid food fortification-its history, effect, concerns, and future directions. Nutrients *3*, 370-384. 10.3390/nu3030370.

Crott, J.W., Liu, Z., Keyes, M.K., Choi, S.W., Jang, H., Moyer, M.P., and Mason, J.B. (2008). Moderate folate depletion modulates the expression of selected genes involved in cell cycle, intracellular signaling and folate uptake in human colonic epithelial cell lines. J Nutr Biochem *19*, 328-335. 10.1016/j.jnutbio.2007.05.003.

de Bono, M., Tobin, D.M., Davis, M.W., Avery, L., and Bargmann, C.I. (2002). Social feeding in Caenorhabditis elegans is induced by neurons that detect aversive stimuli. Nature *419*, 899-903. 10.1038/nature01169.

Dickinson, D.J., and Goldstein, B. (2016). CRISPR-Based Methods for Caenorhabditis elegans Genome Engineering. Genetics *202*, 885-901. 10.1534/genetics.115.182162.

Duda, D.M., Borg, L.A., Scott, D.C., Hunt, H.W., Hammel, M., and Schulman, B.A. (2008). Structural insights into NEDD8 activation of Cullin-RING ligases: Conformational control of conjugation. Cell *134*, 995-1006. 10.1016/j.cell.2008.07.022.

Elnakat, H., and Ratnam, M. (2004). Distribution, functionality and gene regulation of folate receptor isoforms: implications in targeted therapy. Adv Drug Deliv Rev *56*, 1067-1084. 10.1016/j.addr.2004.01.001.

Esposito, G., Di Schiavi, E., Bergamasco, C., and Bazzicalupo, P. (2007). Efficient and cell specific knock-down of gene function in targeted C. elegans neurons. Gene *395*, 170-176. 10.1016/j.gene.2007.03.002.

Faouzi, M., Kilch, T., Horgen, F.D., Fleig, A., and Penner, R. (2017). The TRPM7 channel kinase regulates store-operated calcium entry. J Physiol *595*, 3165-3180. 10.1113/jp274006.

Feng, S., Shen, Y., Sullivan, J.A., Rubio, V., Xiong, Y., Sun, T.P., and Deng, X.W. (2004). Arabidopsis CAND1, an unmodified CUL1-interacting protein, is involved in multiple developmental pathways controlled by ubiquitin/proteasome-mediated protein Degradation. Plant Cell *16*, 1870-1882. 10.1105/tpc.021949.

Geller, J., Kronn, D., Jayabose, S., and Sandoval, C. (2002). Hereditary folate malabsorption: family report and review of the literature. Medicine (Baltimore) *81*, 51-68. 10.1097/00005792-200201000-00004.

Glickman, M.H., and Ciechanover, A. (2002). The ubiquitin-proteasome proteolytic pathway: destruction for the sake of construction. Physiol Rev *82*, 373-428. 10.1152/physrev.00027.2001.

Goldenberg, S.J., Cascio, T.C., Shumway, S.D., Garbutt, K.C., Liu, J., Xiong, Y., and Zheng, N. (2004). Structure of the Cand1-Cul1-Roc1 complex reveals regulatory mechanisms for the assembly of the multisubunit cullin-dependent ubiquitin ligases. Cell *119*, 517-528. 10.1016/j.cell.2004.10.019.

Goodman, M.B. (2006). Mechanosensation. WormBook, 1-14. 10.1895/wormbook.1.62.1.

Grapp, M., Wrede, A., Schweizer, M., Huwel, S., Galla, H.J., Snaidero, N., Simons, M., Buckers, J., Low, P.S., Urlaub, H., et al. (2013). Choroid plexus transcytosis and exosome shuttling deliver folate into brain parenchyma. Nat Commun *4*, 2123. 10.1038/ncomms3123.

Henderson, G.I., Perez, T., Schenker, S., Mackins, J., and Antony, A.C. (1995). Maternal-to-fetal transfer of 5-methyltetrahydrofolate by the perfused human placental cotyledon: evidence for a concentrative role by placental folate receptors in fetal folate delivery. J Lab Clin Med *126*, 184-203.

Holm, J., and Hansen, S.I. (2020). Characterization of soluble folate receptors (folate binding proteins) in humans. Biological roles and clinical potentials in infection and malignancy. Biochim Biophys Acta Proteins Proteom *1868*, 140466. 10.1016/j.bbapap.2020.140466.

Imbard, A., Benoist, J.F., and Blom, H.J. (2013). Neural tube defects, folic acid and methylation. Int J Environ Res Public Health *10*, 4352-4389. 10.3390/ijerph10094352.

Jang, S.M., Redon, C.E., and Aladjem, M.I. (2018). Chromatin-Bound Cullin-Ring Ligases: Regulatory Roles in DNA Replication and Potential Targeting for Cancer Therapy. Front Mol Biosci *5*, 19. 10.3389/fmolb.2018.00019.

Ji, J., Shu, D., Zheng, M., Wang, J., Luo, C., Wang, Y., Guo, F., Zou, X., Lv, X., Li, Y., et al. (2016). Microbial metabolite butyrate facilitates M2 macrophage polarization and function. Sci Rep *6*, 24838. 10.1038/srep24838.

Jia, Z., Zhao, R., Tian, Y., Huang, Z., Tian, Z., Shen, Z., Wang, Q., Wang, J., Fu, X., and Wu, Y. (2009). A novel splice variant of FR4 predominantly expressed in CD4+CD25+ regulatory T cells. Immunol Invest *38*, 718-729. 10.3109/08820130903171003.

Kato, K., Satouh, Y., Nishimasu, H., Kurabayashi, A., Morita, J., Fujihara, Y., Oji, A., Ishitani, R., Ikawa, M., and Nureki, O. (2016). Structural and functional insights into IZUMO1 recognition by JUNO in mammalian fertilization. Nat Commun *7*, 12198. 10.1038/ncomms12198.

Keuss, M.J., Thomas, Y., McArthur, R., Wood, N.T., Knebel, A., and Kurz, T. (2016). Characterization of the mammalian family of DCN-type NEDD8 E3 ligases. J Cell Sci *129*, 1441-1454. 10.1242/jcs.181784.

Kim, A.Y., Bommelje, C.C., Lee, B.E., Yonekawa, Y., Choi, L., Morris, L.G., Huang, G., Kaufman, A., Ryan, R.J., Hao, B., et al. (2008). SCCRO (DCUN1D1) is an essential

component of the E3 complex for neddylation. J Biol Chem *283*, 33211-33220. 10.1074/jbc.M804440200.

Kim, T.Y., Siesser, P.F., Rossman, K.L., Goldfarb, D., Mackinnon, K., Yan, F., Yi, X., MacCoss, M.J., Moon, R.T., Der, C.J., and Major, M.B. (2015). Substrate trapping proteomics reveals targets of the betaTrCP2/FBXW11 ubiquitin ligase. Mol Cell Biol *35*, 167-181. 10.1128/MCB.00857-14.

Kipreos, E.T. (2005). Ubiquitin-mediated pathways in C. elegans. WormBook, 1-24. 10.1895/wormbook.1.36.1.

Kipreos, E.T., Lander, L.E., Wing, J.P., He, W.W., and Hedgecock, E.M. (1996). cul-1 is required for cell cycle exit in C. elegans and identifies a novel gene family. Cell *85*, 829-839. 10.1016/s0092-8674(00)81267-2.

Kipreos, E.T., and Pagano, M. (2000). The F-box protein family. Genome Biol *1*, REVIEWS3002. 10.1186/gb-2000-1-5-reviews3002.

Kwan, C.S., Vazquez-Manrique, R.P., Ly, S., Goyal, K., and Baylis, H.A. (2008). TRPM channels are required for rhythmicity in the ultradian defecation rhythm of C. elegans. BMC Physiol *8*, 11. 10.1186/1472-6793-8-11.

Lambie, E.J., Bruce, R.D., 3rd, Zielich, J., and Yuen, S.N. (2015). Novel Alleles of gon-2, a C. elegans Ortholog of Mammalian TRPM6 and TRPM7, Obtained by Genetic Reversion Screens. PLoS One *10*, e0143445. 10.1371/journal.pone.0143445.

Lau, A.W., Fukushima, H., and Wei, W. (2012). The Fbw7 and betaTRCP E3 ubiquitin ligases and their roles in tumorigenesis. Front Biosci (Landmark Ed) *17*, 2197-2212. 10.2741/4045.

Liu, H., Urbe, S., and Clague, M.J. (2012). Selective protein degradation in cell signalling. Semin Cell Dev Biol *23*, 509-514. 10.1016/j.semcdb.2012.01.014.

Liu, J., Furukawa, M., Matsumoto, T., and Xiong, Y. (2002). NEDD8 modification of CUL1 dissociates p120(CAND1), an inhibitor of CUL1-SKP1 binding and SCF ligases. Mol Cell *10*, 1511-1518. 10.1016/s1097-2765(02)00783-9.

Liu, X., Reitsma, J.M., Mamrosh, J.L., Zhang, Y., Straube, R., and Deshaies, R.J. (2018). Cand1-Mediated Adaptive Exchange Mechanism Enables Variation in F-Box Protein Expression. Mol Cell *69*, 773-786 e776. 10.1016/j.molcel.2018.01.038.

Liu, Z., Ciappio, E.D., Crott, J.W., Brooks, R.S., Nesvet, J., Smith, D.E., Choi, S.W., and Mason, J.B. (2011). Combined inadequacies of multiple B vitamins amplify colonic Wnt signaling and promote intestinal tumorigenesis in BAT-LacZxApc1638N mice. FASEB J *25*, 3136-3145. 10.1096/fj.11-184143.

Luteijn, R.D., Zaver, S.A., Gowen, B.G., Wyman, S.K., Garelis, N.E., Onia, L., McWhirter, S.M., Katibah, G.E., Corn, J.E., Woodward, J.J., and Raulet, D.H. (2019). SLC19A1 transports immunoreactive cyclic dinucleotides. Nature *573*, 434-438. 10.1038/s41586-019-1553-0.

Mangeat, B., Gers-Huber, G., Lehmann, M., Zufferey, M., Luban, J., and Piguet, V. (2009). HIV-1 Vpu neutralizes the antiviral factor Tetherin/BST-2 by binding it and directing its beta-TrCP2-dependent degradation. PLoS Pathog *5*, e1000574. 10.1371/journal.ppat.1000574.

Mathias, N., Johnson, S.L., Winey, M., Adams, A.E., Goetsch, L., Pringle, J.R., Byers, B., and Goebl, M.G. (1996). Cdc53p acts in concert with Cdc4p and Cdc34p to control the G1-to-S-phase transition and identifies a conserved family of proteins. Mol Cell Biol *16*, 6634-6643. 10.1128/MCB.16.12.6634.

Moore, R., and Boyd, L. (2004). Analysis of RING finger genes required for embryogenesis in C. elegans. Genesis *38*, 1-12. 10.1002/gene.10243.

Nadler, M.J., Hermosura, M.C., Inabe, K., Perraud, A.L., Zhu, Q., Stokes, A.J., Kurosaki, T., Kinet, J.P., Penner, R., Scharenberg, A.M., and Fleig, A. (2001). LTRPC7 is a Mg.ATP-regulated divalent cation channel required for cell viability. Nature *411*, 590-595. 10.1038/35079092.

Nakayama, K.I., and Nakayama, K. (2005). Regulation of the cell cycle by SCF-type ubiquitin ligases. Semin Cell Dev Biol *16*, 323-333. 10.1016/j.semcdb.2005.02.010.

Nathoo, A.N., Moeller, R.A., Westlund, B.A., and Hart, A.C. (2001). Identification of neuropeptide-like protein gene families in Caenorhabditiselegans and other species. Proc Natl Acad Sci U S A *98*, 14000-14005. 10.1073/pnas.241231298.

Nguyen, K.M., and Busino, L. (2020). The Biology of F-box Proteins: The SCF Family of E3 Ubiquitin Ligases. Adv Exp Med Biol *1217*, 111-122. 10.1007/978-981-15-1025-0_8.

Nguyen, T.P., and Clarke, C.F. (2012). Folate status of gut microbiome affects Caenorhabditis elegans lifespan. BMC Biol *10*, 66. 10.1186/1741-7007-10-66.

Olma, M.H., and Dikic, I. (2013). Cullins getting undressed by the protein exchange factor Cand1. Cell *153*, 14-16. 10.1016/j.cell.2013.03.014.

Ortbauer, M., Ripper, D., Fuhrmann, T., Lassi, M., Auernigg-Haselmaier, S., Stiegler, C., and Konig, J. (2016). Folate deficiency and over-supplementation causes impaired folate metabolism: Regulation and adaptation mechanisms in Caenorhabditis elegans. Mol Nutr Food Res *60*, 949-956. 10.1002/mnfr.201500819.

Oshikawa, K., Matsumoto, M., Yada, M., Kamura, T., Hatakeyama, S., and Nakayama, K.I. (2003). Preferential interaction of TIP120A with Cul1 that is not modified by NEDD8 and

not associated with Skp1. Biochem Biophys Res Commun *303*, 1209-1216. 10.1016/s0006-291x(03)00501-1.

Patanwala, I., King, M.J., Barrett, D.A., Rose, J., Jackson, R., Hudson, M., Philo, M., Dainty, J.R., Wright, A.J., Finglas, P.M., and Jones, D.E. (2014). Folic acid handling by the human gut: implications for food fortification and supplementation. Am J Clin Nutr *100*, 593-599. 10.3945/ajcn.113.080507.

Pickart, C.M. (2001). Mechanisms underlying ubiquitination. Annu Rev Biochem *70*, 503-533. 10.1146/annurev.biochem.70.1.503.

Pierce, N.W., Lee, J.E., Liu, X., Sweredoski, M.J., Graham, R.L., Larimore, E.A., Rome, M., Zheng, N., Clurman, B.E., Hess, S., et al. (2013). Cand1 promotes assembly of new SCF complexes through dynamic exchange of F box proteins. Cell *153*, 206-215. 10.1016/j.cell.2013.02.024.

Puig-Kroger, A., Sierra-Filardi, E., Dominguez-Soto, A., Samaniego, R., Corcuera, M.T., Gomez-Aguado, F., Ratnam, M., Sanchez-Mateos, P., and Corbi, A.L. (2009). Folate receptor beta is expressed by tumor-associated macrophages and constitutes a marker for M2 anti-inflammatory/regulatory macrophages. Cancer Res *69*, 9395-9403. 10.1158/0008-5472.CAN-09-2050.

Reitsma, J.M., Liu, X., Reichermeier, K.M., Moradian, A., Sweredoski, M.J., Hess, S., and Deshaies, R.J. (2017). Composition and Regulation of the Cellular Repertoire of SCF Ubiquitin Ligases. Cell *171*, 1326-1339 e1314. 10.1016/j.cell.2017.10.016.

Rock, K.L., Gramm, C., Rothstein, L., Clark, K., Stein, R., Dick, L., Hwang, D., and Goldberg, A.L. (1994). Inhibitors of the proteasome block the degradation of most cell proteins and

the generation of peptides presented on MHC class I molecules. Cell *78*, 761-771. 10.1016/s0092-8674(94)90462-6.

Runnels, L.W., Yue, L., and Clapham, D.E. (2002). The TRPM7 channel is inactivated by PIP(2) hydrolysis. Nat Cell Biol *4*, 329-336. 10.1038/ncb781.

Rusnac, D.V., and Zheng, N. (2020). Structural Biology of CRL Ubiquitin Ligases. Adv Exp Med Biol *1217*, 9-31. 10.1007/978-981-15-1025-0_2.

Saha, A., and Deshaies, R.J. (2008). Multimodal activation of the ubiquitin ligase SCF by Nedd8 conjugation. Mol Cell *32*, 21-31. 10.1016/j.molcel.2008.08.021.

Samaniego, R., Dominguez-Soto, A., Ratnam, M., Matsuyama, T., Sanchez-Mateos, P., Corbi, A.L., and Puig-Kroger, A. (2020). Folate Receptor beta (FRbeta) Expression in Tissue-Resident and Tumor-Associated Macrophages Associates with and Depends on the Expression of PU.1. Cells *9*. 10.3390/cells9061445.

Sasagawa, Y., Urano, T., Kohara, Y., Takahashi, H., and Higashitani, A. (2003). Caenorhabditis elegans RBX1 is essential for meiosis, mitotic chromosomal condensation and segregation, and cytokinesis. Genes Cells *8*, 857-872. DOI 10.1046/j.1365-2443.2003.00682.x.

Sawin, E.R., Ranganathan, R., and Horvitz, H.R. (2000). C-elegans locomotory rate is modulated by the environment through a dopaminergic pathway and by experience through a serotonergic pathway. Neuron *26*, 619-631. Doi 10.1016/S0896-6273(00)81199-X.

Schade, M.A., Reynolds, N.K., Dollins, C.M., and Miller, K.G. (2005). Mutations that rescue the paralysis of Caenorhabditis elegans ric-8 (synembryn) mutants activate the G alpha(s) pathway and define a third major branch of the synaptic signaling network. Genetics *169*, 631-649. 10.1534/genetics.104.032334.

Schafer, W.R. (2006). Neurophysiological methods in C. elegans: an introduction. WormBook, 1-4. 10.1895/wormbook.1.111.1.

Selhub, J., Emmanouel, D., Stavropoulos, T., and Arnold, R. (1987). Renal folate absorption and the kidney folate binding protein. I. Urinary clearance studies. Am J Physiol *252*, F750-756.

Sivapalaratnam, S., Basart, H., Watkins, N.A., Maiwald, S., Rendon, A., Krishnan, U., Sondermeijer, B.M., Creemers, E.E., Pinto-Sietsma, S.J., Hovingh, K., et al. (2012). Monocyte gene expression signature of patients with early onset coronary artery disease. PLoS One *7*, e32166. 10.1371/journal.pone.0032166.

Skaar, J.R., Pagan, J.K., and Pagano, M. (2013). Mechanisms and function of substrate recruitment by F-box proteins. Nat Rev Mol Cell Biol *14*, 369-381. 10.1038/nrm3582.

Soucy, T.A., Smith, P.G., Milhollen, M.A., Berger, A.J., Gavin, J.M., Adhikari, S., Brownell, J.E., Burke, K.E., Cardin, D.P., Critchley, S., et al. (2009). An inhibitor of NEDD8-activating enzyme as a new approach to treat cancer. Nature *458*, 732-736. 10.1038/nature07884.

Starostina, N.G., and Kipreos, E.T. (2012). Multiple degradation pathways regulate versatile CIP/KIP CDK inhibitors. Trends Cell Biol *22*, 33-41. 10.1016/j.tcb.2011.10.004.

Sun, A.Y., and Lambie, E.J. (1997). gon-2, a gene required for gonadogenesis in Caenorhabditis elegans. Genetics *147*, 1077-1089. 10.1093/genetics/147.3.1077.

Suzuki, S., Lis, A., Schmitz, C., Penner, R., and Fleig, A. (2018). The TRPM7 kinase limits receptor-induced calcium release by regulating heterotrimeric G-proteins. Cell Mol Life Sci *75*, 3069-3078. 10.1007/s00018-018-2786-z.

Sybesma, W., Starrenburg, M., Tijsseling, L., Hoefnagel, M.H., and Hugenholtz, J. (2003). Effects of cultivation conditions on folate production by lactic acid bacteria. Appl Environ Microbiol *69*, 4542-4548. 10.1128/AEM.69.8.4542-4548.2003.

Sze, J.Y., Victor, M., Loer, C., Shi, Y., and Ruvkun, G. (2000). Food and metabolic signalling defects in a Caenorhabditis elegans serotonin-synthesis mutant. Nature *403*, 560-564. 10.1038/35000609.

Tam, C., O'Connor, D., and Koren, G. (2012). Circulating unmetabolized folic Acid: relationship to folate status and effect of supplementation. Obstet Gynecol Int *2012*, 485179. 10.1155/2012/485179.

Teramoto, T., Lambie, E.J., and Iwasaki, K. (2005). Differential regulation of TRPM channels governs electrolyte homeostasis in the C. elegans intestine. Cell Metab *1*, 343-354. 10.1016/j.cmet.2005.04.007.

Teramoto, T., Sternick, L.A., Kage-Nakadai, E., Sajjadi, S., Siembida, J., Mitani, S., Iwasaki, K., and Lambie, E.J. (2010). Magnesium excretion in C. elegans requires the activity of the GTL-2 TRPM channel. PLoS One *5*, e9589. 10.1371/journal.pone.0009589.

Thrower, J.S., Hoffman, L., Rechsteiner, M., and Pickart, C.M. (2000). Recognition of the polyubiquitin proteolytic signal. EMBO J *19*, 94-102. 10.1093/emboj/19.1.94.

Umapathy, N.S., Gnana-Prakasam, J.P., Martin, P.M., Mysona, B., Dun, Y., Smith, S.B., Ganapathy, V., and Prasad, P.D. (2007). Cloning and functional characterization of the proton-coupled electrogenic folate transporter and analysis of its expression in retinal cell types. Invest Ophthalmol Vis Sci *48*, 5299-5305. 10.1167/iovs.07-0288.

Valimberti, I., Tiberti, M., Lambrughi, M., Sarcevic, B., and Papaleo, E. (2015). E2 superfamily of ubiquitin-conjugating enzymes: constitutively active or activated through phosphorylation in the catalytic cleft. Sci Rep *5*, 14849. 10.1038/srep14849.

Visentin, M., Diop-Bove, N., Zhao, R., and Goldman, I.D. (2014). The intestinal absorption of folates. Annu Rev Physiol *76*, 251-274. 10.1146/annurev-physiol-020911-153251.

Williams, P.J., Mistry, H.D., and Morgan, L. (2012). Folate transporter expression decreases in the human placenta throughout pregnancy and in pre-eclampsia. Pregnancy Hypertens *2*, 123-131. 10.1016/j.preghy.2011.12.001.

Wojcik, C., and DeMartino, G.N. (2003). Intracellular localization of proteasomes. Int J Biochem Cell Biol *35*, 579-589. 10.1016/s1357-2725(02)00380-1.

Xing, J., Yan, X., Estevez, A., and Strange, K. (2008). Highly Ca2+-selective TRPM channels regulate IP3-dependent oscillatory Ca2+ signaling in the C. elegans intestine. J Gen Physiol *131*, 245-255. 10.1085/jgp.200709914.

Yeh, C.H., Bellon, M., and Nicot, C. (2018). FBXW7: a critical tumor suppressor of human cancers. Mol Cancer *17*, 115. 10.1186/s12943-018-0857-2.

Zhang, Y., Lu, H., and Bargmann, C.I. (2005). Pathogenic bacteria induce aversive olfactory learning in Caenorhabditis elegans. Nature *438*, 179-184. 10.1038/nature04216.

Zhao, R., Diop-Bove, N., Visentin, M., and Goldman, I.D. (2011). Mechanisms of membrane transport of folates into cells and across epithelia. Annu Rev Nutr *31*, 177-201. 10.1146/annurev-nutr-072610-145133.

Zhao, R., Min, S.H., Wang, Y., Campanella, E., Low, P.S., and Goldman, I.D. (2009). A role for the proton-coupled folate transporter (PCFT-SLC46A1) in folate receptor-mediated endocytosis. J Biol Chem *284*, 4267-4274. 10.1074/jbc.M807665200.

Zhao, Y.C., and Sun, Y. (2013). Cullin-RING Ligases as Attractive Anti-cancer Targets. Curr Pharm Design *19*, 3215-3225. Doi 10.2174/1381612811319999030O.

Zheng, J., Yang, X., Harrell, J.M., Ryzhikov, S., Shim, E.H., Lykke-Andersen, K., Wei, N., Sun, H., Kobayashi, R., and Zhang, H. (2002a). CAND1 binds to unneddylated CUL1 and regulates the formation of SCF ubiquitin E3 ligase complex. Mol Cell *10*, 1519-1526. 10.1016/s1097-2765(02)00784-0.

Zheng, N., Schulman, B.A., Song, L., Miller, J.J., Jeffrey, P.D., Wang, P., Chu, C., Koepp, D.M., Elledge, S.J., Pagano, M., et al. (2002b). Structure of the Cul1-Rbx1-Skp1-F boxSkp2 SCF ubiquitin ligase complex. Nature *416*, 703-709. 10.1038/416703a.

Zheng, N., Wang, Z., and Wei, W. (2016). Ubiquitination-mediated degradation of cell cycle-related proteins by F-box proteins. Int J Biochem Cell Biol *73*, 99-110. 10.1016/j.biocel.2016.02.005.

Zheng, Y., and Cantley, L.C. (2019). Toward a better understanding of folate metabolism in health and disease. J Exp Med *216*, 253-266. 10.1084/jem.20181965.

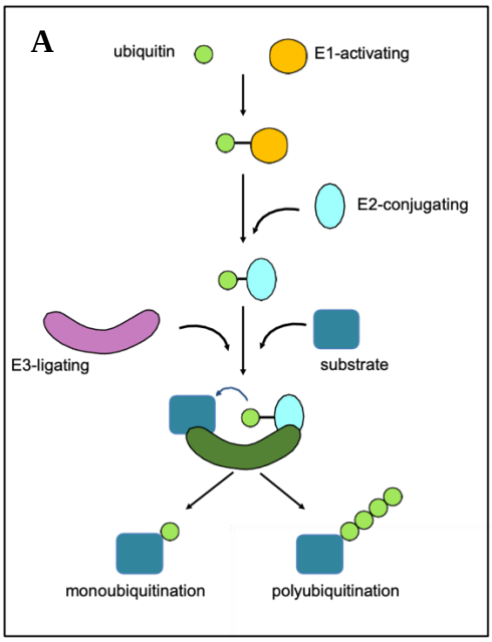
A
ubiquitin
E1-activating
E2-conjugating
E3-ligating
substrate
monoubiquitination
polyubiquitination

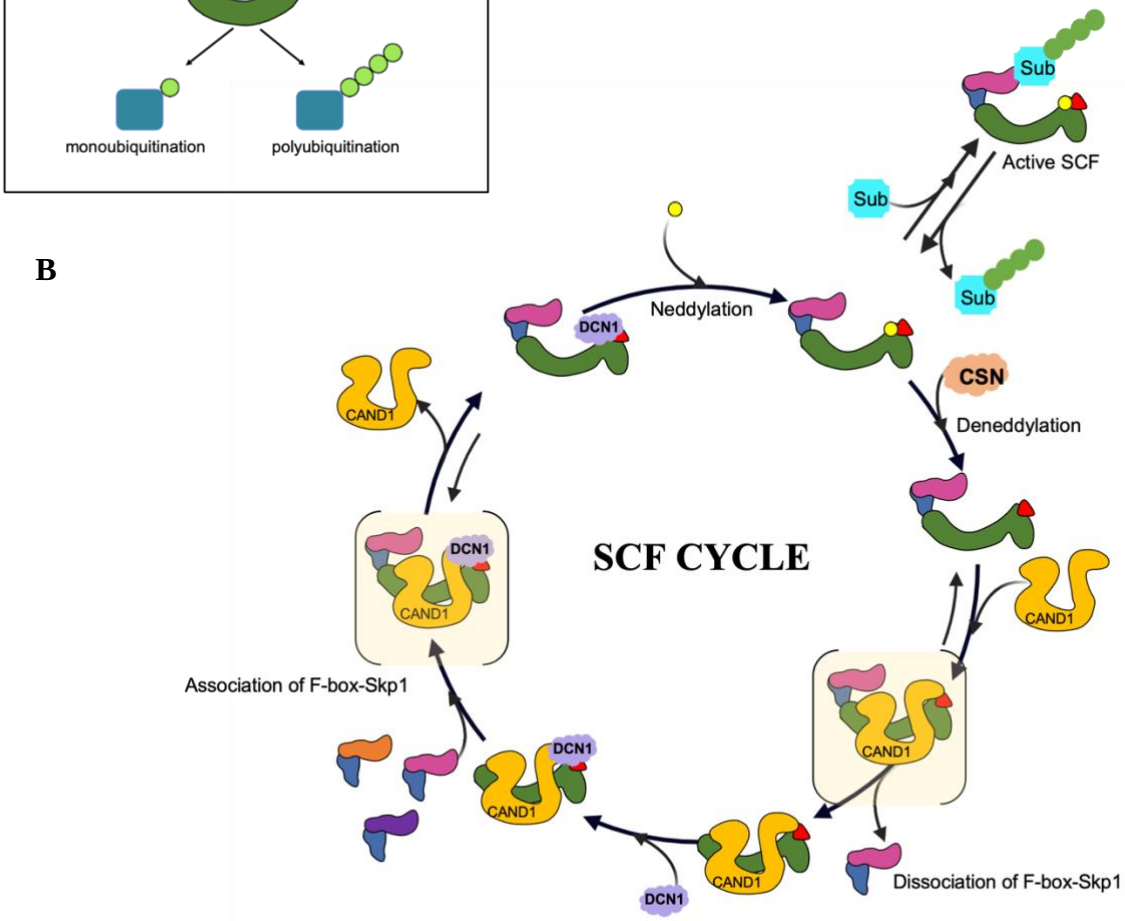
B
Sub
Active SCF
Sub
Sub
Neddylation
DCN1
CSN
Deneddylation
CAND1
SCF CYCLE
DCN1
CAND1
CAND1
Association of F-box-Skp1
CAND1
DCN1
CAND1
DCN1
CAND1
Dissociation of F-box-Skp1

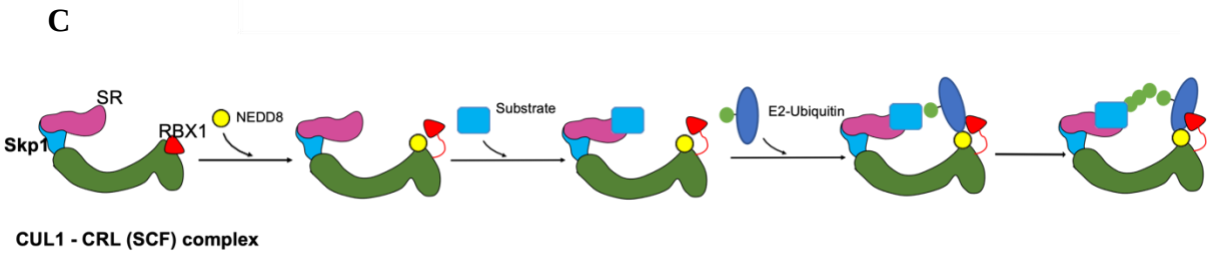
C
SR
Skp1
RBX1
NEDD8
Substrate
E2-Ubiquitin
CUL1 - CRL (SCF) complex

Figure. 1.1 The ubiquitination process; structure and regulation of CRL complexes

(A) The cascade of E1-E2-E3 enzymes tag substrates with ubiquitin.

(B) Regulation of SCFs by CAND1 and the CSN complex.

(C) Structure of CRL E3 ubiquitin ligases, and the process of assembly of structural components, recruitment of the E2 enzyme, and ubiquitination of substrate proteins.

(Figures A and C Modified from the dissertation of Snehal Nitin Chaudhary)

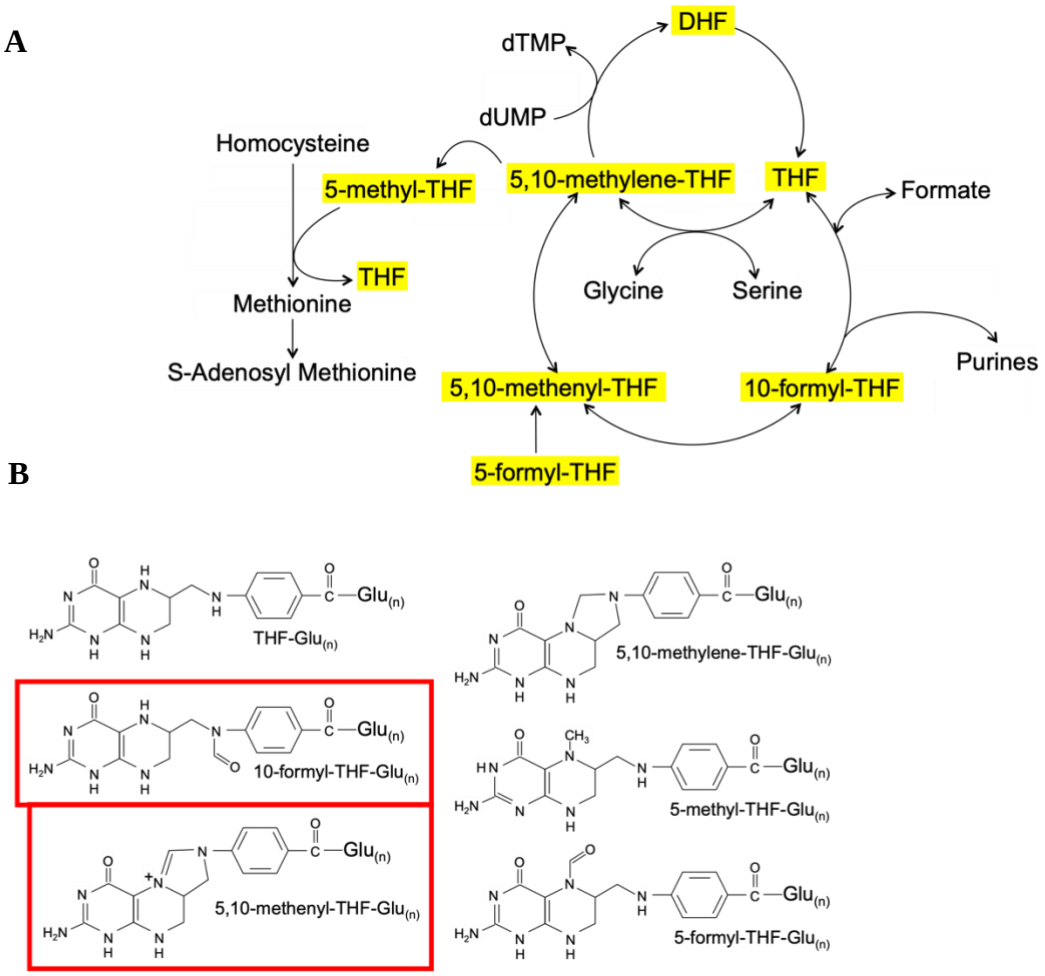

Figure. 1.2. Partial one-carbon metabolism cycle and stimulatory folate structures.

(A) Diagram of partial one-carbon metabolism cycle

(C) Structures of one-carbon metabolism folates.

(Modified from (Chaudhari *et al.*, 2016), Reprinted with permission)

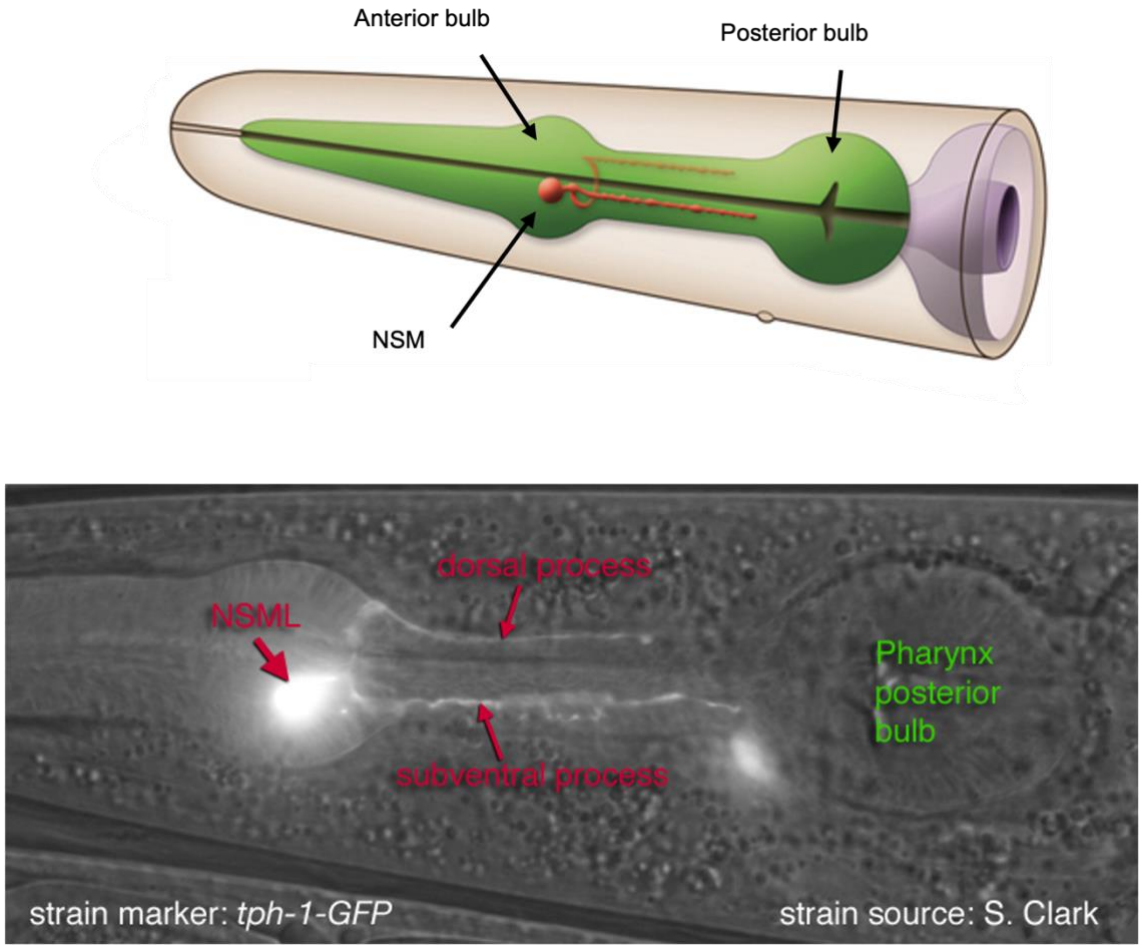

Figure. 1.3. NSM neuron projection contacts the lumen of the pharynx

A) Anterior diagram with the pharynx in green and an NSM neuron in red. : Arrows mark NSM soma; arrowheads mark minor neurite.

B) Diagram of the pharynx with one NSM neuron and two other neurons labeled.

(Reprinted from WormAtlas (http://wormatlas.org) with permission.)

CHAPTER 2

EMERGING ROLES FOR FOLATE IN CANCER CELL SIGNALING

Fathima Zahra Nawaz and Edward T. Kipreos* "Emerging roles for folate in cancer cell signaling", *invited review submitted to Trends in Endocrinology and Metabolism (TEM).*

Abstract

Folates are B vitamins that function in one-carbon metabolism. Folate receptors are one of three major types of folate transporters. The folate receptors FOLR1 and FOLR2 are overexpressed in multiple cancers. The overexpression of FOLR1 is often associated with increased cancer progression and poor patient prognosis. There is emerging evidence that FOLR1 is directly involved in signaling pathways in cancer cells that are independent of its canonical role in metabolism. Recent publications implicate a direct role of FOLR1 in several signaling pathways: JAK–STAT3 and ERK1/2; a direct role as a transcription factor; and interaction with LYN and G-protein coupled receptor subunits. We discuss data that support non-canonical roles for FOLR1, and the limitations of the data.

Introduction

Folate (vitamin B_9) is an essential nutrient that is required for one-carbon metabolism. Folic acid (a synthetic folate) is provided as a supplement during pregnancy to reduce the incidence of neural tube defects, and 82 countries fortify grains with folic acid (Wald et al., 2018). The folate receptors FOLR1 and FOLR2 have restricted tissue expression, but many cancers overexpress one of the two receptors. We will review the overexpression of FOLR1 and FOLR2 in different cancers and the impact on cancer progression. Emerging evidence suggests that folates function as ligands to initiate cell signaling in a surprisingly large number of intracellular signaling pathways. We will critically appraise the data that implicate the role of folate receptor in non-metabolic pathways in cancer cells.

Folates and one-carbon metabolism

Folates have a canonical role in one-carbon metabolism, where they donate and receive one-carbon unit. One-carbon metabolism functions in the synthesis of nucleotides (purines and deoxythymidine monophosphate, dTMP), the amino acid methionine (which is required to generate the methyl-donor S-adenosyl methionine), and the interconversion of glycine and serine (Zheng and Cantley, 2019).

Folates are a family of molecules that are comprised of a pteridine ring, para-aminobenzoic acid (PABA), and one or more glutamates (Glu) (Zheng and Cantley, 2019). Different folates differ in their pteridine rings. In animals, the folate in serum that mediates systemic distribution is 5-methyl-tetrahydrafolate (5-methyl-THF) with a single glutamate (Zheng and Cantley, 2019). Once 5-methyl-THF is taken up by cells, it is converted to other folates and additional Glu are added to create poly-Glu folates that are retained within cells (Zheng and Cantley, 2019).

Folate transporters

Mammals utilize three types of folate transporters: the reduced folate carrier (RFC); the proton-coupled folate transporter (PCFT); and folate receptors (FOLRs). RFC is a low-affinity, high-throughput transporter that is ubiquitously expressed in mammalian cells and mediates the majority of folate transport into the majority of mammalian cells (Zhao et al., 2011) (Fig. 2.1, left). RFC efficiently transports reduced folates (including the serum folate 5-methyl-THF), but has a two-orders of magnitude lower efficiency for folic acid, which is a synthetic folate that is not found in nature. PCFT has a critical role in the small intestine to absorb folate derived from food into the body (Visentin et al., 2014) (Fig. 2.1, middle).

FOLR are high-affinity, low-throughput transporters (Zhao *et al.*, 2011). There are four FOLR1 genes, *FOLR1–4* (aka, folate receptors α, β, γ, and δ; and the historical name of folate binding protein, FBP). FOLR3 is expressed in neutrophil granulocytes and monocytes and is a secreted protein that binds folate in the bloodstream (Holm and Hansen, 2020; Sivapalaratnam et al., 2012). FOLR4 is expressed in regulatory T cells and mammalian eggs, but is unable to bind folate (Bianchi et al., 2014; Jia et al., 2009). In the egg, FOLR4 functions as the receptor for the sperm Izumo protein, and is required for fertilization (Bianchi *et al.*, 2014). FOLR1 and FOLR2 bind folates on the cell surface, and FOLR bound to folate are brought into the cell by endocytosis (Fig. 2.1, right). After endocytosis, folates are released from acidified endosomes into the cytoplasm by PCFT (Zhao et al., 2009).

FOLR1 has limited tissue expression on the luminal (apical) surface of polarized epithelia, including proximal kidney tubules, type 1 and 2 pneumocytes in the lungs, choroid plexus, ovary, fallopian tube, uterus, cervix, epididymis, submandibular salivary gland, bronchial glands, and trophoblasts in the placenta (Elnakat and Ratnam, 2004). In several tissues, the polarized localization of FOLR1 corresponds to its role in the transcytosis of folates across cellular barriers. In the choroid plexus, FOLR1 transports folates from the basolateral to the apical membrane of the choroid plexus, and is then transported in exosomes across the blood brain barrier (Grapp et al., 2013). In the placenta, FOLR1 transports folates from the mother to the fetus (Henderson et al., 1995). And in the kidney, FOLR1 acts to reabsorb folates from pre-urine to transport the folates back into the body (Selhub et al., 1987).

FOLR1 has the highest affinity for folic acid, which is the synthetic folate that is used for vitamin supplements and grain fortification (Wald *et al.*, 2018). The affinity of FOLR1 for folic acid is 14-fold higher than for the serum folate 5-methyl-THF (Leamon et al., 2009).

FOLR2 is expressed in activated M2 macrophages, which are anti-inflammatory/regulatory, but not in M1 macrophages, which are pro-inflammatory (Puig-Kroger et al., 2009). The role of FOLR2 expression in activated M2 macrophages is not known.

Non-canonical signaling roles of folates in non-mammals

There are three examples of potential non-canonical folate signaling in non-mammalian species.

Dictyostelium folate signaling through a G-protein coupled receptor

Dictyostelium discoideum is a type of soil amoeba that live as single cells, but in response to starvation, they form multicellular aggregates that form fruiting bodies, which release spores. As single cells, *D. discoideum* eat bacteria, and they chemotax toward bacteria based on the detection of folates and pterins that are released from the bacteria (Janssens and Van Haastert, 1987). The *D. discoideum* cell surface receptor for folates/pterins is an orphan G-protein-coupled receptor (GPCR) (Pan et al., 2016); and thus differs from the FOLR-directed signaling pathways proposed in animals.

Caenorhabditis elegans folate signaling through FOLR-1

C. elegans is a small roundworm that lives in the soil and eats bacteria. In *C. elegans*, 10-formyl-THF and dihydropteroate (which is a pteroate, structurally similar to folates but lack Glu) act as signals to increase the rate of germ stem cell proliferation (Chaudhari et al., 2016). Three lines of evidence indicate that 10-formyl-THF acts as a signal, rather than through metabolism. First, the stimulation of germ cell proliferation requires FOLR-1, which is not required to provide folates for metabolism (that is the role of RFC). Second, other folates can rescue folate deficiency better than 10-formyl-THF but are unable to increase the basal rate of germ cell proliferation, thereby

decoupling a role in metabolism from the stimulatory role. Third, a ligand that cannot function in metabolism (a pteroate) can stimulate the FOLR-1 pathway.

A potential non-canonical role for FOLR1 in Xenopus

In *Xenopus* neural tube closure, the apical surface constricts to induce the curvature that shapes the neural tube. FOLR1 is localized to the apical surface and is required for the constriction of the neural plate (Balashova et al., 2017). FOLR1 physically interacts with C-cadherin and β-catenin, which are components of adherens junctions (Balashova *et al.*, 2017). FOLR1 is required for the endocytosis of C-cadherin from the apical surface, which facilitates the constriction of the apical surface (Balashova *et al.*, 2017). The physical interaction of FOLR1 with C-cadherin suggests that FOLR1 may directly mediate the endocytosis of C-cadherin endocytosis, which would be a non-metabolic role in regulating adherens junctions.

FOLR overexpression and linkage to cancer progression

FOLR1 is overexpressed in many cancers of epithelial origin. A broad survey of FOLR1 protein (Parker et al., 2005), along with more targeted surveys, have identified the human cancers that have increased FOLR-1 expression relative to normal tissues (Table 1). Among the highest levels of overexpression of FOLR1 are cancers of the female reproductive tissues – the ovary and uterus (Table 1). Significant overexpression of FOLR1 is also observed in brain carcinomas (Parker *et al.*, 2005). FOLR1 overexpression is associated with metastasis of pancreatic carcinomas and lymphomas relative to non-metastatic cancers in those tissues (Parker *et al.*, 2005).

Two mechanisms have been described for how FOLR1 is overexpressed in ovarian cancer. One third of ovarian cancers were found to amplify the genomic region containing FOLR1, and this correlated with increased mRNA levels (Siu et al., 2012). A second mechanism involves

caveolin-1 (CAV1), which functions in caveolae-mediated endocytosis. CAV1 has an antagonistic transcriptional relationship with FOLR1 in ovarian cancer cells. Overexpressing FOLR1 reduces *CAV1* expression in ovarian cancer cell lines, and overexpression of CAV1 reduces *FOLR1* expression (Bagnoli et al., 2000). Ovarian cancer cells have reduced CAV1 expression and increased FOLR1 expression (Bagnoli *et al.*, 2000). Thus, a reduction in CAV1 expression could have increased FOLR1 expression or the increase in FOLR1 expression could have reduced CAV1 expression.

Multiple studies have been conducted to determine the association between FOLR1 and cancer progression or reduced patient survival. A meta-analysis assessing the effect of FOLR1 overexpression on patient survival has reported that breast cancers with high FOLR1 expression had a **hazard ratio (HR)** (see Glossary) of 2.66 for **disease-free survival (DFS)** and a HR of 2.71 for **overall survival (OS)** (Liu et al., 2020). This indicates that FOLR1 overexpression in breast cancer results in a 2.71-fold higher likelihood of patient death. Uterine endometrial cancer had a HR of 1.3 for DFS and 1.72 for OS, indicating a 72% increased likelihood of patient death (Liu *et al.*, 2020). There was no statistical increase in DFS or OS for ovarian and lung cancers (Liu *et al.*, 2020). However, a caveat is that because such a high percentage of ovarian cancers express FOLR1 (Table 1) comparisons between FOLR1 overexpressing and non-expressing cells are not as relevant.

Despite the lack of correlation of FOLR1 expression with patient survival for all types of ovarian cancer (Despierre et al., 2013; Kalli et al., 2008; Liu *et al.*, 2020; Yuan et al., 2009), higher expression of FOLR1 is observed in ovarian cancers with higher histologic grades, more advanced stages, increased aneuploidy, a higher percentage of S phase cells, and higher resistance to chemotherapy – all markers of cancer progression (Chen et al., 2012; Kurosaki et al., 2016; Siu *et*

al., 2012; Toffoli, 1998). Patients with serous ovarian carcinomas with higher FOLR1 expression levels had increased HRs for DFS (2.77) and OS (4.76) (Chen *et al.*, 2012). Additionally, inhibition of FOLR1 in ovarian cancer cells reduced the cancer attributes of cell proliferation, growth in soft agar, and cell migration and invasiveness (Figini et al., 2003; Siu *et al.*, 2012).

The overexpression of FOLR2 has been reported in the placenta, mature neutrophils, and in more than 50% of all myelogenous leukemias (Ross et al., 1994; Wang et al., 2000). When considering solid tumors, higher FOLR2 expression is often associated with cells in the stroma, which primarily reflects the presence of activated macrophages (Puig-Kroger *et al.*, 2009). A careful analysis of anti-FOLR2 staining in the stroma vs. in cancer cells found that nearly 25% of cancer samples express FOLR2, primarily in malignancies of the lung, liver, skin, kidney, and soft tissue, but not in cancers of the head and neck, prostate, and colon (Shen et al., 2015) (Table1). The expression of FOLR2 did not correlate with the stage of cancer, size of tumors, or involvement of lymph nodes (Shen *et al.*, 2015).

Indirect evidence that FOLR1 functions independently of metabolism

FOLR1 could promote cancer by providing increased levels of folates for one-carbon metabolism. However, even when FOLR1 is overexpressed, it generally transports less folate into cells than RFC. In five ovarian cancer cell lines (including SKOV-3), FOLR1 only contributes ~20% of the uptake of the serum folate 5-methyl-THF, while RFC is responsible for ~70% of the uptake (Corona et al., 1998).

In SKOV-3 cells, FOLR1 *knockdown* reduced cell proliferation, migration, and invasiveness, implying that FOLR1 expression promotes these cancer attributes (Siu *et al.*, 2012). Surprisingly, the *overexpression* of RFC had a similar effect in reducing cell proliferation, migration, and invasiveness. This suggests that FOLR1 expression promotes cancer progression while RFC

expression inhibits cancer progression (despite both overexpressions presumably increasing folate uptake). This suggests that increasing folate uptake is not as relevant as which transporter is overexpressed. However, a caveat is that the study was carried out with folic acid as the sole source of folate. RFC is very inefficient at transporting folic acid (Zhao *et al.*, 2011), and when folic acid is provided at low, physiological levels, FOLR1 may transport the majority of the folic acid. Hence, it is possible that the reduction of cancer attributes associated with FOLR1 knockdown resulted from a lack of folates for metabolism.

Additional evidence that suggests FOLR1 acts independently of metabolism is that the proliferation of erythropoietic cells is significantly increased by incubation with anti-FOLR1 antibodies (Antony et al., 1987). The binding of antibodies to cell surface receptors can, in many instances, activate signaling independently of ligand binding. This particular anti-FOLR1 antibody prevents folate from binding to FOLR1 (Antony *et al.*, 1987) suggesting that the stimulation of erythropoiesis was independent of folate transport.

Signaling pathways linked to FOLR1

In this section, we will describe the different signaling pathways that implicate a direct role for FOLR1 in signaling. Our assessment of whether the data supports a non-canonical role for FOLR1 relies on the physical interaction of FOLR1 with signaling components and how rapidly signaling events occur after folate stimulation. Short time frames would suggest a direct effect on signaling rather than a consequence of changes in the levels of amino acids or nucleotides that are generated by one-carbon metabolism.

Currently, for many potential published pathways there is insufficient evidence to infer direct regulation by folate vs. secondary consequences of changes in metabolism or the effects of other signaling pathways. Potential pathways for FOLR1 and FOLR2 that fall in this category and will

not be discussed include a potential FOLR2 pathway linked to AKT and ribosomal S6 kinase (Xu et al., 2018), potential FOLR1 pathways linked to Wnt (Yang et al., 2021), TGFβ (Warner et al., 2011), and NOTCH3 and FGFR1 (Yao et al., 2009). Other folate-linked signaling pathways where the transporter was not defined include mTor (Pan et al., 2017; Silva et al., 2017), Hedgehog (Wang et al., 2012), AKT (Hwang et al., 2015), and GSK-3β (Budni et al., 2018) signaling.

The concentration of folates used in the experiments can be important. Certain studies use excessive, supraphysiological folate concentrations to stimulate cells. Excessive folate levels can potentially induce non-physiological cellular responses. We are mindful that when trying to detect rapid readouts of intracellular signaling pathways (e.g., phosphorylation of signaling proteins), it is often helpful to transiently use a pulse of ligand at high concentration. However, ideally, this would be combined with experiments using lower, physiological concentrations to follow the normal functioning of the pathway.

When considering experiments on potential signaling pathways it is important to consider the level of folate in the cell culture conditions, as tissue culture media contain a wide range of folic acid concentrations (e.g., 0 nM for folate-free RPMI to 9.1 μM for DMEM). The use of too low folate concentrations could make cells reliant on FOLR1 (rather than RFC) to obtain folates for one-carbon metabolism due to its high-affinity binding of folates. Studies have used folate-free medium supplemented with 5% FBS, which would suggest that the level of folate was only ~5% of the physiological level. Conversely, studies have used high-folate culture medium with 9.1 μM of folic acid then stimulated cells with only 1 μM folic acid.

JAK–STAT3 signaling

The JAK–STAT3 pathway is often activated in epithelium-derived cancers, where it promotes proliferation and is associated with poor patient prognosis (Jarnicki et al., 2010). Three laboratories have reported that folate induces the activation of the JAK–STAT3 signaling pathway leading to the activation of the STAT3 transcription factor (Table 2) (Fig. 2.2). Folic acid induces the activating phosphorylation of STAT3 within 5 min in HeLa cells (Hansen et al., 2015), and within 30 min in mouse neural precursor cells (Su et al., 2018). Folic acid also increases the steady-state levels of phospho-STAT3 in mouse embryonic stem cells (Wei et al., 2017). The fast activation (within 5 min) suggests a non-metabolic pathway. Downstream STAT3-inducible genes are activated in response to the folic acid stimulation (Hansen *et al.*, 2015). FOLR1 co-immunoprecipitates (co-IP) with the gp130 co-receptor that binds JAK, suggesting a direct linkage between folate binding by FOLR1 and the initiation of the signaling pathway (Hansen *et al.*, 2015; Su *et al.*, 2018) (Fig. 2.2).

The linkage between FOLR1 and STAT3 activation was also demonstrated in a mouse breast cancer model. Breast cancers were induced in mice by expressing polyoma virus middle T oncogenic protein in mammary epithelium, and the resulting tumors overexpress FOLR1 and have increased levels of phospho-STAT3 (Hansen et al., 2017). Feeding the mice a diet high in folic acid caused a doubling of tumor mass, demonstrating that only a five-fold increase in dietary folic acid can promote tumor growth *in vivo*.

The very high levels of folic acid that were used to induce phospho-STAT3 raises the question of the physiological relevance of the pathway. The concentration of folic acid added to HeLa cells was 567–1360 μM, which is >18,000-fold higher than the median concentration of serum folate in the fortified US population (26 to 31 nM) (Pfeiffer et al., 2007). Stimulation with

1134 µM folic acid in neural precursor cells produced substantially more phospho-STAT3 than stimulation with 453 µM, suggesting that the pathway is not saturated at 453 µM (Su *et al.*, 2018). This does not match the expectation of FOLR1 initiating the pathway because FOLR1 has a K_D for binding folic acid (~0.1 nM) that is 4.5 million-fold lower than 453 µM (Leamon *et al.*, 2009). With such a low K_D, one would expect that FOLR1 binding to folic acid would be saturated at 453 µM, so that further increases would not impact STAT3 activation. This leads to the question of whether FOLR1 is required for the induction of phospho-STAT3. Two FOLR1 knockdown experiments showed either a normal increase of phospho-STAT3 in response to folic acid (despite FOLR1 knockdown to undetectable levels) or a reduced but still significant increase of phospho-STAT3 (Hansen *et al.*, 2015). This suggests that FOLR1 may not be essential for the activation of the JAK–STAT3 pathway.

ERK1/2 signaling

There are multiple papers from several labs that describe FOLR1 promoting signaling that involves the serine/threonine kinase ERK (MAP kinase). The canonical ERK1/2 pathway involves receptor tyrosine kinases that activate the small GTPase protein RAS, which then leads to the sequential phospho-activations of the serine/threonine kinases RAF, MEK, and ERK1/2 (Lavoie et al., 2020). This pathway is often activated in cancer, where it increases cell proliferation and migration (Lavoie *et al.*, 2020). There are other pathways that activate ERK1/2, including a pathway that involves involves the SRC tyrosine kinase (Lavoie *et al.*, 2020).

FOLR1/PGR/SRC/ERK/IκB-α/NF-κB/p53/p21 & p27

Several papers from the Lee laboratory describe a signaling pathway for FOLR1 that includes the progesterone receptor (PGR) and SRC (Kuo et al., 2015; Kuo and Lee, 2016; Lin et al., 2012; Ting et al., 2019; Wang et al., 2020) (Table 2) (Fig. 2.3A). After addition of 10 µM folic acid, FOLR1

is shown to physically associate with PGR, the estrogen receptor (ESR2), and SRC in primary endothelial **HUVEC cells** (Lee et al., 2018; Lin *et al.*, 2012), and with PGR but not SRC in the COLO-205 colon cancer cell line (although PGR independently interacts with SRC) (Kuo and Lee, 2016). The data infers the downstream pathway of activated phospho-SRC inducing the phospho-activation of ERK1/2, which phosphorylates IκB-α to release the NF-κB transcription factor, which translocates to the nucleus where it induces the expression of the tumor suppressor p53 transcription factor. p53 then induces the expression of the CDK-inhibitors $p21^{CIP1}$ and $p27^{KIP1}$, which bind cyclin-dependent kinases (CDKs) to inhibit cell cycle progression (Fig. 2.3A). The pathway also inhibits cell migration and invasiveness (Ting *et al.*, 2019). FOLR1 is required for the folic acid-induced increase in phospho-SRC and p53 levels (Kuo *et al.*, 2015; Lin *et al.*, 2012). Phosphorylation of ERK1/2 and SRC is observed only 2 min after addition of folic acid (Kuo *et al.*, 2015; Kuo and Lee, 2016; Lin *et al.*, 2012; Ting *et al.*, 2019; Wang *et al.*, 2020). Partial inhibition of cell proliferation is observed at 0.1 μM folic acid, which is closer to physiological levels.

The pathway with FOLR1, PGR, and SRC is also present in breast cancer cell lines (Wang *et al.*, 2020). However, in this context, folic acid promotes cell proliferation and migration. Intracellular signaling pathways are often utilized for different functional outcomes depending on the tissue. With breast cancer, the ERK1/2 signaling pathway promotes cancer attributes, consistent with FOLR1 overexpression worsening breast cancer outcomes (Liu *et al.*, 2020). With colon cancer, the ERK1/2 signaling pathway inhibits cancer attributes, consistent with FOLR1 protecting against colon cancer in a mouse model (Ma et al., 2005).

FOLR1/MEK/ERK/TSLC1

Z. Liu et al., 2017, described a different FOLR1 and ERK1/2 pathway in the nasopharyngeal cancer cell line HONE1 (Liu et al., 2017b) (Fig. 2.3B). Folic acid at 10 μM induces an increase in phospho-MEK and phospho-ERK1/2 levels in 10 min (Liu *et al.*, 2017b). FOLR1 is required for the folic acid-induced increase in phospho-ERK1/2 levels, and the inhibition of cell proliferation, migration, and invasiveness (Liu *et al.*, 2017b). The pathway is associated with increased transcription of the tumor suppressor TSLC1 (Liu *et al.*, 2017b), which is downregulated or inactivated in 87% of nasopharyngeal tumors (Lung et al., 2006). The inhibition of cell proliferation by this pathway is consistent with a study that showed that increased dietary folate prevents nasopharyngeal cancer (Zeng et al., 2016).

FOLR1/ERK/FOS–JUN

C. Liu et al., 2017, described a correlation between FOLR1, ERK1/2, and the FOS–JUN (c-Fos–c-Jun) transcription complex and cervical cancer (Liu et al., 2017a) (Fig. 2.3C). A correlation was observed between increasing severity of cervical lesions and increased expression of FOLR1, phospho-ERK1/2, phospho-FOS, and phospho-JUN (Fig. 2.3C). FOS and JUN are proto-oncogenes that together form the transcription factor AP-1, which promotes cell proliferation and cancer (Eferl and Wagner, 2003). The phosphorylation of FOS and JUN by ERK1/2 is known to increase AP-1 activity (Eferl and Wagner, 2003).

FOLR1/ERK/FOS–JUN/Survivin

Zhang et al., 2019, described a correlation between FOLR1, ERK1/2, FOS and JUN, and the apoptosis inhibitor Survivin (BIRC5) in promoting endometrial carcinomas (Zhang et al., 2019). An analysis of endometrial carcinoma samples showed a strong correlation with increasing pathological grade and increased expression of FOLR1, phospho-ERK1/2, and Survivin. ERK1/2

is known to induce the expression of Survivin in other cells (Cao et al., 2011). Inactivation of FOLR1 in the endometrial carcinoma cell line KLE reduced the steady-state levels of phospho-ERK1/2, phospho-JUN, phospho-FOS, and Survivin, and increased apoptosis.

FOLR1 interaction with LYN and $G\alpha_{i-3}$

An analysis of the IGROV1 ovarian cancer cell line found FOLR1 in the detergent-resistant membrane fraction (indicative of lipid rafts) along with several SRC-family tyrosine kinases, and GPCR components (Miotti et al., 2000). FOLR1 and the SRC-family member LYN reciprocally co-IP with each other along with the trimeric GPCR subunit $G\alpha_{i-3}$, suggesting physical interactions within lipid rafts. Adding anti-FOLR1 antibody to the cells reduced the amount of both FOLR1 and LYN in the detergent-resistant membrane fraction, suggesting that FOLR1 affects LYN localization. The functional impact of the interaction of FOLR1 with LYN and $G\alpha_{i-3}$ was not assessed.

FOLR1 as a transcription factor

The Mayanil lab published three papers in which FOLR1 acts as a transcription factor that translocates from the cytoplasm to the nucleus, where it directly regulates gene expression (Boshnjaku et al., 2012; Mohanty et al., 2016; Monick et al., 2019) (Table 2) (Fig. 2.4). Two FOLR1 isoforms of 42 and 38 kDa are initially localized to the cytoplasm. The 38 kDa isoform undergoes folate-regulated nuclear localization 15–30 min after stimulation with 453 µM folic acid in the human medulloblastoma cell line DAOY, and with 22 nM of 5-methyl-THF in the mouse neural crest cell line O9-1 (Boshnjaku *et al.*, 2012; Monick *et al.*, 2019). The effect of the 22 nM 5-methyl-THF is surprising, as the experiment appears to be performed in the context of a medium based on DMEM, which has 9.1 µM folic acid (although the medium was pre-conditioned by

incubation with STO feeder cells (Ishii et al., 2012), which might have removed some folic acid). The nuclear localization of FOLR1 has been previously reported as localization to the nuclear envelope in murine Müller retinal cells (Bozard et al., 2010); however, TEM images in that publication suggest there is also localization to the nucleoplasm (see their Fig. 5C).

The Mayanil lab used a candidate gene approach to identify six genes whose transcription is increased by FOLR1 (Boshnjaku *et al.*, 2012; Mohanty *et al.*, 2016). FOLR1 was shown to bind the regulatory regions of *OCT14*, *SOX2*, and *KLF4* within 15–30 min of stimulation with folic acid (Mohanty *et al.*, 2016). FOLR1 is proposed to bind to AANTT DNA sequences based on in vitro binding and electrophoretic mobility shift assay (Boshnjaku *et al.*, 2012; Mohanty *et al.*, 2016). AANTT has too little information to direct specific binding for a monomeric FOLR1. Most transcription factors increase DNA-binding specificity either by homomeric association or interaction with other DNA-binding proteins, and presumably FOLR1 would use a similar strategy to increase binding specificity.

The Mayanil lab reported that the 38 kDa isoform of FOLR1 physically bound to chromatin assembly factor 1 subunit A (CHAF1A, CAF-1) and the microRNA processing Drosha–DGCR8 complex (Mohanty *et al.*, 2016; Monick *et al.*, 2019). FOLR1 was proposed to act as an inhibitor of both CAF-1 and Drosha–DGCR8, but these scenarios were not directly tested.

Concluding Remarks

FOLR1 is overexpressed in many epithelium-derived cancers and has been associated with neoplastic progression and poor prognosis in a subset of these cancers. In several cancers, FOLR1 promotes proliferation, migration, and invasiveness. Emerging evidence suggests that these cancer attributes can result from signaling events that are initiated by folate and involve FOLR1.

FOLR1 is associated with a plethora of potential signaling pathways. While it is possible that FOLR1 is a jack-of-all trades that functions in multiple signaling pathways, it is also possible that some of the proposed pathways are not physiologically relevant. Several aspects of these pathways are not determined or are of potential concern (see Outstanding Questions). It is also possible that one or more of the pathways are activated in response to an upstream folate-responsive signaling pathway. For example, multiple signaling pathways can activate ERK1/2, which can then lead to the phospho-activation of STAT3 (Lavoie *et al.*, 2020).

The majority of the data supporting a role of FOLR1 in signaling comes from tissue culture studies. Idiosyncrasies among cell lines can sometimes lead to conclusions that do not reflect *in vivo* realities. When there are divergent tissue culture observations, it is often helpful to utilize studies with whole organisms to clarify *in vivo* pathways. Studies with mice could help to identify physiologically relevant pathways, and studies with invertebrate model organisms could identify evolutionarily-conserved pathways.

References

Antony, A.C., Bruno, E., Briddell, R.A., Brandt, J.E., Verma, R.S., and Hoffman, R. (1987). Effect of perturbation of specific folate receptors during in vitro erythropoiesis. J Clin Invest *80*, 1618-1623. 10.1172/JCI113249.

Bagnoli, M., Tomassetti, A., Figini, M., Flati, S., Dolo, V., Canevari, S., and Miotti, S. (2000). Downmodulation of caveolin-1 expression in human ovarian carcinoma is directly related to alpha-folate receptor overexpression. Oncogene *19*, 4754-4763. 10.1038/sj.onc.1203839.

Balashova, O.A., Visina, O., and Borodinsky, L.N. (2017). Folate receptor 1 is necessary for neural plate cell apical constriction during Xenopus neural tube formation. Development *144*, 1518-1530. 10.1242/dev.137315.

Bianchi, E., Doe, B., Goulding, D., and Wright, G.J. (2014). Juno is the egg Izumo receptor and is essential for mammalian fertilization. Nature *508*, 483-487. 10.1038/nature13203.

Boshnjaku, V., Shim, K.W., Tsurubuchi, T., Ichi, S., Szany, E.V., Xi, G., Mania-Farnell, B., McLone, D.G., Tomita, T., and Mayanil, C.S. (2012). Nuclear localization of folate receptor alpha: a new role as a transcription factor. Sci Rep *2*, 980. 10.1038/srep00980.

Bozard, B.R., Ganapathy, P.S., Duplantier, J., Mysona, B., Ha, Y., Roon, P., Smith, R., Goldman, I.D., Prasad, P., Martin, P.M., et al. (2010). Molecular and biochemical characterization of folate transport proteins in retinal Muller cells. Invest Ophthalmol Vis Sci *51*, 3226-3235. 10.1167/iovs.09-4833.

Budni, J., Molz, S., Dal-Cim, T., Martin-de-Saavedra, M.D., Egea, J., Lopez, M.G., Tasca, C.I., and Rodrigues, A.L.S. (2018). Folic Acid Protects Against Glutamate-Induced

Excitotoxicity in Hippocampal Slices Through a Mechanism that Implicates Inhibition of GSK-3beta and iNOS. Mol Neurobiol *55*, 1580-1589. 10.1007/s12035-017-0425-6.

Cao, W., Xie, Y.H., Li, X.Q., Zhang, X.K., Chen, Y.T., Kang, R., Chen, X., Miao, S., and Wang, S.W. (2011). Burn-induced apoptosis of cardiomyocytes is survivin dependent and regulated by PI3K/Akt, p38 MAPK and ERK pathways. Basic Res Cardiol *106*, 1207-1220. 10.1007/s00395-011-0199-3.

Chaudhari, S.N., Mukherjee, M., Vagasi, A.S., Bi, G., Rahman, M.M., Nguyen, C.Q., Paul, L., Selhub, J., and Kipreos, E.T. (2016). Bacterial Folates Provide an Exogenous Signal for C. elegans Germline Stem Cell Proliferation. Dev Cell *38*, 33-46. 10.1016/j.devcel.2016.06.013.

Chen, Y.L., Chang, M.C., Huang, C.Y., Chiang, Y.C., Lin, H.W., Chen, C.A., Hsieh, C.Y., and Cheng, W.F. (2012). Serous ovarian carcinoma patients with high alpha-folate receptor had reducing survival and cytotoxic chemo-response. Mol Oncol *6*, 360-369. 10.1016/j.molonc.2011.11.010.

Corona, G., Giannini, F., Fabris, M., Toffoli, G., and Boiocchi, M. (1998). Role of folate receptor and reduced folate carrier in the transport of 5-methyltetrahydrofolic acid in human ovarian carcinoma cells. Int J Cancer *75*, 125-133.

Despierre, E., Lambrechts, S., Leunen, K., Berteloot, P., Neven, P., Amant, F., O'Shannessy, D.J., Somers, E.B., and Vergote, I. (2013). Folate receptor alpha (FRA) expression remains unchanged in epithelial ovarian and endometrial cancer after chemotherapy. Gynecol Oncol *130*, 192-199. 10.1016/j.ygyno.2013.03.024.

Eferl, R., and Wagner, E.F. (2003). AP-1: a double-edged sword in tumorigenesis. Nat Rev Cancer *3*, 859-868. 10.1038/nrc1209.

Elnakat, H., and Ratnam, M. (2004). Distribution, functionality and gene regulation of folate receptor isoforms: implications in targeted therapy. Adv Drug Deliv Rev *56*, 1067-1084. 10.1016/j.addr.2004.01.001.

Figini, M., Ferri, R., Mezzanzanica, D., Bagnoli, M., Luison, E., Miotti, S., and Canevari, S. (2003). Reversion of transformed phenotype in ovarian cancer cells by intracellular expression of anti folate receptor antibodies. Gene Ther *10*, 1018-1025. 10.1038/sj.gt.3301962.

Grapp, M., Wrede, A., Schweizer, M., Huwel, S., Galla, H.J., Snaidero, N., Simons, M., Buckers, J., Low, P.S., Urlaub, H., et al. (2013). Choroid plexus transcytosis and exosome shuttling deliver folate into brain parenchyma. Nat Commun *4*, 2123. 10.1038/ncomms3123.

Hansen, M.F., Greibe, E., Skovbjerg, S., Rohde, S., Kristensen, A.C., Jensen, T.R., Stentoft, C., Kjaer, K.H., Kronborg, C.S., and Martensen, P.M. (2015). Folic acid mediates activation of the pro-oncogene STAT3 via the Folate Receptor alpha. Cell Signal *27*, 1356-1368. 10.1016/j.cellsig.2015.03.020.

Hansen, M.F., Jensen, S.O., Fuchtbauer, E.M., and Martensen, P.M. (2017). High folic acid diet enhances tumour growth in PyMT-induced breast cancer. Br J Cancer *116*, 752-761. 10.1038/bjc.2017.11.

Henderson, G.I., Perez, T., Schenker, S., Mackins, J., and Antony, A.C. (1995). Maternal-to-fetal transfer of 5-methyltetrahydrofolate by the perfused human placental cotyledon: evidence for a concentrative role by placental folate receptors in fetal folate delivery. J Lab Clin Med *126*, 184-203.

Holm, J., and Hansen, S.I. (2020). Characterization of soluble folate receptors (folate binding proteins) in humans. Biological roles and clinical potentials in infection and malignancy. Biochim Biophys Acta Proteins Proteom *1868*, 140466. 10.1016/j.bbapap.2020.140466.

Hwang, S.Y., Kang, Y.J., Sung, B., Kim, M., Kim, D.H., Lee, Y., Yoo, M.A., Kim, C.M., Chung, H.Y., and Kim, N.D. (2015). Folic acid promotes the myogenic differentiation of C2C12 murine myoblasts through the Akt signaling pathway. Int J Mol Med *36*, 1073-1080. 10.3892/ijmm.2015.2311.

Ishii, M., Arias, A.C., Liu, L., Chen, Y.B., Bronner, M.E., and Maxson, R.E. (2012). A stable cranial neural crest cell line from mouse. Stem Cells Dev *21*, 3069-3080. 10.1089/scd.2012.0155.

Janssens, P.M., and Van Haastert, P.J. (1987). Molecular basis of transmembrane signal transduction in Dictyostelium discoideum. Microbiol Rev *51*, 396-418. 10.1128/mr.51.4.396-418.1987.

Jarnicki, A., Putoczki, T., and Ernst, M. (2010). Stat3: linking inflammation to epithelial cancer - more than a "gut" feeling? Cell Div *5*, 14. 10.1186/1747-1028-5-14.

Jia, Z., Zhao, R., Tian, Y., Huang, Z., Tian, Z., Shen, Z., Wang, Q., Wang, J., Fu, X., and Wu, Y. (2009). A novel splice variant of FR4 predominantly expressed in CD4+CD25+ regulatory T cells. Immunol Invest *38*, 718-729. 10.3109/08820130903171003.

Kalli, K.R., Oberg, A.L., Keeney, G.L., Christianson, T.J., Low, P.S., Knutson, K.L., and Hartmann, L.C. (2008). Folate receptor alpha as a tumor target in epithelial ovarian cancer. Gynecol Oncol *108*, 619-626. 10.1016/j.ygyno.2007.11.020.

Kuo, C.T., Chang, C., and Lee, W.S. (2015). Folic acid inhibits COLO-205 colon cancer cell proliferation through activating the FRalpha/c-SRC/ERK1/2/NFkappaB/TP53 pathway: in vitro and in vivo studies. Sci Rep *5*, 11187. 10.1038/srep11187.

Kuo, C.T., and Lee, W.S. (2016). Progesterone receptor activation is required for folic acid-induced anti-proliferation in colorectal cancer cell lines. Cancer Lett *378*, 104-110. 10.1016/j.canlet.2016.05.019.

Kurosaki, A., Hasegawa, K., Kato, T., Abe, K., Hanaoka, T., Miyara, A., O'Shannessy, D.J., Somers, E.B., Yasuda, M., Sekino, T., and Fujiwara, K. (2016). Serum folate receptor alpha as a biomarker for ovarian cancer: Implications for diagnosis, prognosis and predicting its local tumor expression. Int J Cancer *138*, 1994-2002. 10.1002/ijc.29937.

Lavoie, H., Gagnon, J., and Therrien, M. (2020). ERK signalling: a master regulator of cell behaviour, life and fate. Nat Rev Mol Cell Biol *21*, 607-632. 10.1038/s41580-020-0255-7.

Leamon, C.P., You, F., Santhapuram, H.K., Fan, M., and Vlahov, I.R. (2009). Properties influencing the relative binding affinity of pteroate derivatives and drug conjugates thereof to the folate receptor. Pharm Res *26*, 1315-1323. 10.1007/s11095-009-9840-3.

Lee, W.S., Lu, Y.C., Kuo, C.T., Chen, C.T., and Tang, P.H. (2018). Effects of female sex hormones on folic acid-induced anti-angiogenesis. Acta Physiol (Oxf) *222*, e13001. 10.1111/apha.13001.

Lin, S.Y., Lee, W.R., Su, Y.F., Hsu, S.P., Lin, H.C., Ho, P.Y., Hou, T.C., Chou, Y.P., Kuo, C.T., and Lee, W.S. (2012). Folic acid inhibits endothelial cell proliferation through activating the cSrc/ERK 2/NF-kappaB/p53 pathway mediated by folic acid receptor. Angiogenesis *15*, 671-683. 10.1007/s10456-012-9289-6.

Liu, C., Ding, L., Bai, L., Chen, X., Kang, H., Hou, L., and Wang, J. (2017a). Folate receptor alpha is associated with cervical carcinogenesis and regulates cervical cancer cells growth by activating ERK1/2/c-Fos/c-Jun. Biochem Biophys Res Commun *491*, 1083-1091. 10.1016/j.bbrc.2017.08.015.

Liu, Y., Lian, T., and Yao, Y. (2020). A systematic review and meta-analysis of higher expression of folate receptor alpha (FOLR1) predicts poor cancer prognosis. Biomarkers *25*, 367-374. 10.1080/1354750X.2020.1771420.

Liu, Z., Jin, X., Pi, W., and Liu, S. (2017b). Folic acid inhibits nasopharyngeal cancer cell proliferation and invasion via activation of FRalpha/ERK1/2/TSLC1 pathway. Biosci Rep *37*. 10.1042/BSR20170772.

Lung, H.L., Cheung, A.K., Xie, D., Cheng, Y., Kwong, F.M., Murakami, Y., Guan, X.Y., Sham, J.S., Chua, D., Protopopov, A.I., et al. (2006). TSLC1 is a tumor suppressor gene associated with metastasis in nasopharyngeal carcinoma. Cancer Res *66*, 9385-9392. 10.1158/0008-5472.CAN-06-0590.

Ma, D.W., Finnell, R.H., Davidson, L.A., Callaway, E.S., Spiegelstein, O., Piedrahita, J.A., Salbaum, J.M., Kappen, C., Weeks, B.R., James, J., et al. (2005). Folate transport gene inactivation in mice increases sensitivity to colon carcinogenesis. Cancer Res *65*, 887-897.

Miotti, S., Bagnoli, M., Tomassetti, A., Colnaghi, M.I., and Canevari, S. (2000). Interaction of folate receptor with signaling molecules lyn and G(alpha)(i-3) in detergent-resistant complexes from the ovary carcinoma cell line IGROV1. J Cell Sci *113 Pt 2*, 349-357.

Mohanty, V., Shah, A., Allender, E., Siddiqui, M.R., Monick, S., Ichi, S., Mania-Farnell, B., D, G.M., Tomita, T., and Mayanil, C.S. (2016). Folate Receptor Alpha Upregulates Oct4,

Sox2 and Klf4 and Downregulates miR-138 and miR-let-7 in Cranial Neural Crest Cells. Stem Cells *34*, 2721-2732. 10.1002/stem.2421.

Monick, S., Mohanty, V., Khan, M., Yerneni, G., Kumar, R., Cantu, J., Ichi, S., Xi, G., Singh, B.R., Tomita, T., and Mayanil, C.S. (2019). A Phenotypic Switch of Differentiated Glial Cells to Dedifferentiated Cells Is Regulated by Folate Receptor alpha. Stem Cells. 10.1002/stem.3067.

Pan, M., Xu, X., Chen, Y., and Jin, T. (2016). Identification of a Chemoattractant G-Protein-Coupled Receptor for Folic Acid that Controls Both Chemotaxis and Phagocytosis. Dev Cell *36*, 428-439. 10.1016/j.devcel.2016.01.012.

Pan, S., Lin, H., Luo, H., Gao, F., Meng, L., Zhou, C., Jiang, C., Guo, Y., Ji, Z., Chi, J., and Guo, H. (2017). Folic acid inhibits dedifferentiation of PDGF-BB-induced vascular smooth muscle cells by suppressing mTOR/P70S6K signaling. Am J Transl Res *9*, 1307-1316.

Parker, N., Turk, M.J., Westrick, E., Lewis, J.D., Low, P.S., and Leamon, C.P. (2005). Folate receptor expression in carcinomas and normal tissues determined by a quantitative radioligand binding assay. Anal Biochem *338*, 284-293. 10.1016/j.ab.2004.12.026.

Pfeiffer, C.M., Johnson, C.L., Jain, R.B., Yetley, E.A., Picciano, M.F., Rader, J.I., Fisher, K.D., Mulinare, J., and Osterloh, J.D. (2007). Trends in blood folate and vitamin B-12 concentrations in the United States, 1988 2004. Am J Clin Nutr *86*, 718-727. 10.1093/ajcn/86.3.718.

Puig-Kroger, A., Sierra-Filardi, E., Dominguez-Soto, A., Samaniego, R., Corcuera, M.T., Gomez-Aguado, F., Ratnam, M., Sanchez-Mateos, P., and Corbi, A.L. (2009). Folate receptor beta is expressed by tumor-associated macrophages and constitutes a marker for M2 anti-

inflammatory/regulatory macrophages. Cancer Res *69*, 9395-9403. 10.1158/0008-5472.CAN-09-2050.

Ross, J.F., Chaudhuri, P.K., and Ratnam, M. (1994). Differential regulation of folate receptor isoforms in normal and malignant tissues in vivo and in established cell lines. Physiologic and clinical implications. Cancer *73*, 2432-2443. 10.1002/1097-0142(19940501)73:9<2432::aid-cncr2820730929>3.0.co;2-s.

Selhub, J., Emmanouel, D., Stavropoulos, T., and Arnold, R. (1987). Renal folate absorption and the kidney folate binding protein. I. Urinary clearance studies. Am J Physiol *252*, F750-756.

Shen, J., Putt, K.S., Visscher, D.W., Murphy, L., Cohen, C., Singhal, S., Sandusky, G., Feng, Y., Dimitrov, D.S., and Low, P.S. (2015). Assessment of folate receptor-beta expression in human neoplastic tissues. Oncotarget *6*, 14700-14709. 10.18632/oncotarget.3739.

Silva, E., Rosario, F.J., Powell, T.L., and Jansson, T. (2017). mTOR Is a novel molecular mechanism linking folate availability and cell function. The Journal of Nutrition *147*, 1237-1242.

Siu, M.K., Kong, D.S., Chan, H.Y., Wong, E.S., Ip, P.P., Jiang, L., Ngan, H.Y., Le, X.F., and Cheung, A.N. (2012). Paradoxical impact of two folate receptors, FRalpha and RFC, in ovarian cancer: effect on cell proliferation, invasion and clinical outcome. PLoS One *7*, e47201. 10.1371/journal.pone.0047201.

Sivapalaratnam, S., Basart, H., Watkins, N.A., Maiwald, S., Rendon, A., Krishnan, U., Sondermeijer, B.M., Creemers, E.E., Pinto-Sietsma, S.J., Hovingh, K., et al. (2012). Monocyte gene expression signature of patients with early onset coronary artery disease. PLoS One *7*, e32166. 10.1371/journal.pone.0032166.

Su, L., Xia, W., Shen, T., Liang, Q., Wang, W., Li, H., and Jiao, J. (2018). H2A.Z.1 crosstalk with H3K56-acetylation controls gliogenesis through the transcription of folate receptor. Nucleic Acids Res *46*, 8817-8831. 10.1093/nar/gky585.

Ting, P.C., Lee, W.R., Huo, Y.N., Hsu, S.P., and Lee, W.S. (2019). Folic acid inhibits colorectal cancer cell migration. J Nutr Biochem *63*, 157-164. 10.1016/j.jnutbio.2018.09.020.

Toffoli, G., Russo, A., Gallo, A., Cernigoi, C., Miotti, S., Sorio, R., Tumolo, S., & Boiocchi, M. (1998). Expression of folate binding protein as a prognostic factor for response to platinum-containing chemotherapy and survival in human ovarian cancer. International Journal of Cancer *79*, 121-126.

Visentin, M., Diop-Bove, N., Zhao, R., and Goldman, I.D. (2014). The intestinal absorption of folates. Annu Rev Physiol *76*, 251-274. 10.1146/annurev-physiol-020911-153251.

Wald, N.J., Morris, J.K., and Blakemore, C. (2018). Public health failure in the prevention of neural tube defects: time to abandon the tolerable upper intake level of folate. Public Health Rev *39*, 2. 10.1186/s40985-018-0079-6.

Wang, H., Zheng, X., Behm, F.G., and Ratnam, M. (2000). Differentiation-independent retinoid induction of folate receptor type beta, a potential tumor target in myeloid leukemia. Blood *96*, 3529-3536.

Wang, H.C., Huo, Y.N., and Lee, W.S. (2020). Folic acid prevents the progesterone-promoted proliferation and migration in breast cancer cell lines. Eur J Nutr *59*, 2333-2344. 10.1007/s00394-019-02077-3.

Wang, T.P., Hsu, S.H., Feng, H.C., and Huang, R.F. (2012). Folate deprivation enhances invasiveness of human colon cancer cells mediated by activation of sonic hedgehog

signaling through promoter hypomethylation and cross action with transcription nuclear factor-kappa B pathway. Carcinogenesis *33*, 1158-1168. 10.1093/carcin/bgs138.

Warner, D.R., Webb, C.L., Greene, R.M., and Pisano, M.M. (2011). Altered signal transduction in Folr1-/- mouse embryo fibroblasts. Cell Biol Int *35*, 1253-1259. 10.1042/CBI20110025.

Wei, T., Jia, W., Qian, Z., Zhao, L., Yu, Y., Li, L., Wang, C., Zhang, W., Liu, Q., Yang, D., et al. (2017). Folic Acid Supports Pluripotency and Reprogramming by Regulating LIF/STAT3 and MAPK/ERK Signaling. Stem Cells Dev *26*, 49-59. 10.1089/scd.2016.0091.

Xu, X., Jiang, J., Yao, L., and Ji, B. (2018). Silencing the FOLR2 Gene Inhibits Cell Proliferation and Increases Apoptosis in the NCI-H1650 Non-Small Cell Lung Cancer Cell Line via Inhibition of AKT/Mammalian Target of Rapamycin (mTOR)/Ribosomal Protein S6 Kinase 1 (S6K1) Signaling. Med Sci Monit *24*, 8064-8073. 10.12659/MSM.911384.

Yang, H., Qin, D., Xu, S., He, C., Sun, J., Hua, J., and Peng, S. (2021). Folic acid promotes proliferation and differentiation of porcine pancreatic stem cells into insulin-secreting cells through canonical Wnt and ERK signaling pathway. J Steroid Biochem Mol Biol *205*, 105772. 10.1016/j.jsbmb.2020.105772.

Yao, C., Evans, C.O., Stevens, V.L., Owens, T.R., and Oyesiku, N.M. (2009). Folate receptor alpha regulates cell proliferation in mouse gonadotroph alphaT3-1 cells. Exp Cell Res *315*, 3125-3132. 10.1016/j.yexcr.2009.05.006.

Yuan, Y., Nymoen, D.A., Dong, H.P., Bjorang, O., Shih Ie, M., Low, P.S., Trope, C.G., and Davidson, B. (2009). Expression of the folate receptor genes FOLR1 and FOLR3 differentiates ovarian carcinoma from breast carcinoma and malignant mesothelioma in serous effusions. Hum Pathol *40*, 1453-1460. 10.1016/j.humpath.2009.02.013.

Zeng, F.F., Liu, Y.T., Lin, X.L., Fan, Y.Y., Zhang, X.L., Xu, C.H., and Chen, Y.M. (2016). Folate, vitamin B6, vitamin B12 and methionine intakes and risk for nasopharyngeal carcinoma in Chinese adults: a matched case-control study. Br J Nutr *115*, 121-128. 10.1017/S0007114515004146.

Zhang, J., Li, Y., Wang, L., Zhang, Y., Zhang, Q., and Liu, J. (2019). Folate receptor alpha promotes endometrial carcinoma cell proliferation and inhibits apoptosis by regulating the ERK signaling pathway. International Journal of Clinical and Experimental Medicine *12*, 8791-8979.

Zhao, R., Diop-Bove, N., Visentin, M., and Goldman, I.D. (2011). Mechanisms of membrane transport of folates into cells and across epithelia. Annu Rev Nutr *31*, 177-201. 10.1146/annurev-nutr-072610-145133.

Zhao, R., Min, S.H., Wang, Y., Campanella, E., Low, P.S., and Goldman, I.D. (2009). A role for the proton-coupled folate transporter (PCFT-SLC46A1) in folate receptor-mediated endocytosis. J Biol Chem *284*, 4267-4274. 10.1074/jbc.M807665200.

Zheng, Y., and Cantley, L.C. (2019). Toward a better understanding of folate metabolism in health and disease. J Exp Med *216*, 253-266. 10.1084/jem.20181965.

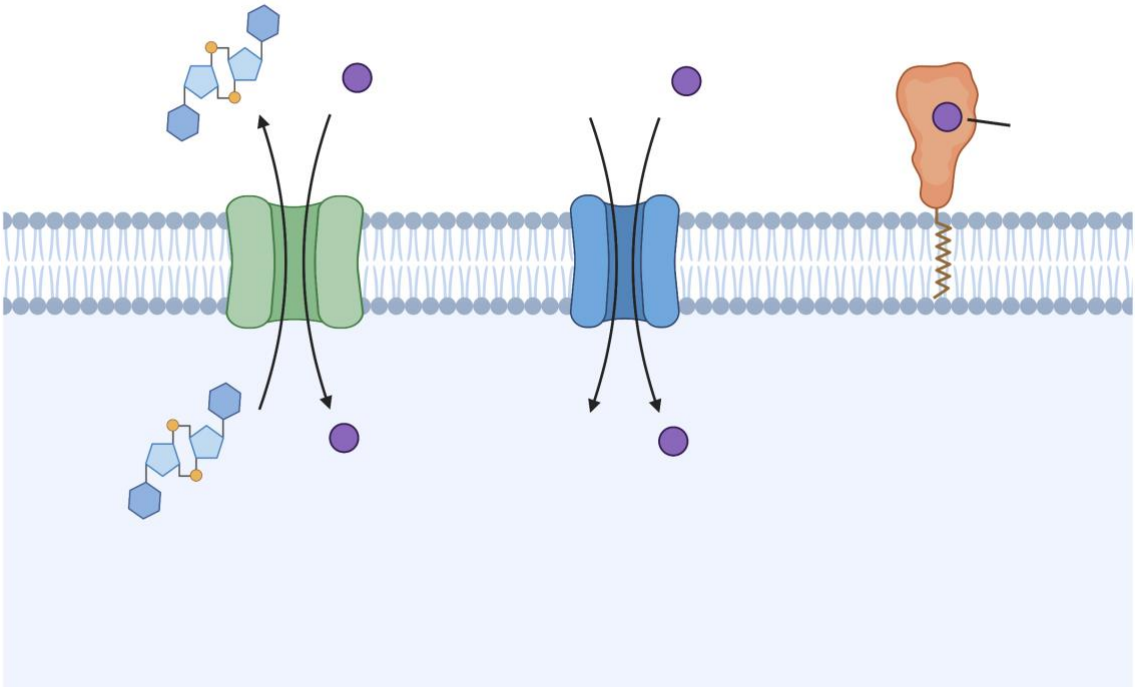

Figure. 2.1. The three types of folate transporters. Left) RFC (aka, the solute transport carrier SLC19A1) is an anion antiporter that uses a gradient of higher organic phosphate in the cell to transport folate into the cell while transporting organic phosphate out of the cell. The term "organic phosphate" refers to phosphate linked to organic molecules, and these can be relatively large molecules such as cyclic dinucleotides (Luteijn et al., 2019). **Middle)** PCFT (aka, SLC46A1) couples the transport of folates with protons (H^+) along the pH gradient from the lower pH environment of the lumen of the intestine to the higher pH within intestinal cells. PCFT also releases folate from acidified endosomes after the endocytosis of FOLRs. **Right)** FOLR1 and FOLR2 are high-affinity, low throughput transporters of folate. Each FOLR only binds one folate and brings the folate into cells via endocytosis of the FOLR–folate complex. The reliance on endocytosis to bring in a singly-bound folate ensures that this is a relatively slow, low-throughput transport mechanism. FOLR1 and 2 are linked to the plasma membrane by a carboxy terminal glycosylphosphatidylinositol (GPI) anchor. Figure created with BioRender.com.

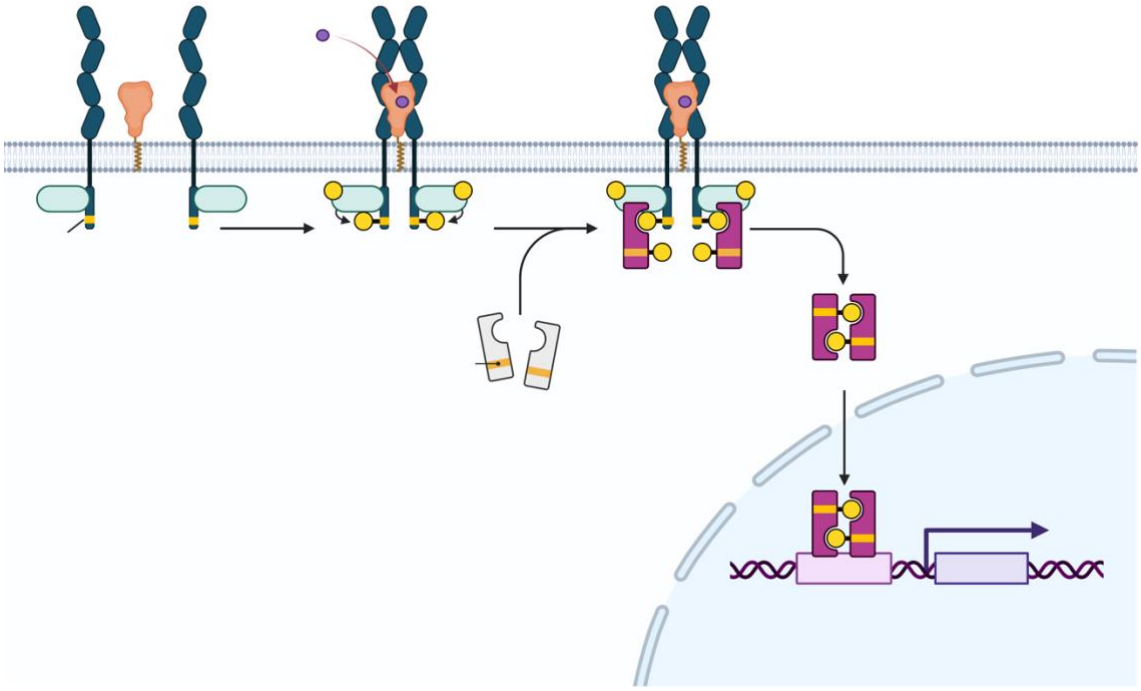

Figure. 2.2. Proposed role for FOLR1 in JAK–STAT3 signaling. JAK is the Janus kinase, a tyrosine kinase that associates with the intracellular domains of specific receptors (Jarnicki *et al.*, 2010). Ligand binding brings together two receptors (or co-receptors), the associated JAK then cross-phosphorylate the receptors, which allows two STAT3 proteins to bind the tyrosine-phosphorylated receptors, the STAT3 are subsequently phosphorylated by JAK. The two phospho-STAT3 dimerize and enter the nucleus where they function as transcription factors. In the proposed signaling pathway, the gp130 co-receptor, which is associated with JAK, binds to FOLR1. Folate binding would then bring two gp130 together to initiate the JAK–STAT3 pathway to generate phospho-STAT3 dimers, which act as transcription factors. Figure created with BioRender.com.

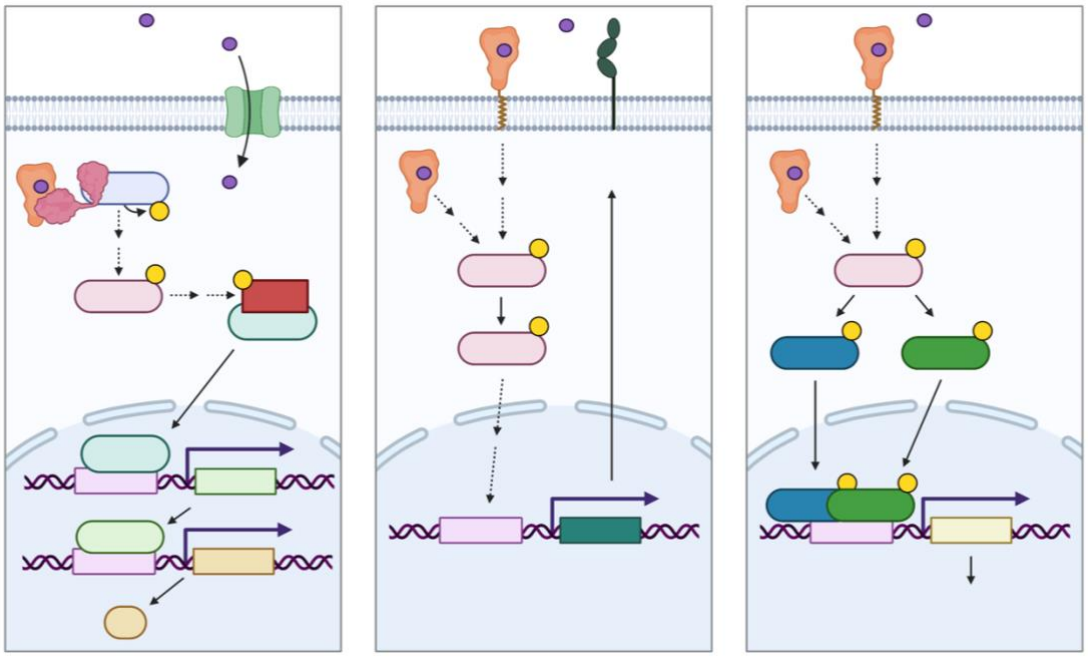

Figure. 2.3. Proposed roles for FOLR1 in ERK1/2 signaling. In the diagrams of proposed pathways, dashed-line double arrows indicate uncertainty in how a step is accomplished. **A)** Folate signaling through FOLR1–PGR–SRC. Folate is brought into the cell through RFC or plasma membrane-localized FOLR1. Cytoplasmic-localized FOLR1 (which may or may not have a GPI anchor, shown without) physically interacts with PGR. PGR interacts with both FOLR1 and SRC, either separately (Kuo and Lee, 2016) or in a trimeric complex (Lee *et al.*, 2018). SRC autophosphorylates to activate itself and promotes the phospho-activation of ERK1/2. Activated ERK1/2 phosphorylates IκB-α, releasing NF-κB to translocate to the nucleus and induce the transcription of p53, which induces the transcription of $p21^{CIP1}$. $p21^{CIP1}$ inhibits CDK–cyclin complexes to block cell cycle progression. **B)** FOLR1 signaling through MEK–ERK. It is not known if FOLR1 initiates this pathway from the plasma membrane or intracellularly. MEK is phospho-activated, and phospho–activates ERK1/2 (Liu *et al.*, 2017b).

Activated ERK1/2 induces transcription of *TSLC1* (aka cell adhesion molecule 1, *CADM1*), which acts on the plasma membrane to prevent cell proliferation. **C)** FOLR–ERK1/2 signaling through FOS and JUN. ERK1/2 phosphorylates FOS and JUN to promote their activity as a transcription factor (Liu *et al.*, 2017a). Figure created with BioRender.com.

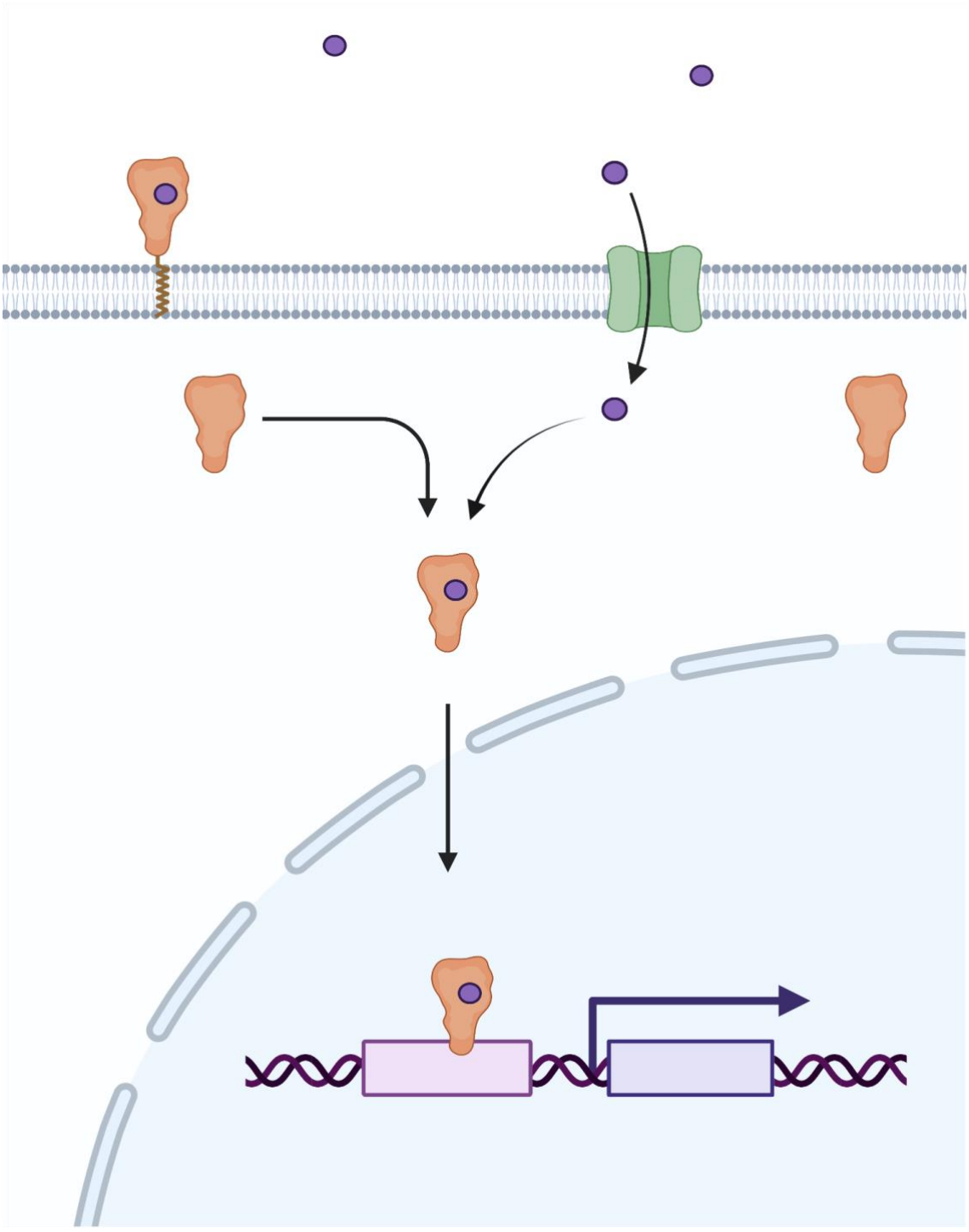

Figure. 2.4. Proposed role of FOLR1 as a transcription factor. Folate is brought into the cytoplasm either through the action of RFC or membrane-localized FOLR1. Cytoplasmic FOLR1 (which may or may not have the GPI anchor, shown without) binds folate and then translocates to the nucleus, where it functions as a transcription factor, directly binding gene regulatory regions. Figure created with BioRender.com.

Glossary

Disease-free survival (DFS): the length of time after primary treatment during which the patient does not show symptoms of cancer.

Hazard ratio (HR): a ratio of how often a particular deleterious event happens in one group compared to another group (generally the control group) over time. For example, a HR above 1 for DFS means that the analyzed group had less DFS (with less DFS being the deleterious event) than the control group.

HUVEC cells: primary human umbilical venous endothelial cells obtained from the umbilical cord.

Overall survival (OS): the length of time from either the date of diagnosis or the start of treatment that patients remain alive.

Table 2.1. Expression of FOLR1 and FOLR2 in different cancers

Tissue and cancer	Express high FOLR1 (%)	Reference	Ratio cancer/normal FOLR1 protein (Parker *et al.*, 2005)	Express FOLR2 (%) (Shen *et al.*, 2015)
Ovary				
Primary tumor	70%-100%	(Kalli *et al.*, 2008)		
Serous carcinoma	82%-100%	(Crane et al., 2012; Kalli *et al.*, 2008; Parker *et al.*, 2005)	22.3	50%
Endometrioid carcinoma	22%, 67%, 100%	(Crane *et al.*, 2012; Kalli *et al.*, 2008; Parker *et al.*, 2005)	10.2	
Mucinous carcinoma	0%, 22%, 55%	(Crane *et al.*, 2012; Kalli *et al.*, 2008; Parker *et al.*, 2005)	1.2	14%
Clear cell carcinoma	63%	(Kalli *et al.*, 2008)		
Metastatic	100%	(Parker *et al.*, 2005)	30.1	
Papillary serous cystadenocarcinoma				8%
Normal	0%	(Parker *et al.*, 2005)	1.0	0%
Uterus				
Endometrial Primary carcinoma	20%	(Parker *et al.*, 2005)	9.8	

Endometrial Metastatic	100%	(Parker *et al.*, 2005)	8.6	0%
Uterine serous carcinoma	69%	(Parker *et al.*, 2005)		
Squamous cell carcinoma				20%
Endometrial adenocarcinoma				5%
Normal	0%	(Dainty et al., 2007)	1.0	0%
Brain				
Primary carcinoma	35%	(Parker *et al.*, 2005)	14.1	
Glioblastoma				18%
Astrocytoma				10%
Normal	0%	(Parker *et al.*, 2005)	1.0	0%
Pancreas				
Primary carcinoma	10%	(Parker *et al.*, 2005)	1.5	
Metastatic	100%	(Parker *et al.*, 2005)	3.6	
pancreatic ductal adenocarcinoma	80%	(Cai, 2017)		5%

Normal	0%	(Parker *et al.*, 2005)	1.0	0%
Lymphoma				
Primary	0%	(Parker *et al.*, 2005)	1.0	
Metastatic	50%	(Parker *et al.*, 2005)	2.1	75%
Normal	0%	(Parker *et al.*, 2005)		0%
Breast				
Primary carcinoma	43%	(Parker *et al.*, 2005)	1.9	0%
Triple-negative breast cancer	71%	(O'Shannessy et al., 2012b)		
- Metastatic	86%	(O'Shannessy et al., 2012a)		
Infiltrating ductal carcinoma				20%
Invasive ductal carcinoma				3%
Normal	20%	(Parker *et al.*, 2005)	1.0	0%
Lung				
Primary carcinoma	36%	(Parker *et al.*, 2005)	0.8	

Adenocarcinoma	59.6%, 72%, 76%	(Cagle et al., 2013; O'Shannessy *et al.*, 2012b; Tie et al., 2020)	0.9	56%
Mesothelioma	67%	(Parker *et al.*, 2005)	1.0	
Metastatic	50%	(Parker *et al.*, 2005)	0.8	
Squamous cell carcinoma	13%, 33%, 51%	(Cagle *et al.*, 2013; O'Shannessy *et al.*, 2012b; Tie *et al.*, 2020)		14%
Non-small cell carcinoma				100%
Normal	75%	(Parker *et al.*, 2005)	1.0	
Kidney				
Primary carcinoma	86%	(Parker *et al.*, 2005)	0.9	
Metastatic	50%	(Parker *et al.*, 2005)	0.3	
Renal cell carcinoma				100%
Clear cell carcinoma				15%

Normal	100%	(Parker *et al.*, 2005)	1.0	
Liver				
Primary carcinoma	0%	(Parker *et al.*, 2005)	1.3	
Hepatocellular carcinoma				53%
Normal	0%	(Parker *et al.*, 2005)	1.0	0%
Prostate				
Primary carcinoma	0%	(Parker *et al.*, 2005)	1.2	
Normal	0%	(Parker *et al.*, 2005)	1.0	
Colorectal				
Primary carcinoma	33%	(Shia et al., 2008)	0.1	
Metastatic	44%	(Shia *et al.*, 2008)	0.8	
Normal	7%	(Shia *et al.*, 2008)	1.0	0%
Bladder				
Primary carcinoma	20%	(Parker *et al.*, 2005)	0.7	
Transitional cell carcinoma				9%

Normal	50%	(Parker *et al.*, 2005)	1.0	
Bone				
Acute Myelogenous Leukemia				68%
Head and Neck				
Squamous cell carcinoma				0%
- primary tumors	45%	(Saba et al., 2009)		
- lymph node metastases (LNM)	40%	(Saba *et al.*, 2009)		
Normal	0%	(Saba *et al.*, 2009)		0%
Cervix				
Squamous cell carcinoma	41%	(Liu *et al.*, 2017a)		5%
Normal	12%	(Liu *et al.*, 2017a)		
Soft tissue				
Spindle cell type liposarcoma				100%
Fibrosarcoma				70%
Mucinous liposarcoma				25%
Liposarcoma				20%

Skin				
Malignant melanoma				40%
Thyroid				
Papillary carcinoma				30%
Follicular carcinoma				22%
Normal				0%
Stomach				
Adenocarcinoma				11%
Normal				0%
Esophagus				
Squamous cell carcinoma				10%
Normal				0%
Testis				
Seminoma				7%
Normal				0%

Table 2.2. Papers that describe a direct role for FOLR1 in signaling.

Cells	Folate added (μM)	Increase in markers (time post folate) *requires FOLR1	FOLR1 physical interaction	Notes	Ref.
JAK–STAT signaling					
HeLa (cervical cancer cell)	FA (567–1360)	- p-STAT3 (5 min)	- co-IP gp130 with FOLR1	- STAT3-regulated genes increase with folic acid (FA)	(Hansen *et al.*, 2015)
mouse neural precursor cells	FA (453–1134)	- p-STAT3 (30 min)	- co-IP FOLR1 with gp130	- FOLR1 promotes astrocyte differentiation	(Su *et al.*, 2018)
mouse embryonic stem cells (ESC)	FA (1000)	- nuclear p-STAT3 (steady state)		- no increase in p-STAT3 but translocation to nucleus	(Wei *et al.*, 2017)
mouse mammary epithelium tumors				- induced breast cancers that express FOLR1 and p-STAT3	(Hansen *et al.*, 2017)
ERK1/2 signaling					
FOLR1/PGR/SRC/ERK/IκB-α/NF-κB/p53/p21 & p27					
HUVEC	FA (10)	- p-SRC (2 min)* - p-ERK1/2 (5 min) - nuclear NF-κB (13 hrs) - p53 (14 hrs)* - p21 & p27 (17 hrs)	- co-IP SRC with FOLR1	- inhibition of cell proliferation starts at 0.1 μM FA (max 10 μM) - interaction of SRC and FOLR1 is in cytosolic fraction	(Lin *et al.*, 2012)
HUVEC	FA (10)	- p-SRC (2 min) - p-ERK1/2 (2 min) - p21 & p27 (21 hrs) - RhoA and Rac1 increase cytosol, decrease membrane fraction (6 hrs)	- co-IP PGR, ESR2, SRC with FOLR1 - co-IP FOLR1, PGR, ESR2 with SRC - co-IP FOLR1, SRC, ESR2 with PGR	- inhibition of cell migration with 10 μM FA	(Lee *et al.*, 2018)

COLO-205 (colon cancer cell line)	FA (1–10)	- p-SRC (2 min)* - p-ERK1/2 (2 min) - nuclear NF-κB - p53 (12 hrs)* - p21 & p27 (12 hrs)*		- inhibition of cell proliferation starts at 0.1 μM FA (max 10 μM)	(Kuo *et al.*, 2015)
COLO-205	FA (10)	- p-SRC (2 min) - p-ERK (2 min) - p53 (18 hrs) - p21 & p27 (18–20 hrs)	- co-IP SRC with PGR - co-IP FOLR1 with PGR	- PGR required for increase in FA-induced signaling markers	(Kuo and Lee, 2016)
COLO-205	FA (10)	- p-SRC (2 min) - p-p21 (18-20 hrs) - p(Ser32)-IκB-α - RhoA increased cytosol, decreased membrane frac.		- inhibition of cell migration starts at 0.1 μM FA (max 10 μM)	(Ting *et al.*, 2019)
T47D and MCF-7 (breast cancer cell lines)	FA (1)	- p-SRC (5 min) - RhoA increase membrane fraction, decrease cytosol	- co-IP FOLR1, PGR with SRC - co-IP FOLR1, SRC with PGR	- increased proliferation and migration starts at 1 μM FA (max 10 μM)	(Wang *et al.*, 2020)
FOLR1/MEK/ERK/TSLC1					
HONE1 (nasopharyngeal cell line)	FA (10)	- p-MEK (10 min) - p-ERK1/2 (10 min)* - TSLC1*		- FOLR1 and TSLC1 inhibit proliferation, migration, invasiveness	(Liu *et al.*, 2017b)
FOLR1/ERK/FOS–JUN					
HeLa		- steady-state levels of p-ERK, p-FOS, p-JUN*		- FOLR1 p-ERK, p-FOS, p-JUN correlated severity of squamous cervical carcinomas	(Liu *et al.*, 2017a)
FOLR1/ERK/Survivin					
KLE (endometrial carcinoma cell line)		- steady-state levels of p-		- FOLR1, p-ERK1/2, and	(Zhang *et al.*, 2019)

		ERK1/2, p-JUN, p-FOS, and Survivin*		Survivin correlated pathological grade of endometrial carcinomas	
FOLR1 interaction with LYN and $G\alpha_{i-3}$					
IGROV1 (ovarian cancer cell line)			- co-IP FOLR1, $G\alpha_{i-3}$ with LYN - co-IP LYN, $G\alpha_{i-3}$ with FOLR1	- FOLR1, LYN, and $G\alpha_{i-3}$ in detergent-resistant membrane	(Miotti *et al.*, 2000)
FOLR1 as a transcription factor					
DAOY (medullo-blastoma cell line)	FA (453)	- nuclear localization of FOLR1 p38 (15-30 min)		- before FA stimulation, FOLR1 p48 and p38 in cytosol fraction	(Boshnjaku *et al.*, 2012)
O9-1 (neural crest cell line)	FA (0.23)	- FOLR1 ChIP of *Oct4*, *Sox2*, *Klf4* regul. DNA (15-30 min) - *Oct4*, *Sox2*, *Klf4*, *Trim71* expression (12-24 hrs)* - decrease miR-let-7, miR-138 (6 hrs)*	- co-IP of DGCR8, Drosha with FOLR1	- FA- and FOLR1-induced genes promote pluripotency	(Mohanty *et al.*, 2016)
O9-1 (differentiated into glial cells)	5-m-THF (0.022)	- nuclear localization of FOLR1 p38 (30 min)	- co-IP of FOLR1 with CAF-1	- FOLR1 is required for 5-m-THF to dedifferentiate glial cells	(Monick *et al.*, 2019)

The information in this Table is not comprehensive, many aspects of the signaling pathways are not included.

CHAPTER 3

CAND1 CATALYZES THE REDISTRIBUTION OF SCF COMPLEXES TO PROMOTE MITOTIC PROGRESSION

Fathima Zahra Nawaz, Kyoengwoo Min, and Edward T. Kipreos2 "CAND1 catalyzes the redistribution of SCF complexes to promote mitotic progression", to be submitted to *Molecular Cell*

Abstract

SCF (Skp1-Cullin-F-box) ubiquitin ligases regulate diverse cellular processes including multiple aspects of the cell cycle, transcription, signal transduction, and apoptosis. Several SCF complexes function to regulate cell cycle progression, including the F-box proteins SKP2, FBW7, and FBXW11. There are 69 human F-box proteins that function as substrate receptors (SRs) for SCF complexes. The binding of each F-box protein to the core SCF complex produces a unique E3 ubiquitin ligase that targets different subsets of substrates that regulate different cellular pathways. The CAND1 protein is a SR exchange factor for SCF complexes. CAND1 strips off adaptor–SR complexes from the SCF core complex and allows new adapter–SRs to bind to create new active SCF complexes. We have analyzed the SR proteins present in SCF complexes throughout the cell cycle and found systematic changes in SR association with SCF complexes during mitosis. The differences in SCF complexes occur even when the SRs are constitutively present throughout the cell cycle. We show that CAND1 is required to reorganize the diversity of SCF complexes during mitosis. CAND1 is required for the removal of multiple SRs from SCF complexes during mitosis and promoting the integration of a specific SR, FBXW11/β-TrCP2, into SCF complexes. Inactivating CAND1/2 causes mitotic arrest that often leads to cell death, and these mitotic defects have been observed in human cells, including HeLa, U2OS, and normal hTERT-derived fibroblasts. Broad inactivation of CRL complexes with the small molecule MLN4924 rescues the CAND1/2 phenotype, suggesting that the mitotic defects are caused by the ectopic activation of SCF complexes. This is consistent with the hypothesis that the reorganization of SCF complexes that is dependent on CAND1 is required predominantly to prevent ectopic SCF activity to allow normal mitotic progression. These results highlight a novel mechanism by which SCF complexes can undergo large-scale reorganization through a CAND1-dependent process.

Introduction

The ubiquitin proteasome system (UPS) is responsible for the degradation of the vast majority of proteins in the cell (Rock et al., 1994). In UPS, a cascade of E1-activating, E2-conjugating, and E3-ligating enzymes function in tandem to tag substrate proteins with a polyubiquitin chain to target them for degradation by the 26S proteasome. E3 ubiquitin ligases provide the specificity by recognizing the substrate proteins for ubiquitylation (Kipreos, 2005).

Cullin-RING ubiquitin ligases (CRLs) are the largest single classes of E3 ubiquitin ligases and have a multitude of diverse functions in cells (Bosu and Kipreos, 2008; Sarikas et al., 2011). CRLs are comprised of: a cullin protein that acts as a scaffold; a RING finger protein that binds and activates the ubiquitin-conjugating enzyme; a substrate receptor (SR) that binds the substrate; and an adapter that links the substrate receptor to the core complex. SRs are variable components, and core CRL complexes function separately with multiple SRs. The binding of a particular SR to the core CRL complex determines the substrates that are targeted and the cellular functions of the complex.

The most-studied family of CRLs are the SCF (Skp1-CUL1-F-box proteins) complexes (Reitsma et al., 2017). The SCF complex is made of three invariable, core components: the scaffold CUL1; the RING H2 finger protein RBX1/ROC1/Hrt1 that binds the E2; and the adaptor Skp1, which links the SRs to the complex (Petroski and Deshaies, 2005; Skaar et al., 2013). The only variable SCF component are the SRs, which contain an F-box protein motif. The F-box motif binds to the adaptor Skp1 to link the SR to the core SCF complex (Nakayama and Nakayama, 2005; Zheng et al., 2002).

Animal and plant species have multiple SRs for SCF complexes. There are 69 F-box proteins identified in humans, and they fall into three categories based on their additional protein-

protein interaction domains (Nakayama and Nakayama, 2005; Zheng et al., 2016b). FBXWs contain WD40 repeats, FBXLs contain leucine-rich repeats, and FBXOs contain no defined motifs other than the F-box.

Each time a different SR binds the core SCF complex it forms a unique SCF complex with specific substrates and cellular functions. The current model posits that the cellular repertoire of SCFs is regulated by a post-translational modification of CUL1 by the ubiquitin-like protein Nedd8, the SR exchange factor CAND1, and substrate binding to the F-box protein (Pierce et al., 2013; Reitsma *et al.*, 2017; Zemla et al., 2013). CAND1, is an SR exchange factor that equilibrates CUL1 with the cellular pool of SR modules by replacing SR–Skp1 (adaptor) complexes that are bound to the core SCF complex with new SR–Skp1 complexes (Pierce *et al.*, 2013; Reitsma *et al.*, 2017; Wu et al., 2013; Zemla *et al.*, 2013). When Cand1 encounters an SCF complex, it competes with the adaptor Skp1 for an overlapping binding site on CUL1. This results in the release of the SR–Skp1 complex. A new SR–Skp1 complex can then displace CAND1 to form a new SCF complex thereby mediating one full exchange of the SR–Skp1 module (Deshaies, 2014; Olma and Dikic, 2013; Reitsma *et al.*, 2017; Zemla *et al.*, 2013). When SCF binds to a substrate via a specific SR, Nedd8 is conjugated to the CUL1 C-terminus by the Nedd8-conjugating enzyme Ubc12 (Lydeard et al., 2013). Nedd8 prevents CAND1 from interacting with the SCF complex. Removal of NEDD8 is catalyzed by the COP9 signalosome (CSN), and this allows CAND1 to interact with CUL1, thus removing the SR–Skp1 module and inactivating the SCF complex while CAND1 is bound (Cope and Deshaies, 2003).

Members of Cyclin-dependent kinase (CDK) family, controlled by key regulators such as cyclins and CDK inhibitors (CKI)s, drives the cell cycle. This progression is tightly regulated by the ubiquitin-mediated proteolysis of those cell cycle regulators by ubiquitin ligases; mainly the

(SCF) complex and the anaphase-promoting complex/cyclosome (APC/C) (Nakayama and Nakayama, 2005). The F-box proteins S-phase kinase-associated protein 2 (SKP2), F-box and WD-40 domain protein 7 (FBXW7/Cdc4) and β-transducin repeat-containing protein (β-TrCP) are well studied cell cycle regulators (Nakayama and Nakayama, 2005; Zheng et al., 2016a).

In humans, there are two paralogs of the β-TrCP SR: β-TrCP1/BTRC/FBXW1A and β-TrCP2/FBXW11. FBXW11/β-TrCP recognizes their substrate through the canonical DSGXXS, degron sequence where both serines are phosphorylated, thereby inducing their ubiquitination and subsequent proteasomal degradation (Kim et al., 2015; Kipreos and Pagano, 2000). Despite having high similarity between BTRC and FBXW11, these proteins display a significant difference in subcellular localization, as BTRC is nuclear localized, while FBXW11 is cytosolic (Mangeat et al., 2009). Moreover, a protein-protein interaction study utilizing tandem affinity purification and mass spectrometry (TAPMS) revealed distinct substrates for the two SRs (FBXW11 and BTRC were found to interact with 96 and 26 proteins, respectively, while twenty proteins co-complexed with both FBXW11 and BTRC) (Kim *et al.*, 2015).

SCFs regulate diverse cellular processes including multiple aspects of cell signaling and physiology, including the cell cycle, transcription, signal transduction, apoptosis, angiogenesis, and cell migration (Nakayama and Nakayama, 2005). Defects in SCF activity has been linked to many human diseases, including sleep and mood disorders, diabetes, Parkinson's disease, bacterial and viral infections, and multiple cancers (Nguyen and Busino, 2020; Zheng *et al.*, 2016b). In this study, we present evidence that CAND1 is required to selectively load the SR FBXW11 onto SCF complexes during mitosis, while at the same time, removing other substrate receptors from mitotic SCF complexes: thereby effecting a reorganization of SCF complexes. This reorganization of SCF complexes is important to allow normal mitotic progression.

Results

CAND1 has increased interaction with CUL1 during mitosis

CAND1 is the SR exchange factor that regulates the switching of SRs on and off the CUL1-RBX1 module. We wanted to understand the involvement of CAND1 in regulating CRLs through the cell cycle phases. To test if the interaction between CAND1 and CUL1 varied throughout the cell cycle, we analyzed the association of endogenous CAND1 with FLAG-tagged human CUL1 in the human embryonic kidney HEK293T cell line during different cell cycle phases. We observed an increase in CAND1 binding to CUL1 in mitosis compared to G1, S, and G2 phases (Fig. 1A). CAND1 bound to immunoprecipitated FLAG-CUL1 at approximately 3.5 times higher levels in mitotic cells than in S-phase cells. The next highest level of CAND1 bound to FLAG-CUL1 was in G1-phase cells, which had 1.75 times higher levels than in S-phase cells.

We did not analyze whether CAND1 binding to other cullins is increased during mitosis because CUL3, CUL4A, and CUL5 did not stably associate with FLAG-CUL1 during IPs using a buffer with Triton-X100 detergent (Fig. 1B). The interaction of CAND1 with CUL1 is increased during mitosis relative to asynchronous cells, but interaction between CAND1 and the other cullins is not observed in either mitosis or asynchronous cells. This is consistent with another study that only showed stable interaction between CAND1 and CUL1 but not with other cullins (Chew and Hagen, 2007). However, a later study by the same group found that a different choice of detergent in the immunoprecipitation (IP) buffer, NP40 rather than Triton X-100, allows CAND1 to interact stably with CUL1, CUL2, CUL3, CUL4a and CUL5 in HEK293T cells (Chua et al., 2011). Given our initial results of non-interaction with the other cullins, our study subsequently focused solely on CAND1 interaction with CUL1.

Increased levels of unneddylated CUL1 generally correlates with increased association with CAND1, as CAND1 can only bind to unneddylated cullins (Pierce *et al.*, 2013; Zheng *et al.*, 2002). When we assessed the neddylation status of CUL1 in different cell cycle phases, we observed a lower level of neddylation in mitosis and G1 (44% and 45% of CUL1 was neddylated) compared to S and G2 (71% and 67% neddylated CUL1) (Fig. 1A). However, the increased association of CAND1 with CUL1 in mitosis is not a consequence of changes in CUL1 neddylation, based on two observations. First, there is not a significant difference in the level of neddylated CUL1 between mitosis and G1 phase, yet there is a 2-fold higher interaction of CAND1 with CUL1 in mitosis than G1 phase. Second, when neddylation is blocked in both asynchronous and mitotic cells by adding the Nedd8 E1 inhibitor MLN4924, increased binding of CAND1 to CUL1 is still observed in mitotic cells (Fig. 2A). These observations suggest that CAND1 has increased association with CUL1 during mitosis through a mechanism other than the regulation of neddylation. Consistently, we did not observe a change in the rate of deneddylation between asynchronous and mitotic cells (Fig. 2B).

Since the increased association of CAND1 to CUL1 during mitosis appears to be regulated independently of the state of neddylation, we wanted to assess if there was a difference between the stability of the CAND1-CUL1 complexes formed in mitosis vs. interphase. To test this, we co-expressed FLAG-CUL1 and Myc-CAND1 in HEK293T cells and then immunoprecipitated FLAG-CUL1 from mitotic cells or S-phase cells using anti-FLAG affinity beads (Fig. 3A). This will also precipitate Myc-CAND1–FLAG-CUL1 complexes. After washing the anti-FLAG-affinity beads, the beads with precipitated Myc-CAND1–FLAG-CUL1 complexes were placed into S-phase or M-phase HEK293T cell lysates and incubated for 0, 5, or 30 minutes to allow Myc-CAND1 to dissociate from FLAG-CUL1. After the incubation period,

the beads were spun down and washed, and the amount of Myc-CAND1 still associated with FLAG-CUL1 was analyzed by western blot to assess how much CAND1 remained associated with FLAG-CUL1. After 30 minutes of incubation in the S-phase lysate, the mitotic CAND1–CUL1 complex had less dissociation than the S-phase CAND1–CUL1 complex (Fig. 3B). At the same time, the S-phase CAND1–CUL1 complex was more stable in the mitotic lysate than when it was in the S-phase lysate. These results suggest that the CAND1–CUL1 complex from different cell cycle phases have different stabilities (with the mitotic complex more stable than the S-phase complex). Additionally, the ability of the lysate to dissociate the CAND1–CUL1 complex differs during the cell cycle (with more dissociation activity in S phase lysate).

CAND1 and CAND2 are required for mitotic progression

Since the interaction between CAND1 and CUL1 seems to be mitotically regulated, we wanted to determine if CAND1 is required for mitosis. Human cells have two CAND1 paralogs, CAND1 and CAND2 (Aoki et al., 2002). CAND2 was found to occupy less than 0.25% of endogenous CUL1 in HEK293T cells, however, inactivation of CAND1 increases the CAND2 association with CUL1 (Reitsma *et al.*, 2017). Inactivating CAND1 and CAND2 in HEK293T cells increased the percentage of cells in G2/M phase from 8.8% to 21.6%. (Fig. 4A). We confirmed these cells, to be arrested in mitosis by evaluating the mitotic index on HEK293T cells (control siRNA 4.5%; siCAND1 4%; siCAND2 3.8%; siCAND1+siCAND2 28.1%). This suggests that the inactivation of both CAND1 and CAND2 causes cells to take longer to progress through mitosis, thereby leading to the accumulation of mitotic cells.

To determine directly whether CAND1/2 is important for mitotic progression, we made time-lapse movies of U2OS cells after CAND1/2 knockdowns. U2OS cells are human osteosarcoma cells that were utilized because they are relatively adherent during mitosis, thereby allowing a

determination of mitotic stages using non-invasive visualization with differential interference contrast (DIC) microscopy. The DIC movies showed that the loss of CAND1 and CAND2 caused a delay in mitosis, with the most pronounced increases in timing occurring in prometaphase and telophase, although all mitotic stages were statistically longer (Fig. 4B and 4C). Inactivating CAND1/2 also affects the mitotic progression of normal IMR90-hTERT human fibroblasts, with a 3-fold increase in mitotic timing: 215.6 ± 26 min for CAND1/2 siRNA vs. 70.5 ± 5.3 min for control siRNA (Fig. 4D). The non-flat morphology of IMR90-hTERT cells did not allow a determination of progression through the individual mitotic stages.

We then analyzed CAND1 knockdown in HeLa cells expressing α-tubulin-YFP, and histone-H2B-RFP. HeLa cells do not express detectable levels of CAND2 (data not shown) therefore it wasn't necessary to KD CAND2 in these cells. Time lapse videos of the HeLa cells showed statistically significant delays in metaphase and telophase and specific mitotic defects in response to two different CAND1 siRNAs (Fig. 5A and 5B). We noticed that U2OS mitotic cells treated with both CAND1 and CAND2 siRNA undergo significant levels of cell death compared to control siRNA-treated cells (Fig, 5C). Of the cells that showed a mitotic delay but ultimately divided, many did so in a different cleavage-plane orientation. Most of the control siRNA-treated cells divided horizontally (98%) (n=16), while approximately half of the CAND1/2 siRNA-treated cells divided vertically (46% n=10). Overall, CAND1 siRNA results in: an increase in multipolar spindles relative to control HeLa cells (0% to 8.3%,); perduring cytokinetic bridge (2.4% to 11.1%, where the average timing is increased from 20 min in control to 43 min, and some cells retain the bridge for >60 min); surface blebbing during mitosis that does not lead to cell death (3.6% to 13.9%); and cell death (9.6% to 51.4%) (control, n=83; and siCAND1, n=72).

Reitsma et al, 2017 recently reported a double knockout (DKO) of CAND1 and CAND2 in HEK293 cells.On its surface, that would suggest that loss of CAND1/2 may not be that deleterious because the cell line can be maintained. However, we obtained the DKO cell line (as well as the parental, non-knockout HEK293 cells) from the authors. We found that the DKO cells have a significantly reduced proliferation rate – the doubling time increases from 24.9 ± 1.0 hrs for the parental strain to 42.0 ± 1.1hrs for the DKO cells – an increase of 69%. Time lapse video of the CAND1/2 DKO cells showed that all cells either died (47%, 7/15) or had a substantial mitotic arrest that perdured over the video period of 24 hrs (53%, 8/15) (Fig. 7). In contrast, the parental HEK293 cells did not exhibit cell death during mitosis (0/21). The fact that the CAND1/2 DKO cells can be maintained in culture suggests that the stress of the video conditions led to a higher percentage of cell death during mitosis. Overall, our results suggest that the CAND1/2 DKO HEK293 cells are impaired for mitotic progression.

SCF complexes undergo subunit reorganization during mitosis that is dependent on CAND1

As we observed mitotic defects and delays in progression after CAND1/2 knockdown, we wanted to evaluate if the loss of CAND1/2 influences mitotic SCF complex formation. We analyzed the components of the SCF complex in the presence and absence of CAND1/CAND2 in HEK293T cells. To analyze how the SRs associated with SCF complexes changed during mitosis, we immunoprecipitated FLAG-CUL1 stably expressed in HEK293T cells and affinity eluted with FLAG peptide, and then analyzed the associating proteins by LC-MS/MS. Intriguingly the only SR that was detected to interact with FLAG-CUL1 in mitotic cells was FBXW11 (Fig. 6A). Significantly, knocking down CAND1 in M phase cells resulted in a larger complement of 10 SRs associating with FLAG-CUL1 (Fig. 6A). We obtained similar results by performing a Western blot for specific CUL1 SRs (Fig. 5B). Recent data on analyzing SCF complex formation

throughout the cell cycle from the Deshaies lab showed that FBXW11 was enriched in SCF complexes in mitosis, while the proteins SKP2, FBXO22, FBX09, FBXL15, FBXL18, and FBXO30 exhibited increased assembly with Cul1 in S phase, while showing a negative association in mitosis (Reitsma *et al.*, 2017).

These results suggest two potential mechanisms by which CAND1 and CAND2 promotes mitotic progression. The first mechanism is that CAND1/CAND2 reorganize the mitotic CRL complexes to load specific SRs (e.g., FBXW11) into SCF or CRL complexes that promote mitotic progression. The second mechanism is that CAND1/CAND2 selectively remove SRs from the core SCF/CRL complexes to reduce unwanted SCF/CRL activity that would inhibit mitotic progression. To test these hypotheses, we used the small molecule inhibitor MLN4924, which inhibits the Nedd8-activating enzyme, to broadly inhibit CRL complexes (Soucy et al., 2009). Treatment with MLN4924 would be expected to inhibit all SCF and CRL complexes. MLN4924 treatment alone does not have an appreciable effect on mitotic progression in U2OS cells (Balachandran et al., 2016). The fact that MLN4924 treatment does not affect mitotic progression argues against the hypothesis that the defect in mitotic progression in CAND1/2 knockout cells is due to a failure to activate specific CRL(s), as inhibiting all CRLs with MLN4924 would then be expected to produce mitotic defects. On the other hand, if knocking down CAND1/2 results in the ectopic activation of CRL complexes during mitosis that are deleterious for mitotic progression then inhibiting all CRL complexes with MLN4924 should rescue the mitotic defects.

As expected, treatment of CAND1/2 knockdown cells with MLN4924 rescued the accumulation of mitotic cells in prometaphase and telophase, as well as the aberrant orientation of the cell division plane (Fig. 7; and data not shown). This suggests that the mitotic defects are caused by the ectopic activity of SCF (or CRL) complexes. This implies that one of the major

functions of CAND1 in mitosis is to eliminate deleterious SCF/CRL activity so that mitotic progression can occur properly.

CAND1 interacts with SCF- FBXW11

In order to gain insights into how CAND-1 regulates SCF complexes during mitosis, we sought to identify novel proteins that interact with CAND1 during mitosis. We immunoprecipitated FLAG-CAND1 from HEK293T cells and analyzed the interacting proteins by LC-MS/MS. (Fig. 8A). Interestingly, FBXW11 co-precipitated with FLAG-CAND1 from mitotic cells, but not from asynchronous cells. To confirm these results, we co-expressed pGlue-tagged FBXW11 (Angers et al., 2006) along with FLAG-CAND1 and found that FLAG-CAND1 was robustly co-precipitated with FBXW11 (which was pulled down with anti-HA antibody, as the pGlue tag has a HA tag) relative to the negative control protein HA-CDL-1 (Fig. 8B). CDL-1 is a *C. elegans* mRNA binding protein, which would not be expected to interact with human CAND1 or the SCF complex. We obtained a similar interaction when we co-expressed Venus-CAND1 with HA-FBXW11 and immunoprecipitated Venus-CAND1 and probed for co-precipitated HA- FBXW11 (data not shown).

Discussion

Ubiquitylation and degradation of specific substrate proteins via SCF complexes allow the rapid removal of cell cycle regulators, promoting irreversible transitions between cell cycle phases. In this work, we demonstrate that CAND1 knockdown during mitosis in human cells significantly increases the binding of the SRs to the CUL1-RBX1 complex, that are not typically found to interact with CUL1 during mitosis. CAND1 mediates the exchange of F-box protein from the active SCF complexes(Pierce *et al.*, 2013; Reitsma *et al.*, 2017). The current paradigm is that the repertoire of active SCF complexes is determined by the non-biased action of CAND1 and

substrate binding to the SCF complex, which blocks SR exchange (Liu et al., 2018). We wanted to understand the role of CAND1 in this process in the context of cell cycle regulation, as transitioning between cell cycle stages is tightly regulated.

Interestingly we observed that the level of CAND1 interacting with the CUL1-RBX1 module varied throughout the cell cycle with stronger interaction during mitosis. According to the prevailing model, CAND1 interacts with the unneddylated form of CUL1 when it is not bound to the adaptor Skp1 (Goldenberg et al., 2004; Pierce *et al.*, 2013). The neddylation of the CUL1-RBX1 inhibits the binding of CAND1 to the CUL1-RBX1 module (Liu et al., 2002). However, the strong association of CAND with CUL1 during mitosis was not due to differences in the neddylation state of CUL1 nor to differences in the rate of deneddylation. CUL1 is known to localize in both cytoplasm and nucleus, while CAND1 is predominantly a cytoplasmic protein. Therefore, one can question if the difference in CAND1 binding to CUL1 in asynchronous and mitosis population is due to the proteins being expressed in different subcellular locations. But analyzing both subcellular fractions, proved otherwise, with the variation in interaction being independent of subcellular localization. These results suggested that other factors regulate the mitotic CAND1-CUL1 association.

We observed that the M-phase CAND1–CUL1 complex is more stable than the S-phase complex. Additionally, M-phase lysate stabilizes an S-phase CAND1–CUL1 complex better than S-phase lysate. These results suggest the possibility of a modification of CAND1 or CUL1 that promotes stronger CAND1 association, and a component of the M-phase lysate that can stabilize the complex, possibly through such modification. Or alternatively, a modification of the S-phase CAND1 or CUL1 that weakens the interaction and a component of S-phase lysate that destabilizes the interaction. SR–Skp1 are involved in dissociating CAND1 from the CAND1–CUL1 complex

(Liu *et al.*, 2018). Therefore, it is possible that the differential modification of the adaptor Skp1 between S phase and mitosis may alter multiple SR–Skp1 interactions with the CAND1–CUL1 complex.

Our CAND1/2 knockdown data indicates that CAND1/2 inactivation not only causes delays in mitotic progression, but also produces multiple phenotypes like altered orientation of the division plane, multipolar spindles, perduring cytokinetic bridge, and cell surface blebbing (without death). These defects may allow us to deduce possible mechanisms that are affected by inactivation CAND1 and CAND2.

Misoriented cell division can result from alterations in cell polarity proteins, spindle orientation defects, defects in adhering proteins, and changes in tissue adhering microenvironment (Finegan and Bergstralh, 2019; Sun et al., 2018). Defects in cell division plane have been associated with developmental disorders and many cancers (Finegan and Bergstralh, 2019). Multipolar spindles are often formed during prometaphase/metaphase are associated with either prior centrosome amplification or loss of spindle pole integrity. Prior centrosome amplification can result from centriole overduplication in S phase, or a prior failure in cytokinesis or mitotic slippage (escape from mitotic arrest) (Maiato and Logarinho, 2014). Abnormal chromatin segregation, defective assembly of nuclear pore complex or DNA replication stress can cause an arrest due to the "abscission checkpoint", which relies on prolonged Aurora B activity (Nähse et al., 2017). This arrest in "abscission checkpoint" can result in chromosomal breakage or aneuploidy. Formation of "chromatin bridges" is a phenotype associated with "abscission checkpoint" (Nähse *et al.*, 2017), and we have observed such bridges in CAND1/2 siRNA movies. We did not observe centriole overduplication nor abnormal chromatin segregation. There were cells that round up, form the metaphase plate, and then exit mitosis without cell division, which can be due to failed mitosis

(Telentschak et al., 2015). The resulting G1 phase cell would then have two centrosomes rather than one, and the subsequent duplication of the centrosomes would create a multipolar spindle with four centrosomes in the next mitosis. Hence multipolar spindles or aneuploidy could be a secondary consequences of a prior failed mitosis rather than a direct effect of CAND1/CAND2 knockdown. In contrast, a failure of cytokinesis would produce cells with two nuclei, which we do not observe at high frequency in CAND1/2 knockdowns.

Knowing that CAND1 is involved in forming a stable complex during mitosis, and inactivation of CAND1 is associated with mitotic delay, led us to investigate if there was any perturbation in SCF complex formation. Examining the SRs associated with CUL1-RBX1 in the presence and absence of CAND1/2 during mitosis revealed that there was a difference between the SRs that are associated with CUL1-RBX1. It was striking to see the only SR that was detected with FLAG-CUL1 in M phase cells was β-TrCP2/FBXW11. Recent data from the Deshaies lab similarly shows that β-TrCP2 is enriched in SCF complexes in mitotic cells (Reitsma *et al.*, 2017). It is interesting that the *C. elegans* ortholog of β-TrCP2, LIN-23, was the SR that was particularly reliant on CAND-1 for activity (Bosu et al., 2010). Thus, CAND1 appears to promote β-TrCP2/LIN-23 activity in both organisms.

Based on our results we hypothesized if CAND1/2 promotes preferential loading of a particular SR, β-TrCP2/FBXW11, which plays an important role in mitotic regulation or alternatively if CAND1/2 prevents binding of SR(s) to the CUL1-RBX1 complex that would inhibit mitotic progression. Treating with broad CRL inhibitor MLN4924 rescued the mitotic delays caused by the CAND1/2 knocked down phenotype. As MLN4924 inhibits all CRL complexes, this suggests that the mitotic defects are caused by the ectopic activity of SCF (or CRL) complexes that are normally not active in mitosis. This further implies that one function of the mitotic SR

reorganization is to limit SCF/CRL activity during mitosis so that mitotic progression can occur properly. Further experiments are required to identify the CRL complex(es) whose ectopic activity contributes to the mitotic arrest in CAND1/2 knockdown cells.

Another intriguing observation was that β-TrCP2/FBXW11 physically interacts with CAND1. There are several possibilities for how this physical interaction could result in functional outcomes, including that CAND1 facilitates β-TrCP2/FBXW11 loading onto the mitotic core SCF module, or that CAND1 and β-TrCP2/FBXW11 interact together in a CAND1–$SCF^{\beta\text{-}TrCP2}$ complex. CAND1 appears to interact with β-TrCP2/FBXW11 in the context of an SCF complex, forming a trimeric CAND1–$SCF^{\beta\text{-}TrCP2}$ (data not shown). This could explain why we observe a higher CAND1 association with the CUL1-RBX1 during mitosis. The questions that remain are if the SKP1 adaptor is included in this trimeric complex and if the trimeric complex is active in ubiquitylating substrates? In a broader context, we have yet to evaluate of what makes the complex mitosis specific.

Here we show for the first time that CAND1 can act in a directed manner towards a particular SRs which is important for mitotic progression. SCF complexes regulate hundreds of cellular processes and are implicated in multiple human diseases (Hindley et al., 2011; Skaar et al., 2014). SRs define the substrates and cellular processes that are regulated. The reorganization of SRs during mitosis is likely to have important implications for developmental and cellular processes that occur in dividing cells. CAND1 SR exchange is one of the major mechanisms that regulates the diversity of SCF complexes, and so demonstrating that CAND1 can act in a directed manner toward particular SRs provides a paradigm shift in understanding CAND1's functions that may operate in other cellular processes. Loss or deregulation of CAND1 is associated with many cancers (Kamburov et al., 2015; Kang et al., 2018; Korzeniewski et al., 2012; Murata et al., 2010;

Salon et al., 2007). Hence, understating the role of CAND1 in cell division can provide insights for potential anticancer targets.

Materials and Methods

Cell culture, selection, and synchronization

Human embryonic kidney HEK293T cells, HeLa cells and human osteosarcoma cells (U2OS) were obtained from the American Type Culture Collection and were cultured in DMEM in the presence of 10% fetal bovine serum (Sigma), 100μg/ml penicillin, and streptomycin (Hyclone). 293T stable cell line expressing FLAG-CUL1, CUL2, CUL3, CUL4A, and CUL5 was generated by transfecting pcDNA-FLAG-CUL1, pcDNA-CUL2, pcDNA-CUL3, pcDNA-CUL4A, and pcDNA-CUL5 followed by puromycin selection. 3xFLAGCul1 WT and DKO (CAND1 and CAND2 knockdown cells), were kind gifts from Dr. Xing Liu and as described in (Reitsma *et al.*, 2017). HeLa cells stably expressing fluorescently tagged tubulin and histone H2B was a kind gift from Dr. Don W. Cleveland and as mentioned in (Silk et al., 2009).

Cells were synchronized at S phase with a double thymidine (Sigma Aldrich) block. The first block with 2.5 mM thymidine was for 18 hrs, followed by a 9 hr release into fresh media, and a second 2.5 mM thymidine block for 18 hrs. Cells arrested in G2 phase were obtained by releasing cells from double thymidine block for 3 hrs, followed by the addition of 9 μM RO-3306 (Sigma Aldrich), a CDK1 inhibitor, for 8 hrs. Cells arrested in prometaphase were obtained by releasing cells from a double thymidine block for 3 hrs, followed by incubation with 100 ng/ml nocodazole (Sigma Aldrich) for 10 hrs.

DNA transfections, siRNA knockdowns, immunoprecipitations

Proteins were expressed in HEK293T cells and immunoprecipitated as described (Kim et al. 2008, Starostina et al. 2007). HEK293T cells and HeLa cells were transfected with plasmids for human protein expression with polyethylenimine (PEI) (Boussif et al., 1995). U2OS cells were transfected with plasmids for protein expression using Lipofectamine 2000 (Invitrogen) according to the manufacturer's instructions. For immunoprecipitation of human proteins, cells were collected 48 hrs after transfection and lysed in NP40 buffer (0.5% NP-40, 150 mM NaCl, 50 mM Tris pH 7.4, 1 mM EDTA, protease inhibitor cocktail (Roche), 2 mM DTT, and 50 μM LLnL). Cell lysates were centrifuged at 13,000 rpm for 25 min at 4°C and the supernatant was pre-cleared with sepharose 4B beads (Sigma Aldrich). Anti-FLAG immunocomplexes were eluted by incubation with FLAG peptide solution (400mM FLAG peptide in lysis buffer) for 20 minutes at 4°C.

Antibodies

Primary antibodies used were: anti-Cul1 (rabbit, Epitomics, ProteinTech at 1:1000) and (mouse, Invitrogen Zymed 32-2400 at 1:1000); anti-Cand1 (goat, Santa Cruz A-13 at 1:2000); anti- FLAG (rabbit and mouse from Sigma at 1:5000); anti-HA (rabbit and mouse from Invitrogen at1:20000); anti-Myc (mouse 9E10 serum at 1:500); anti-actin (mouse, ICN clone C4, 1:5000); anti-α-tubulin (mouse Sigma DM1A); anti-β-TRCP(rabbit, Cell signaling (D12C8 at 1:1000); anti-SKP1 (rabbit, Epitomics at 1:1000); anti-SKP2 (rabbit, Epitomics at1:1000); anti-CDC4 (rabbit, Millipore); and anti-EMI1 (mouse, Invitrogen at 1:30).

siRNA knockdowns

siRNA pools were transfected using RNAiMAX (Invitrogen) according to the manufacturer's instructions. siRNA transfections were performed twice, separated by an interval of 24 hrs.

siRNA pools were purchased from Thermo Scientific as ON-TARGET pools for CAND1 and CAND2.

	Sense strand	Anti-Sense strand
siCAND1 :	UAAGGCUAUGAAGAGAUACtt,	GUAUCUCUUCAUAGCCUUAtt
SiCAND2:	GCUGGUCCUUGUGAACCCUtt	AGGGUUCACAAGGACCAGCtt
	CCUCCAUAUGCUACGUGGAtt	UCCACGUAGCAUAUGGAGGtt
	CGUCUUCACUGCUUACAUCtt	GAUGUAAGCAGUGAAGACGtt

siRNA controls were purchased from Invitrogen.

Control siRNA was GUAUCUCUUCAUAGCCUUAdTdT.

For the knockdown of overexpressed proteins in U2OS cells, DNA was transfected using Lipofectamine 2000 (Invitrogen) according to the manufacturer's instructions followed by the siRNA transfections after 24 hrs.

Time-lapse microscopy

Microscopy for time-lapse movies of human cells (Figs 4, 5, 6) was performed with a DeltaVision Microscope System II in a heated chamber at 37°C. The microscope was controlled by SoftWoRX software (GE Healthcare). Images were taken with an Olympus UPlanSApo 20x DIC objective with a numerical aperture of 0.75. DIC images were taken every 3 or 5 min using a 25 ms exposure time. Epifluorescence images of α-tubulin/DAPI were taken every 5 min using a 400 ms exposure time. Images were 16-bit gray scale at a resolution of 1024 x 1024 pixels. U2OS or IMR90-hTERT cells were plated for imaging on 35 mm glass bottom plates (MatTek) and transfected with siRNA when 70% confluent, as described above. Immediately before imaging, the medium was changed to CO_2-independent media (Gibco). For the mitotic arrest rescue experiment (Fig. 5E) a

concentration of 1 μM MLN4924 (Caymen Chemicals) was used to broadly inhibit CRL complexes. Images were processed with Adobe Photoshop; movies were processed with ImageJ software (Schneider et al., 2012). Epifluorescence images for quantitative comparison were taken with the same exposure and treated identically with no gamma adjustments. Signal levels were determined using Adobe Photoshop, with the background level from the same image subtracted from the signal.

Statistical Analysis

Student's t-test was used to determine significance for Figs 4C, 4D, 4E and 5E. Error bars in all figures represent standard error of the mean (SEM).

Reference

Angers, S., Thorpe, C.J., Biechele, T.L., Goldenberg, S.J., Zheng, N., MacCoss, M.J., and Moon, R.T. (2006). The KLHL12-Cullin-3 ubiquitin ligase negatively regulates the Wnt-beta-catenin pathway by targeting Dishevelled for degradation. Nat Cell Biol *8*, 348-357. 10.1038/ncb1381.

Aoki, T., Okada, N., Wakamatsu, T., and Tamura, T.A. (2002). TBP-interacting protein 120B, which is induced in relation to myogenesis, binds to NOT3. Biochem Biophys Res Commun *296*, 1097-1103. 10.1016/s0006-291x(02)02031-4.

Balachandran, R.S., Heighington, C.S., Starostina, N.G., Anderson, J.W., Owen, D.L., Vasudevan, S., and Kipreos, E.T. (2016). The ubiquitin ligase CRL2ZYG11 targets cyclin B1 for degradation in a conserved pathway that facilitates mitotic slippage. J Cell Biol *215*, 151-166. 10.1083/jcb.201601083.

Bosu, D.R., Feng, H., Min, K., Kim, Y., Wallenfang, M.R., and Kipreos, E.T. (2010). C. elegans CAND-1 regulates cullin neddylation, cell proliferation and morphogenesis in specific tissues. Dev Biol *346*, 113-126. 10.1016/j.ydbio.2010.07.020.

Bosu, D.R., and Kipreos, E.T. (2008). Cullin-RING ubiquitin ligases: global regulation and activation cycles. Cell Div *3*, 7. 10.1186/1747-1028-3-7.

Chew, E.H., and Hagen, T. (2007). Substrate-mediated regulation of cullin neddylation. J Biol Chem *282*, 17032-17040. 10.1074/jbc.M701153200.

Chua, Y.S., Boh, B.K., Ponyeam, W., and Hagen, T. (2011). Regulation of cullin RING E3 ubiquitin ligases by CAND1 in vivo. PLoS One *6*, e16071. 10.1371/journal.pone.0016071.

Cope, G.A., and Deshaies, R.J. (2003). COP9 signalosome: a multifunctional regulator of SCF and other cullin-based ubiquitin ligases. Cell *114*, 663-671. 10.1016/s0092-8674(03)00722-0.

Deshaies, R.J. (2014). Structural biology: Corralling a protein-degradation regulator. Nature *512*, 145-146. 10.1038/nature13644.

Finegan, T.M., and Bergstralh, D.T. (2019). Division orientation: disentangling shape and mechanical forces. Cell Cycle *18*, 1187-1198. 10.1080/15384101.2019.1617006.

Goldenberg, S.J., Cascio, T.C., Shumway, S.D., Garbutt, K.C., Liu, J., Xiong, Y., and Zheng, N. (2004). Structure of the Cand1-Cul1-Roc1 complex reveals regulatory mechanisms for the assembly of the multisubunit cullin-dependent ubiquitin ligases. Cell *119*, 517-528. 10.1016/j.cell.2004.10.019.

Hindley, C.J., McDowell, G.S., Wise, H., and Philpott, A. (2011). Regulation of cell fate determination by Skp1-Cullin1-F-box (SCF) E3 ubiquitin ligases. Int J Dev Biol *55*, 249-260. 10.1387/ijdb.103171ch.

Kamburov, A., Lawrence, M.S., Polak, P., Leshchiner, I., Lage, K., Golub, T.R., Lander, E.S., and Getz, G. (2015). Comprehensive assessment of cancer missense mutation clustering in protein structures. Proc Natl Acad Sci U S A *112*, E5486-5495. 10.1073/pnas.1516373112.

Kang, M., Li, Y., Zhao, Y., He, S., and Shi, J. (2018). miR-33a inhibits cell proliferation and invasion by targeting CAND1 in lung cancer. Clin Transl Oncol *20*, 457-466. 10.1007/s12094-017-1730-2.

Kim, T.Y., Siesser, P.F., Rossman, K.L., Goldfarb, D., Mackinnon, K., Yan, F., Yi, X., MacCoss, M.J., Moon, R.T., Der, C.J., and Major, M.B. (2015). Substrate trapping proteomics reveals targets of the betaTrCP2/FBXW11 ubiquitin ligase. Mol Cell Biol *35*, 167-181. 10.1128/MCB.00857-14.

Kipreos, E.T. (2005). Ubiquitin-mediated pathways in C. elegans. WormBook, 1-24. 10.1895/wormbook.1.36.1.

Kipreos, E.T., and Pagano, M. (2000). The F-box protein family. Genome Biol *1*, REVIEWS3002. 10.1186/gb-2000-1-5-reviews3002.

Korzeniewski, N., Hohenfellner, M., and Duensing, S. (2012). CAND1 promotes PLK4-mediated centriole overduplication and is frequently disrupted in prostate cancer. Neoplasia *14*, 799-806. 10.1593/neo.12580.

Liu, J., Furukawa, M., Matsumoto, T., and Xiong, Y. (2002). NEDD8 modification of CUL1 dissociates p120(CAND1), an inhibitor of CUL1-SKP1 binding and SCF ligases. Mol Cell *10*, 1511-1518. 10.1016/s1097-2765(02)00783-9.

Liu, X., Reitsma, J.M., Mamrosh, J.L., Zhang, Y., Straube, R., and Deshaies, R.J. (2018). Cand1-Mediated Adaptive Exchange Mechanism Enables Variation in F-Box Protein Expression. Mol Cell *69*, 773-786 e776. 10.1016/j.molcel.2018.01.038.

Lydeard, J.R., Schulman, B.A., and Harper, J.W. (2013). Building and remodelling Cullin-RING E3 ubiquitin ligases. EMBO Rep *14*, 1050-1061. 10.1038/embor.2013.173.

Maiato, H., and Logarinho, E. (2014). Mitotic spindle multipolarity without centrosome amplification. Nat Cell Biol *16*, 386-394. 10.1038/ncb2958.

Mangeat, B., Gers-Huber, G., Lehmann, M., Zufferey, M., Luban, J., and Piguet, V. (2009). HIV-1 Vpu neutralizes the antiviral factor Tetherin/BST-2 by binding it and directing its beta-TrCP2-dependent degradation. PLoS Pathog *5*, e1000574. 10.1371/journal.ppat.1000574.

Murata, T., Takayama, K., Katayama, S., Urano, T., Horie-Inoue, K., Ikeda, K., Takahashi, S., Kawazu, C., Hasegawa, A., Ouchi, Y., et al. (2010). miR-148a is an androgen-responsive microRNA that promotes LNCaP prostate cell growth by repressing its target CAND1 expression. Prostate Cancer Prostatic Dis *13*, 356-361. 10.1038/pcan.2010.32.

Nähse, V., Christ, L., Stenmark, H., and Campsteijn, C. (2017). The Abscission Checkpoint: Making It to the Final Cut. Trends Cell Biol *27*, 1-11. 10.1016/j.tcb.2016.10.001.

Nakayama, K.I., and Nakayama, K. (2005). Regulation of the cell cycle by SCF-type ubiquitin ligases. Semin Cell Dev Biol *16*, 323-333. 10.1016/j.semcdb.2005.02.010.

Nguyen, K.M., and Busino, L. (2020). The Biology of F-box Proteins: The SCF Family of E3 Ubiquitin Ligases. Adv Exp Med Biol *1217*, 111-122. 10.1007/978-981-15-1025-0_8.

Olma, M.H., and Dikic, I. (2013). Cullins getting undressed by the protein exchange factor Cand1. Cell *153*, 14-16. 10.1016/j.cell.2013.03.014.

Petroski, M.D., and Deshaies, R.J. (2005). Function and regulation of cullin-RING ubiquitin ligases. Nat Rev Mol Cell Biol *6*, 9-20. 10.1038/nrm1547.

Pierce, N.W., Lee, J.E., Liu, X., Sweredoski, M.J., Graham, R.L., Larimore, E.A., Rome, M., Zheng, N., Clurman, B.E., Hess, S., et al. (2013). Cand1 promotes assembly of new SCF complexes through dynamic exchange of F box proteins. Cell *153*, 206-215. 10.1016/j.cell.2013.02.024.

Reitsma, J.M., Liu, X., Reichermeier, K.M., Moradian, A., Sweredoski, M.J., Hess, S., and Deshaies, R.J. (2017). Composition and Regulation of the Cellular Repertoire of SCF Ubiquitin Ligases. Cell *171*, 1326-1339 e1314. 10.1016/j.cell.2017.10.016.

Rock, K.L., Gramm, C., Rothstein, L., Clark, K., Stein, R., Dick, L., Hwang, D., and Goldberg, A.L. (1994). Inhibitors of the proteasome block the degradation of most cell proteins and the generation of peptides presented on MHC class I molecules. Cell *78*, 761-771. 10.1016/s0092-8674(94)90462-6.

Salon, C., Brambilla, E., Brambilla, C., Lantuejoul, S., Gazzeri, S., and Eymin, B. (2007). Altered pattern of Cul-1 protein expression and neddylation in human lung tumours: relationships with CAND1 and cyclin E protein levels. The Journal of pathology *213*, 303-310.

Sarikas, A., Hartmann, T., and Pan, Z.Q. (2011). The cullin protein family. Genome Biol *12*, 220. 10.1186/gb-2011-12-4-220.

Silk, A.D., Holland, A.J., and Cleveland, D.W. (2009). Requirements for NuMA in maintenance and establishment of mammalian spindle poles. J Cell Biol *184*, 677-690. 10.1083/jcb.200810091.

Skaar, J.R., Pagan, J.K., and Pagano, M. (2013). Mechanisms and function of substrate recruitment by F-box proteins. Nat Rev Mol Cell Biol *14*, 369-381. 10.1038/nrm3582.

Skaar, J.R., Pagan, J.K., and Pagano, M. (2014). SCF ubiquitin ligase-targeted therapies. Nat Rev Drug Discov *13*, 889-903. 10.1038/nrd4432.

Soucy, T.A., Smith, P.G., Milhollen, M.A., Berger, A.J., Gavin, J.M., Adhikari, S., Brownell, J.E., Burke, K.E., Cardin, D.P., Critchley, S., et al. (2009). An inhibitor of NEDD8-activating enzyme as a new approach to treat cancer. Nature *458*, 732-736. 10.1038/nature07884.

Sun, X., Qi, H., Zhang, X., Li, L., Zhang, J., Zeng, Q., Laszlo, G.S., Wei, B., Li, T., Jiang, J., et al. (2018). Src activation decouples cell division orientation from cell geometry in mammalian cells. Biomaterials *170*, 82-94. 10.1016/j.biomaterials.2018.03.052.

Telentschak, S., Soliwoda, M., Nohroudi, K., Addicks, K., and Klinz, F.J. (2015). Cytokinesis failure and successful multipolar mitoses drive aneuploidy in glioblastoma cells. Oncol Rep *33*, 2001-2008. 10.3892/or.2015.3751.

Wu, S., Zhu, W., Nhan, T., Toth, J.I., Petroski, M.D., and Wolf, D.A. (2013). CAND1 controls in vivo dynamics of the cullin 1-RING ubiquitin ligase repertoire. Nat Commun *4*, 1642. 10.1038/ncomms2636.

Zemla, A., Thomas, Y., Kedziora, S., Knebel, A., Wood, N.T., Rabut, G., and Kurz, T. (2013). CSN- and CAND1-dependent remodelling of the budding yeast SCF complex. Nat Commun *4*, 1641. 10.1038/ncomms2628.

Zheng, N., Schulman, B.A., Song, L., Miller, J.J., Jeffrey, P.D., Wang, P., Chu, C., Koepp, D.M., Elledge, S.J., Pagano, M., et al. (2002). Structure of the Cul1-Rbx1-Skp1-F boxSkp2 SCF ubiquitin ligase complex. Nature *416*, 703-709. 10.1038/416703a.

Zheng, N., Wang, Z., and Wei, W. (2016a). Ubiquitination-mediated degradation of cell cycle-related proteins by F-box proteins. Int J Biochem Cell Biol *73*, 99-110. 10.1016/j.biocel.2016.02.005.

Zheng, N., Zhou, Q., Wang, Z., and Wei, W. (2016b). Recent advances in SCF ubiquitin ligase complex: Clinical implications. Biochim Biophys Acta *1866*, 12-22. 10.1016/j.bbcan.2016.05.001.

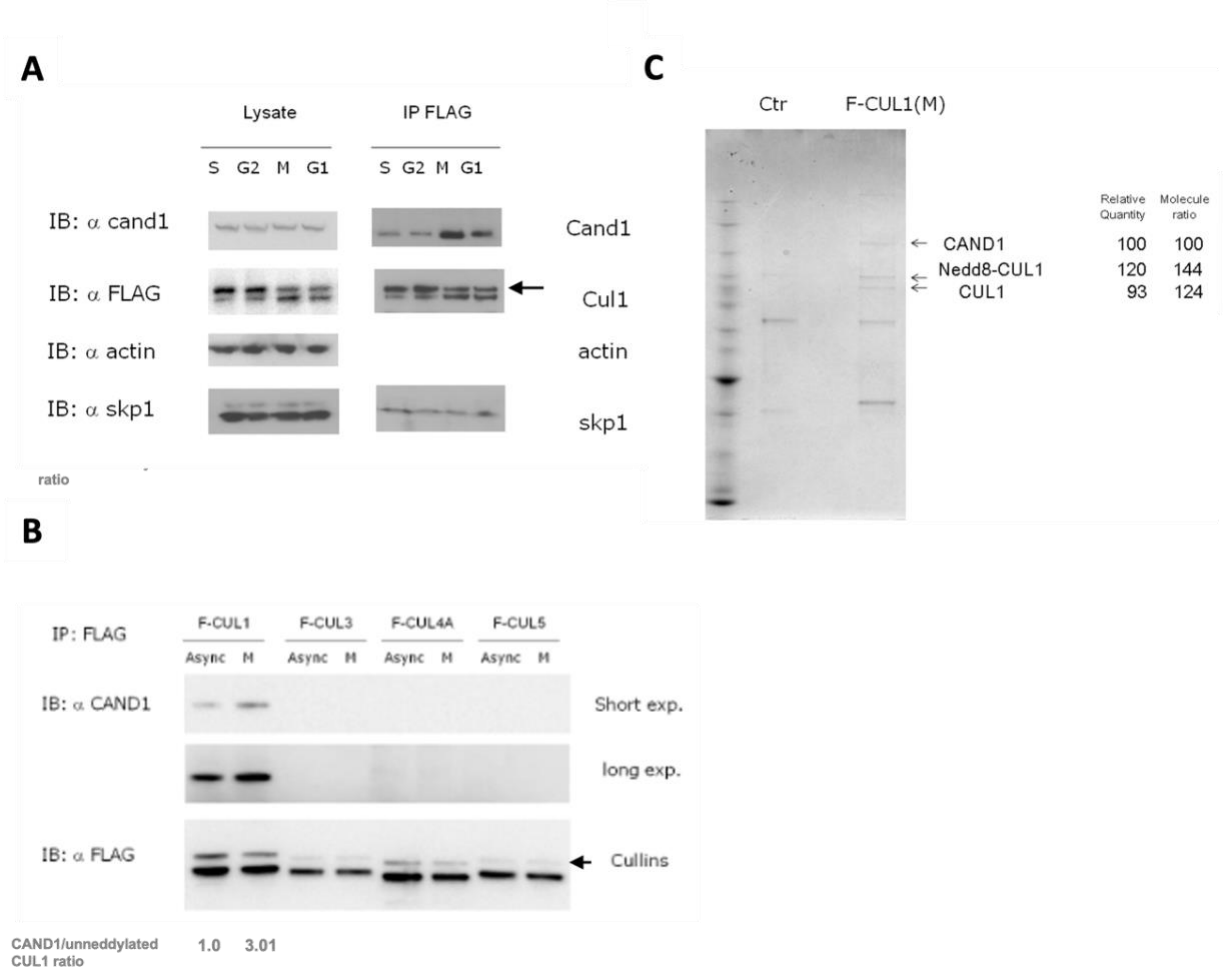
A
Lysate
IP FLAG
S G2 M G1
S G2 M G1
IB: α cand1
IB: α FLAG
IB: α actin
IB: α skp1
Cand1
Cul1
actin
skp1
ratio
B
IP: FLAG
F-CUL1
F-CUL3
F-CUL4A
F-CUL5
Async M
Async M
Async M
Async M
IB: α CAND1
Short exp.
long exp.
IB: α FLAG
Cullins
CAND1/unneddylated CUL1 ratio
1.0 3.01
C
Ctr
F-CUL1(M)
Relative Quantity
Molecule ratio
CAND1 100 100
Nedd8-CUL1 120 144
CUL1 93 124

Figure. 3.1. CAND1 has increased interaction with CUL1 during mitosis.

A. Stronger CAND1 binding to CUL1 in Mitosis than in G1, S, and G2 phases.

A HEK293T FLAG-CUL1 stable cell line was synchronized at G1, S, G2, and M phases. FLAG-CUL1 was immunoprecipitated, and analyzed by western blot (immunoblot, IB) probed with the indicated antibodies. When comparing the ratio of CAND1 to FLAG-CUL1 levels, the mitotic fraction has a higher ratio of CAND1 to CUL1 levels than in other cell cycle phases.

B. CAND1 stably interacts with CUL1 (but not other cullins).

HEK293T cells stably expressing FLAG-CUL1, 3, 4A, and 5 (both asynchronous and mitotic cells) were used for immunoprecipitation of FLAG-CUL proteins, and then probed for CAND1. Only CUL1 exhibited stable interaction with CAND1. The ratio of CAND1 to CUL1 increased from 1.0 in asynchronous cells to 3.0 in mitotic cells. (Images provided by KW Min)

C. The majority of unneddylated CUL1 interacts with CAND1 in Mitosis.

FLAG-CUL1 was immunoprecipitated from FLAG-CUL1 HEK293T cells synchronized in mitosis by thymidine block and release into nocodazole arrest. The control cells are asynchronous HEK293T cells, which was not pretreated before collection. Immunoprecipitated proteins were eluted with FLAG peptide, followed by SDS PAGE and Coomassie G-250 staining. The ratio of CAND1 to unneddylated CUL1 during mitosis indicates that 91% of the unneddylated CUL1 is occupied by CAND1. (Images provided by KW Min)

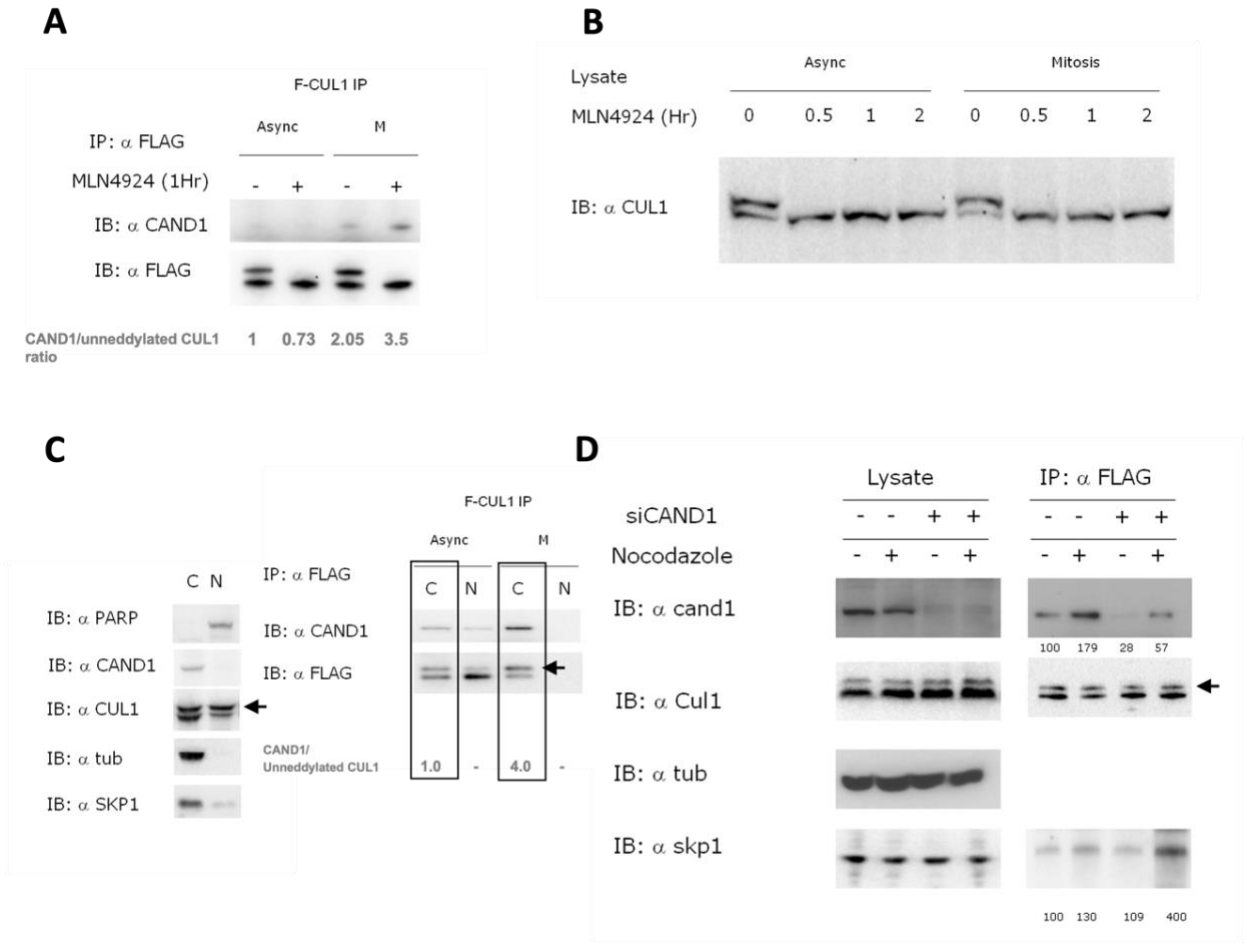

Figure. 3.2. Increased CAND1 interaction with CUL1 during mitosis does not correlate with neddylation

A. CAND1 has increased binding to mitotic CUL1 irrespective of neddylation status. HEK293T cells expressing FLAG-CUL1 were treated with (+) or without (–) the neddylation inhibitor MLN4924. FLAG-CUL1 was immunoprecipitated and analyzed by WB after probing with the indicated antibodies. In the absence of MLN4924, the ratio of CAND1 bound to CUL1 increased 2-fold from asynchronous to mitosis, while inhibiting neddylation did not increase CAND1 binding in asynchronous cells. Neddylated FLAG-CUL1 is the upper band, unneddylated FLAG-CUL1 is the lower band.

B. Deneddylation of CUL1 still occurs rapidly during mitosis.

MLN4924 was added to asynchronous vs. mitotic HEK293T cells expressing FLAG-CUL1 at time 0. Cells were harvested at the indicated time points and analyzed by western blot with anti-CUL1 antibody. No change in the rate of deneddylation was observed between asynchronous and mitotic cells.

C. Increased CAND1–CUL1 interaction is not due the abundance of CUL1 in the cytosol.

Cytoplasmic (C), or nuclear (N) fractions of HEK293T cells expressing FLAG-CUL1cell lysates were analyzed by western blot with the indicated antibodies. Immunoblots of anti-α-tubulin (a cytoplasmic marker) and anti-PARP-1 (a nuclear marker) demonstrate the purity of the fractionation.

FLAG-CUL1 was immunoprecipitated with FLAG agarose beads then analyzed by WB after probing with the indicated antibodies. 4.3 fold more CAND1 was bound to unneddylated CUL1 in mitosis (mitosis).

(Images provided by KW Min)

D. Knockdown of CAND1 and CAND2 increases SKP1–CUL1 interaction in mitosis.

HEK293T-FLAG-CUL1 cells were treated with control (–) or CAND1/2 siRNA (+) and with (+) or without (–) nocodazole. FLAG-CUL1 was immunoprecipitated and then analyzed by WB after probing with the indicated antibodies. CAND1/2 knockdown increased SKP1 binding to CUL1 by 4-fold.

A

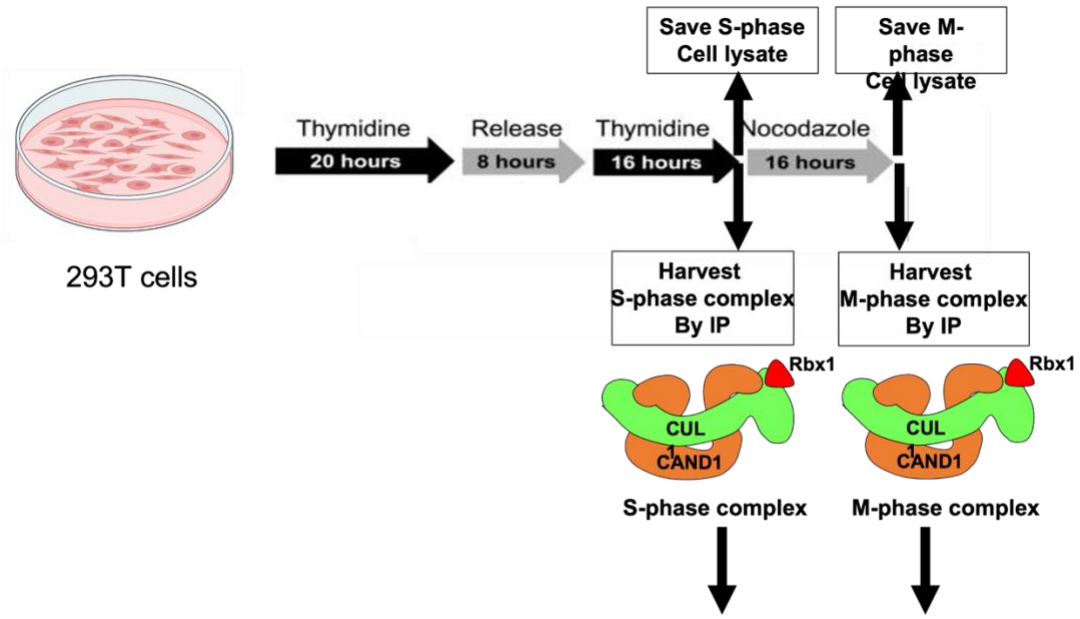

1. 0 min – before adding the complex to the lysate
2. x min – incubate the IPed beads in S/M phase lysate for x minute of time and complete IP western

B

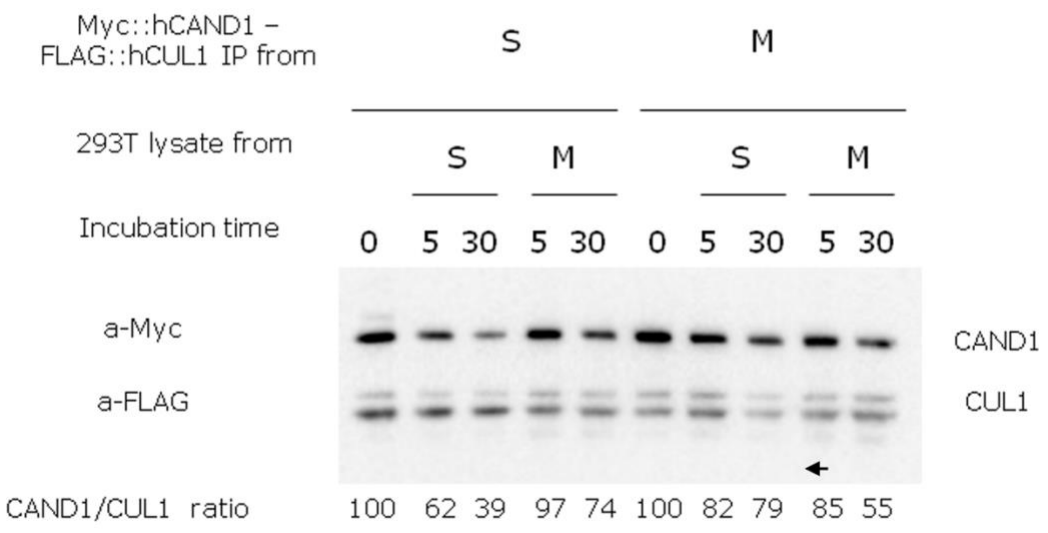

Figure. 3.3. Differential interaction of CAND1 with CUL1 in mitosis is due to variation between S-phase and mitotic CAND1-CUL1 complexes and lysates.

A. Cartoon image summarizing the experimental procedure to test the stability of S-phase and M-phase CAND1–CUL1 complexes in S-phase vs. M-phase lysates. Myc-CAND1 and FLAG-CUL1 were co-expressed in HEK293T cells, synchronized by double thymidine block (for S phase) and thymidine-nocodazole block (for M phase arrest), and immunoprecipitated using FLAG-M2 agarose beads. Each complex was then incubated with untransfected HEK293T cell lysates (S or M phase arrested), followed by 3 times washing and WB analysis blot with the indicated antibodies.

B. Mitotic CAND1–CUL1 complex is more stable and there is differences in dissociation activity of S- and M-phase lysates.

   The amount of Myc-CAND1 remain bound to CUL1 in the M-phase complex is higher at 5 min and 30 mins, compared to the S-phase complex (when both the complexes are in S-phase lysate). The amount of Myc-CAND1 remain bound to CUL1 in the S-phase complex in mitotic lysate is higher at 5 min and 30 mins, compared to the S-phase complex in S-phase lysate. (Images provided by KW Min)

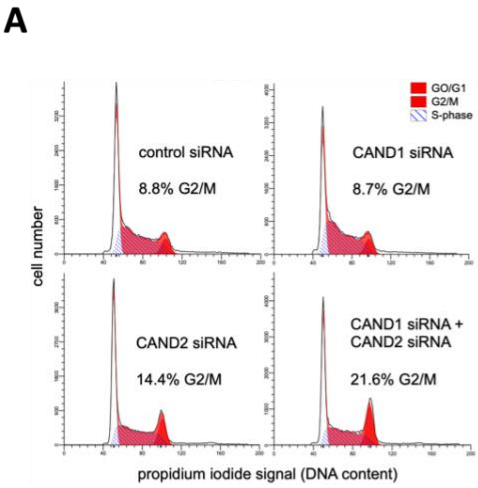
A
GO/G1
G2/M
S-phase
control siRNA
8.8% G2/M
CAND1 siRNA
8.7% G2/M
CAND2 siRNA
14.4% G2/M
CAND1 siRNA +
CAND2 siRNA
21.6% G2/M
cell number
propidium iodide signal (DNA content)

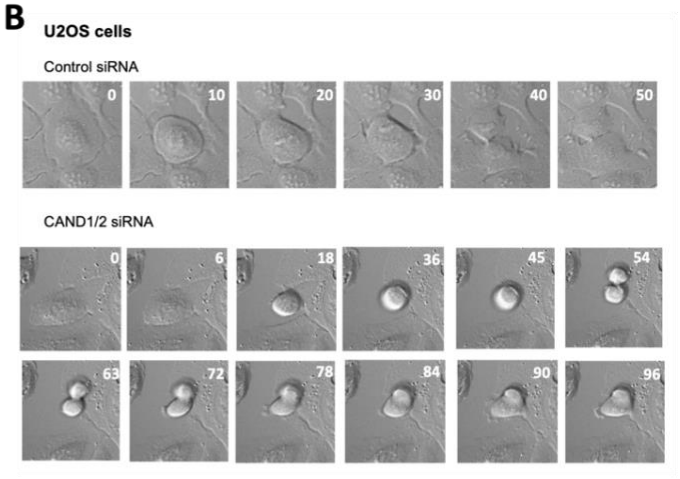
B
U2OS cells
Control siRNA
0
10
20
30
40
50
CAND1/2 siRNA
0
6
18
36
45
54
63
72
78
84
90
96

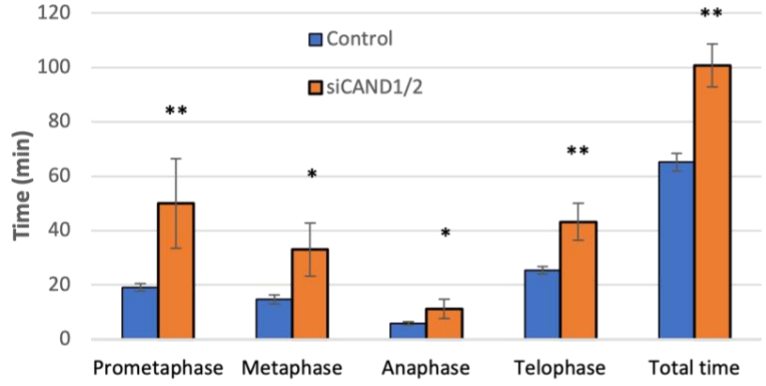
C
Mitotic timing of U2OS cells
Control
siCAND1/2
Time (min)
120
100
80
60
40
20
0
**
*
*
**
**
Prometaphase
Metaphase
Anaphase
Telophase
Total time

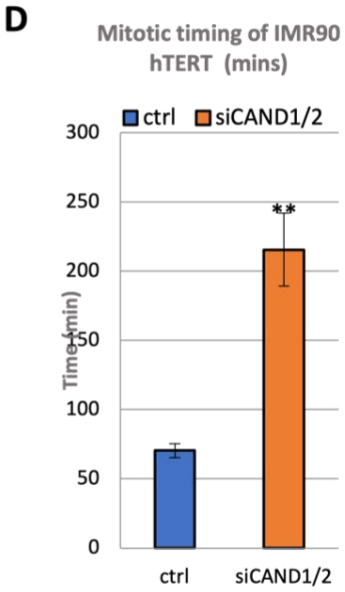
D
Mitotic timing of IMR90
hTERT (mins)
ctrl
siCAND1/2
Time (min)
300
250
200
150
100
50
0
**
ctrl
siCAND1/2

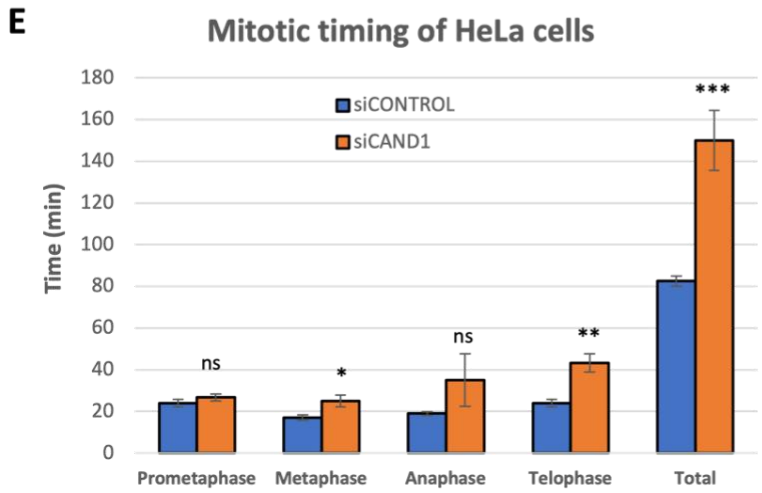
E
Mitotic timing of HeLa cells
siCONTROL
siCAND1
Time (min)
180
160
140
120
100
80
60
40
20
0
ns
*
ns
**
***
Prometaphase
Metaphase
Anaphase
Telophase
Total

Figure. 3.4. CAND1 & CAND2 are required for normal mitotic progression.

A. Double Knockdown of CAND1 and CAND2 increases the percentage of cells in G2-M in asynchronous cells.

   Flow cytometry profiles of DNA content of HEK293T cells transfected with siRNA for control, CAND1, CAND2, and CAND1 and CAND2.

B. Double Knockdown of CAND1 and CAND2 causes a mitotic arrest.

   DIC micrographs of U2OS cells treated with the indicated siRNAs as they progress through mitosis. Timing in minutes is shown in the top right corner of images; the 0 time point denotes nuclear envelope breakdown. The last time point reflects mitotic exit.

C. Bar graph of mitotic timing ± SEM for siRNA treated U2OS cells.

   Timing data from two to four independent experiments are summarized in the graph; for the conditions listed from top to bottom, n = 18, 9, respectively.

D. Bar graph of total mitotic timing ± SEM for siRNA treated hTERT IMR90 cells.

   Timing data from two independent experiments are summarized in the graph; for the conditions listed from top to bottom, n=34, and 32, respectively.

E. Bar graph of total mitotic timing ± SEM for siRNA treated HeLa cells.

   Timing data from two independent experiments are summarized in the graph; for the conditions listed from top to bottom, n=10, and 9, respectively.

   *, $P < 0.05$; **, $P < 0.005$.

A

HeLa cells treated with control siRNA - DIC

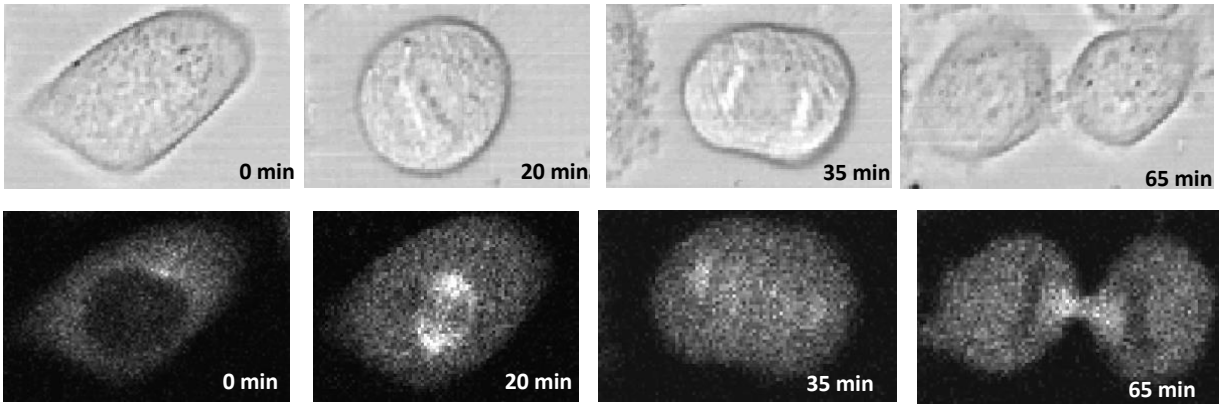

HeLa cells treated with CAND1 siRNA - DIC

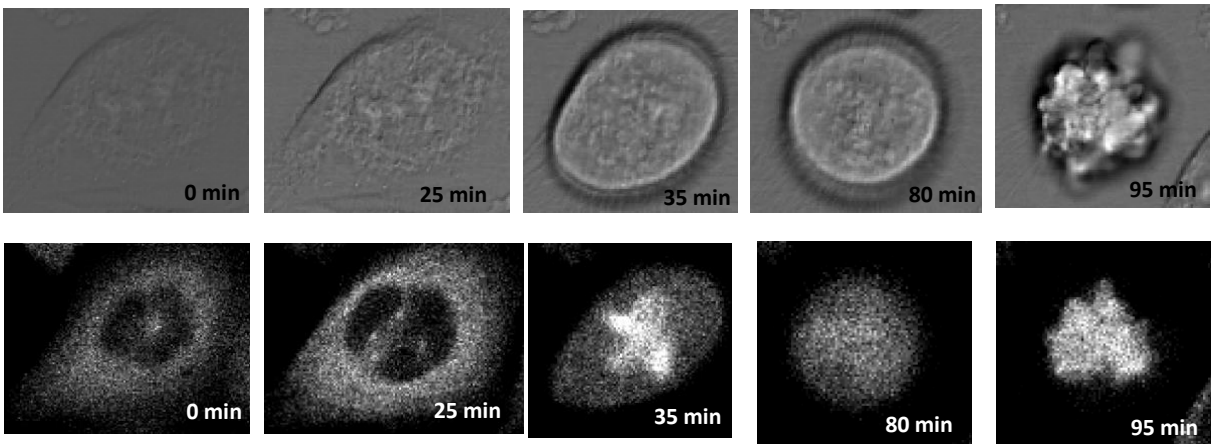

B

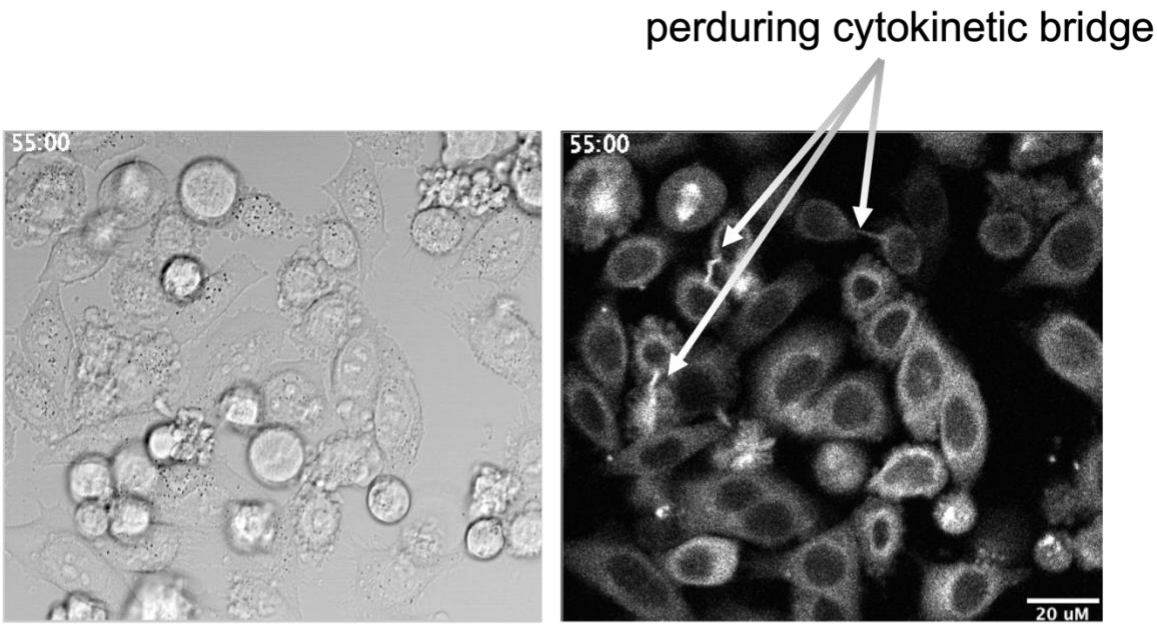
perduring cytokinetic bridge
55:00
55:00
20 uM

C

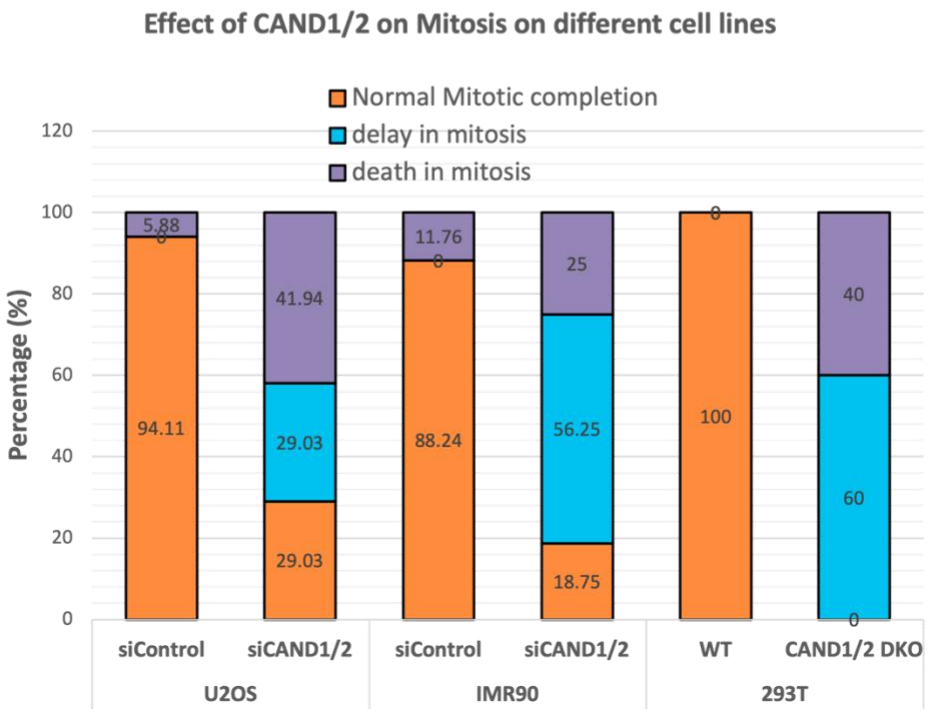
Effect of CAND1/2 on Mitosis on different cell lines
Normal Mitotic completion
delay in mitosis
death in mitosis
Percentage (%)
120
100
80
60
40
20
0
5.88
0
94.11
41.94
29.03
29.03
11.76
0
88.24
25
56.25
18.75
0
100
40
60
0
siControl
siCAND1/2
siControl
siCAND1/2
WT
CAND1/2 DKO
U2OS
IMR90
293T

Figure. 3.5. Inactivating CAND1/2 causes mitotic defects.

A. Matching DIC and epifluorescence micrographs of HeLa cell expressing alpha-Tubulin-YFP treated with control and CAND1 siRNA, in which CAND1 treated cell showing multipolar spindle and cell death at completing.
B. Matching DIC and epifluorescence micrograph at a given time, of HeLa cells expressing alpha-Tubulin-YFP treated with CAND1 siRNA.
C. Mitotic phenotypes: % of cells that undergo normal mitosis vs shows delay in mitosis vs cell death during or after completing mitosis.

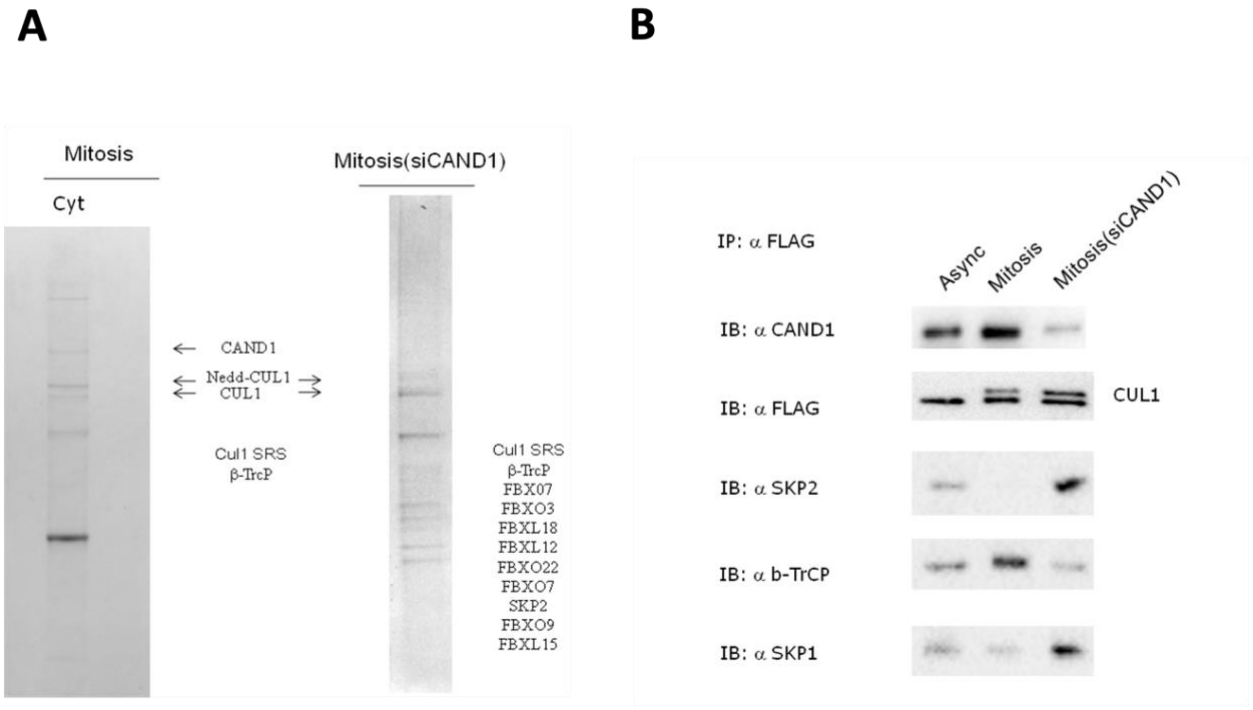

Figure. 3.6. SCF complexes undergo subunit reorganization during mitosis that is dependent on CAND1.

A. CAND1 affects SR loading onto SCF complexes during mitosis.

   Asynchronous and mitotic FLAG-CUL1 HEK293T cells were transfected with control or CAND1/2 siRNA. The cells were lysed and immunoprecipitated with FLAG M2 agarose beads. The immunoprecipitated protein complexes were eluted using FLAG peptide, followed by SDS PAGE and Coomassie G-250 staining. Protein complexes were analyzed by LC-MS/MS. (The proteins listed next to the Coomassie gel, are the proteins detected through LC-MS/MS after IP) (Images provided by KW Min)

B. Cells were treated and collected as described in (B) and then analyzed by western blot probed with the indicated antibodies.

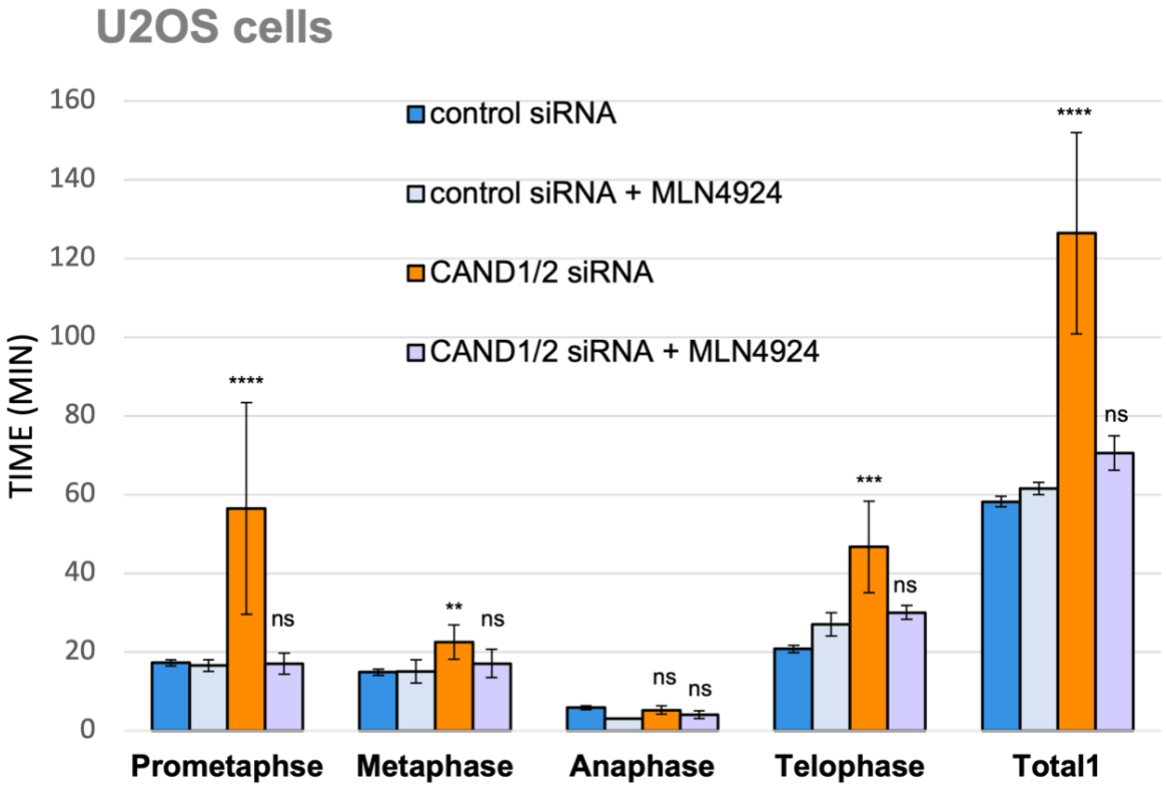

Figure. 3.7. Effect of CAND1/2 knockdown has been rescued by MLN4924 treatment.

Bar graph of the timing of mitotic stages ± SEM for control and CAND1/2 siRNA treated U2OS cells.

Timing data from two independent experiments are summarized in the graph; for the conditions listed from top to bottom, n = 16, 10, 8, and 6, respectively.

*, P < 0.05; **; P < 0.005; ***, <0.0005

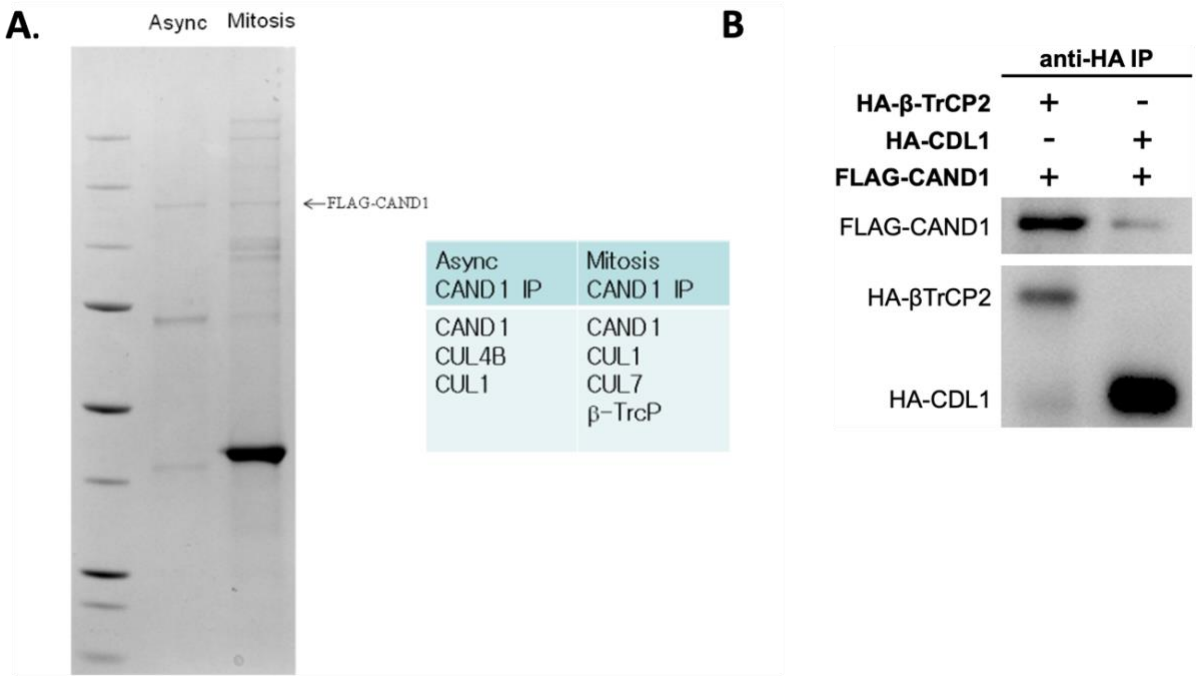

Figure. 3.8. CAND1 interacts with SCF^{FBXW11}

A. CAND1 binds to β-TrCP2/FBXW11 in mitosis.

Asynchronous and mitotic (release of thymidine block into nocodazole arrest) FLAG-CAND1 HEK293T cells were lysed and immunoprecipitated with FLAG M2 agarose beads. The protein complexes were eluted using FLAG peptide solution and followed by SDS PAGE and Coomassie G-250 staining. Protein complexes were analyzed by LC-MS/MS. 1st column of the blue box lists the proteins that are IPed with asynchronous FLAG-CAND1. The second column lists the proteins IPed with mitotic FLAG-CAND1. CAND1 shows to interact with cullins except in mitosis where is interacts with a SR- β-TrCP (Images provided by KW Min)

B. CAND1 physically interacts with the SR β-TrCP2/FBXW11.

pGLUE-β-TrCP2/FBXW11 was transfected into FLAG-CAND1 HEK293T cells. The cells were lysed and immunoprecipitated with FLAG M2 agarose beads. The immunoprecipitated proteins were analyzed by western blot probed with the indicated antibodies. HA-CDL-1 was transfected as a negative control.

CHAPTER 4

THE ROLE OF *CAENORHABDITIS ELEGANS* FOLATE RECEPTOR IN NEURONAL SIGNALING

Fathima Zahra Nawaz and Edward T. Kipreos* "*Caenorhabditis elegans* folate receptor FOLR-1 in neuronal signaling" to be submitted to *Current Biology*

Abstract

Folate (vitamin B_9) is an essential nutrient that is required for one-carbon metabolism. Emerging evidence indicates that vertebrate folate receptors have functions that do not rely on one-carbon metabolism. We have discovered a novel role for the C. elegans protein FOLR1 in neuronal signaling. We have identified that FOLR-1 expresses in the adult C. elegans NSM neurons, localizing in the two major processes. We also identify GON-2, a calcium channel protein that is required for calcium entry into the NSM neuron upon its activation by adding folate, physically interact with the FOLR-1 protein, and co-localize in the same NSM processes, suggesting a direct mechanism through which FOLR-1 promotes calcium entry during neuronal activation. This proposed study will elucidate the molecular pathway(s) by which folates function in neuronal signaling in *C. elegans*. Definitive results would provide a model to spur and guide research to explore potential non-canonical human folate pathways. The majority of *C. elegans* signaling pathways are conserved in humans, and so this study will have direct implications for folate signaling in humans.

Introduction

Folates cannot be synthesized de novo by animals, and hence are classified as an essential vitamin that must be obtained through diet or microbiota. *C. elegans,* like other animals relies on dietary folates for one-carbon metabolism. Folate deficiency in *C. elegans* has resulted in severe reduction in germ cell number and sterility (Austin et al., 2010).

Emerging evidence suggests that vertebrate folate receptors have functions that do not rely on one-carbon metabolism. There are several settings in vertebrates in which folates appear to act independently of one-carbon metabolism, including neural tube defects (NTDs) and cancer. Folate deficiency is a significant risk factor for NTDs, wherein the developing neural tube fails to close, exposing the spinal cord or brain (Copp et al., 2013). In *Xenopus*, neural tube closure depends on FOLR1, which is required for proper morphogenetic movements (Balashova et al., 2017). Notably, it has been suggested that FOLR1 promotes *Xenopus* neural tube closure independently of one-carbon metabolism (Balashova *et al.*, 2017). This conclusion was based on the use of different DHFR inhibitors, all of which block one-carbon metabolism. DHFR inhibitors that prevent FOLR1 from binding to folate induced NTDs, while DHFR inhibitors that did not affect FOLR1 binding to folate did not induce NTDs (Balashova *et al.*, 2017). Based on this, the authors suggested that NTDs result from the disruption of FOLR1 binding to folate rather than from the inhibition of one-carbon metabolism (Balashova *et al.*, 2017).

FOLR-1 is not required to provide folates for one-carbon metabolism. Rather, the reduced folate carrier (RFC) mediates the bulk of folate uptake (~78%) in *C. elegans* (Balamurugan et al., 2007), just as is observed in mammals (Zhao et al., 2009). RFC mutants are folate deficient and therefore produce very few germ cells (Austin *et al.*, 2010). In contrast, *folr-1* mutants have normal numbers of germ cells and eggs (Chaudhari et al., 2016).

Bacterial folates arising from the *C. elegans* diet acts as an exogenous signal to stimulate the adult germ stem cell population (Chaudhari *et al.*, 2016). This germ cell stimulatory activity has only been observed with the folates 10-formyl-THF-Glu_n and 5,10-methenyl-$THFGlu_n$ (which converts to 10-formyl-THF-Glu_n at physiological pH) and the stimulation depends on the presence of FOLR-1. The role of folates in germ cell proliferation appears to be independent of its role in one-carbon metabolism based on several lines of evidence (Chaudhari *et al.*, 2016). Most significantly, dihydropteroate (DHP), a pteroate that cannot function in one-carbon metabolism, also increases the germ cell proliferation rate in a FOLR-1-dependent manner. Pteroates have the same pteridine ring–PABA structure as folates but lack glutamates. Animals cannot convert pteroates to folates to function in one-carbon metabolism (Suckling et al., 1977). Consistently, DHP is unable to act as a vitamin to rescue folate deficiency in *C. elegans* (Chaudhari *et al.*, 2016). Nevertheless, DHP stimulates DNA replication in isolated germ cells and germ cell proliferation in both wild type animals and tumorous germline mutants at low (nM) concentrations (Chaudhari *et al.*, 2016). Thus, DHP stimulates increased germ cell proliferation independently of one-carbon metabolism.

FOLR-1 has a predicted signal peptide and a transmembrane domain that suggests cell surface localization (Cserzo et al., 2002; Petersen et al., 2011; Suh and Hutter, 2012). Recently it has been showed that starved *C. elegans*, when placed on agar plates near bacteria, move toward the bacterial food, but upon reaching the bacteria, they transiently stop their forward motion within 1-3 seconds (Iwanir et al., 2016). This "stopping" behavior is controlled by two NSM neurons that are located within the pharynx, the organ that ingests bacteria (Gurel et al., 2012; Iwanir *et al.*, 2016).

The NSM neurons release serotonin to paralyze the body wall muscles, so that animals stop their forward movement when encountering bacteria (Gurel *et al.*, 2012). The *folr-1* gene is expressed in the NSM neurons (Spencer et al., 2014). When *folr-1* mutants encounter bacteria, they fail to stop and instead slowly continue their forward motion (E.T.K. unpublished data). This indicates that FOLR-1 is required for the full stopping behavior. In contrast, RFC mutants, which are severely depleted for folates for use in metabolism (Austin *et al.*, 2010) stop normally in response to bacteria, indicating that folate deficiency does not affect the stopping behavior (E.T.K. unpublished data). The molecular pathway through which FOLR-1 promotes NSM stopping behavior is not known.

Neurotransmitter release is generally triggered by an influx of Ca^{2+} driven by a Ca^{2+} channel. Identifying the channel that mediates Ca^{2+} entry into the NSM neurons is important for understanding how FOLR-1 regulates NSM activation, as we expect the channel to function with or downstream of FOLR-1. Our laboratory has found that the GON-2 TRPM calcium channel is required for the full NSM-mediated stopping behavior and partially contributes to full NSM activation (E.T.K. unpublished data).

This study explores the subcellular localization of FOLR-1 and GON-2 in NSM neurons and describes a previously unrecognized physical interaction between the folate receptor FOLR-1 and the *C. elegans* TRPM channel GON-2. These results suggest a novel signaling pathway in *C. elegans* NSM neurons.

Results

Subcellular localization of FOLR-1 in the NSM neurons

The signal from bacteria that causes the NSM neurons to initiate the stopping behavior is not known. The previous paper by Spencer et al had reported that FOLR-1 was expressed in the

NSM of the L1 larvae (Spencer *et al.*, 2014), we wanted to know if FOLR-1 was expressed in the NSM of adults.

To identify the tissues in which FOLR-1 functions to allow NSM activation, we have analyzed Pfolr1::FOLR-1::GFP driven by its own promoter from an extrachromosomal array (Fig. 4.1). We observe expression of Pfolr-1::FOLR-1::GFP in the NSM neurons, the isthmus of the pharynx, and the pharyngeal-intestinal valve cell. The expression of FOLR-1::GFP in the isthmus obscures the localization of Pfolr-1::FOLR-1::GFP in the NSM neuronal processes, which are embedded within the isthmus.

To more clearly visualize the subcellular localization of FOLR-1 with the NSM neurons, we created constructs that expresses FOLR-1:: wrmScarlet and a membrane-localized myr-mNeonGreen specifically in the NSM neurons using the *tph-1* promoter, which is expressed in the NSM neurons (Sze et al., 2000) (Fig. 4.3). The membrane-localized myristoylated myr-mNeonGreen is used to highlight the NSM neuronal processes. We generated strains with both of these expression constructs in an extrachromosomal array. Analysis of these transgenic animals shows that FOLR-1::wrmScarlet is present in the two large NSM neuronal processes, but not in the thin process – extending about two-thirds of the length of the neuronal processes from the cell body.

Role of the GON-2 calcium channel in the NSM neuron

Ca^{2+} influxes generally trigger neurotransmitter release. The Ca^{2+} influx is driven by a Ca^{2+} channel. We have found that the GON-2 TRPM calcium channel is required for the full NSM-mediated stopping behavior and is partially required for NSM activation. We hypothesize that GON-2 functions as a component of the folate-signaling pathway in the NSM neuron.

To determine if GON-2 is expressed in the NSM neurons (and where in the neurons), the GFP-tagged *gon-2* locus was co-expressed with Ds-Red2 reporter expressed in the NSM neuron. We see that the GON-2 is localized in the two large NSM neuronal processes (Fig. 4.4).

FOLR-1 is required for calcium entry into NSM neurons in *C. elegans* (E. T. K unpublished data), yet the molecular pathway by which FOLR1 promotes the calcium entry is not known. Based on this information we wanted to know if both FOLR-1 and GON-2 are colocalize in the NSM neurons.

We used a worm strain with GFP tagged *folr-1,* co-expressed with the Ds-Red2 reporter expressed in the NSM neuron, and observed FOLR-1 to colocalize with the same reporter protein which was co-localized with GON-2.

FOLR1 physically interacts with GON-2 calcium channel

Since we observed colocalization of FOLR1 with GON-2, we hypothesize that FOLR-1 may directly regulate GON-2 activity, and it may do so by physically interacting with GON-2. Thus, we wanted to test for physical interaction between FOLR-1 and GON-2., as a direct physical interaction of FOLR-1 and the calcium channel was more likely if this was an evolutionarily conserved pathway. The *C.elegans gon-2* is a very large gene with a coding region of over 6000 bp. We had the cDNA for *gon-2* synthesized in three pieces and then combined those together to form the full cDNA. The gene synthesis also allowed us to optimize the codons for expression in human cells.

We then co-expressed 3xHA-FOLR-1 and 3xFLAG-GON-2 ectopically in both human HEK293T and HeLa cells and used co-immunoprecipitation to determine if the two proteins physically interact with each other. We used 3xFLAG-FBW7 (FBW7 is a F-box protein, that is

not known to associate with FOLR1) and 3xHA-Rab23WT (Rab23 is a small GTPase, that control membrane trafficking, that is not known to associate with FOLR1) as negative controls.

When we Immunoprecipitated the HA tagged proteins, we saw that 3xFLAG-GON2, co-immunoprecipitated with FOLR1, but not with the beads nor the negative control (Fig. 4.6). Similarly, immunoprecipitating FLAG tagged proteins, we observed 3xHA-FOLR1 to co-immunoprecipitated with GON2, not with the negative controls. Our data suggest that there is physical interaction between 3xFLAG-GON-2 and 3xHA-FOLR-1.

Once we observed a physical interaction with between the FOLR1 and GON2, we wanted to determine if we could detect their localization in the cell. We, co-transfected both 3xFLAG-GON2 and 3xHA-FOLR1 ectopically into HEK 293T cells, then confirmed that FOLR-1 colocalizing with GON-2 by expressing 3xHA-FOLR-1 and 3XFLAG-GON-2 in HEK 293T cells (Fig. 4.7).

Discussion

Through this work we have discovered that FOLR-1 and the calcium channel GON-2 both localize to the NSM neurons. FOLR-1 and GON-2 both promote calcium entry into the NSM neuron upon its activation when starved animals encounter bacteria. When NSM neurons are activated, they release serotonin to transiently paralyze body wall muscles so that animals stop their forward movement when encountering bacteria. This work shows that FOLR-1 and GON-2 physically interact. This result suggests a direct mechanism through which FOLR-1 promotes calcium entry to initiate neuronal activation and control behavior.

We hypothesize that the folate that is found in the bacteria is acting as a signaling molecule, to stimulate this behavior. Previous work done by our lab describes a novel signaling role of a stimulatory folate (10-formyl-THF) in germ stem cell proliferation (Chaudhari *et al.*, 2016). It's

reasonable to question why two different tissues (neurons and germ cells) use folate as a signal. We hypothesize that *C. elegans* uses stimulatory folate as a marker for the presence of live bacteria, the NSM "stopping" behavior functions under food-limiting conditions and allows animals who encounter small clumps of bacteria to stop quickly to eat the bacteria.

A study conducted by Rhoades et al have described a different mechanism to regulate the same stopping behavior (Rhoades et al., 2019). Here, the novel acid-sensing ion channels (ASICs) DEL-3 and DEL-7 are required to activate NSM in response to bacteria (Rhoades *et al.*, 2019). The ASICs DEL-3 and DEL-7 are Na^+ channels, for which the ligand is unknown (Rhoades *et al.*, 2019). DEL-3 and DEL-7 channels are expressed in the thin NSM neuronal process at the point that it touches the grinder in the posterior pharyngeal bulb. The proximity of the ASICs to the site of the mechanical disruption of bacteria in the grinder of the posterior bulb, suggests that those channels are directly involved in transducing sensory input that can be amplified by the NSM (Rhoades *et al.*, 2019).

Unlike the ASICS, we find that both the FOLR-1 and GON-2 are expressed in the two large neuronal processes of the NSM, but not in the thin process. Therefore, FOLR-1 and GON-2 are localized further from the lumen of the pharynx (Fig. 1-4). An additional neuronal process from NSM contacts the lumen of the anterior pharyngeal bulb (WormAtlas; https://www.wormatlas.org/neurons/Individual%20Neurons/NSMframeset.html). However, this process is so thin that it does not appear in fluorescence images and was only detected by transmission electron microscopy (WormAtlas). It is thus possible that FOLR-1 and/or GON-2 may be localized to this lumen contact point, but we have not observed this in our images (data not shown).

Alternatively, it is possible that FOLR-1 receives stimulatory folate via an indirect route. We can postulate that the FOLR-1 that is present in the lumen of the isthmus of the pharynx, which connects the posterior and anterior bulbs transports folate into the pharynx, where it can interact with the FOLR-1 in the large NSM processes. Alternatively, FOLR-1 is highly expressed in the vpi1 pharyngeal-intestinal valve cell that is localized immediately after the pharynx (Fig. 1.3). FOLR-1is thus be positioned to bind stimulatory folate soon after the bacteria were disrupted and before the folate could be absorbed by the intestine. This folate could then be distributed through the animal and enter the pharynx where it would be bound by FOLR-1 on the NSM. Notably, in mammalian cells FOLR-1 functions to transport folates across cell barriers by transcytosis ((Zhao *et al.*, 2009)). Thus, it is possible that a similar role of FOLR-1 in C. elegans transports stimulatory folate into the body for recognition by the NSM neurons and germ cells.

Neurotransmitters are releases is response to an influx of Ca^{2+} driven by a Ca^{2+} channel. Identifying the channel that mediates Ca^{2+} entry into the NSM neurons is important for understanding how FOLR-1 regulates NSM activation, as we expect the channel to function downstream of FOLR-1. Given that folate signaling regulates both NSM neurons and germ cells, this initiated our interest in exploring the Ca^{2+} channel GON-2 because of the report of its indirect role in regulating germ cell proliferation (Sun and Lambie, 1997). GON-2 is a transient receptor potential-M (TRPM) channel that is orthologous to mammalian TRPM7, which is overexpressed in diverse cancers and promotes cancer progression (Hantute-Ghesquier et al., 2018). TRPM channels activate Ca^{2+} entry in response to ligand binding. Our demonstration of FOLR-1 interaction with GON-2 suggests that potentially ligand binding by FOLR-1 may activate or potentiate GON-2 Ca^{2+} calcium channel activity.

Emerging evidence in vertebrates suggests that non-canonical folate pathways regulate neural tube closure and cancer through cell signaling. The majority of *C. elegans* signaling pathways are conserved in humans (Shaye and Greenwald, 2011). Multiple signaling pathways have been implicated in FOLR1-directed signaling in human cells (see Chapter 2). The multitude of proposed FOLR1 signaling pathways raises the possibility that several of these pathway activations may occur in response to the activation of different upstream signaling pathways.

Materials and Methods

Expression constructs

C. elegans-expression constructs

The expression construct pCFJ350/Pfolr-1::FOLR-1::GFP::tbb-2 3'UTR expresses the full-length FOLR-1 genomic coding region fused to GFP under the control of *folr-1* regulatory sequences. It was constructed using the pCFJ350 plasmid (Addgene plasmid # 34866) (Frokjaer-Jensen et al., 2012), which contains the *Caenorhabditis briggsae unc-119(+)* gene, allowing rescue of *unc-119* mutants. The expression insert was introduced into pCFJ350 by sequential In-Fusion cloning (Takara Bio) into the XhoI site of pCFJ350. The *folr-1* genomic sequence includes 1857 bp of region upstream of the ATG start codon and the entire *folr-1* coding sequence. This was fused in-frame to the open-reading frame (ORF) of the *C. elegans*-codon-optimized GFP and the 3'UTR of β-tubulin *tbb-2*, both from plasmid pCFJ1415 (Addgene plasmid #110550) (Frokjaer-Jensen et al., 2016). PCR amplifications for all cloning steps were with Q5 polymerase (NEB).

The expression construct pCFJ350/Ptph-1::myr-mNeonGreen:unc-54 3'UTR expresses myristoylated mNeonGreen in the NSM neuron. It was constructed by introducing overlapping PCR inserts into the pCFJ350 plasmid (between AvrII and AflIII sites) using In-Fusion cloning. A 619 bp region of the tph-1 genomic sequence that includes 158 bp upstream of the ATG start

codon, the first full exon, the first full intron, and the first bp of the second exon, was fused in-frame to *C. elegans* codon-optimized myr-mNeonGreen that was PCR amplified from plasmid dg357 (Hostettler et al., 2017). The *unc-54* 3'UTR was PCR amplified from plasmid pPD49.26 (the kind gift of Andy Fire).

The expression construct pCFJ350/Ptph-1::FOLR-1::wrmScarlet::unc-54 3'UTR was created through the same process using In-Fusion cloning into pCFJ350 between the AvrII and AflIII sites. wrmScarlet was PCR amplified from plasmid pZCS16 (Stevenson et al., 2020).

Mammalian-expression constructs

The mammalian expression construct pcDNA3.1(-)/FOLR-1-3xHA was created by gene synthesis by BioMatik. The FOLR-1 cDNA sequence fused to a C-terminal 3xHA tag was synthesized and placed into the expression vector pcDNA3.1(-) (Invitrogen) between the NotI and KpnI sites.

The mammalian expression construct pcDNA3.1(-)/GON-2-3xFLAG was created by gene synthesis of 3 non-overlapping fragments by BioMatik. The GON-2 cDNA sequence with a C-terminal 3xFLAG tag was split into 3 gene synthesis constructs in pcDNA3.1. Restriction digestion was then used to fuse the three pieces into the full pcDNA3.1(-)/GON-2-3xFLAG construct.

Worm strains

Strain ET562, *unc-119(ed3)*; *ekEx38*[pCFJ350/P*folr-1*::FOLR-1::GFP::*unc-54* 3'UTR], was created by injecting 100 ng/µl of plasmid pCFJ350/Pfolr-1::FOLR-1::GFP::tbb-2 3'UTR into strain DP38, *unc-119(ed3)*, to create the extrachromosomal array *ekEx38* that is maintained by picking non-Unc animals.

Strain ET827, *vsIs97*[P*tph-1*::DsRed2 + lin-15(+)]; *ekEx38*[pCFJ350/P*folr-1*::FOLR-1::GFP::*unc-54* 3'UTR], expresses P*folr-1*::FOLR-1::GFP with the NSM-marker P*tph-1*::DsRed.

The strain was created by crossing strain ET562 to strain LX960, *vsIs97*[tph-1p::DsRed2 + *lin-15(+)*].

Strain EJ938, *gon-2(q388)*; *dxIs1*[P*gon-2*::GON-2::GFP::gon-2 3'UTR], expresses GFP that is integrated into the *gon-2* locus on cosmid T01H8. The dxIs1 integrant rescues *gon-2(q388)* sterility. Strain EJ938 was the kind gift of Eric Lambie.

Strain ET622, *gon-2(q388)*; *dxIs1*[P*gon-2*::GON-2::GFP::gon-2 3'UTR]; *vsIs97*[P*tph*-p::DsRed2 + *lin-15(+)*], was created by crossing strain EJ938 with strain LX960.

Four strains were obtained by coinjection of pCFJ350/Ptph-1::myr-mNeonGreen:unc-54 3'UTR and pCFJ350/Ptph-1::FOLR-1::wrmScarlet::unc-54 3'UTR into unc-119(ed3) mutants. The four strains gave similar localization of FOLR-1::wrmScarlet and myr-mNeonGreen in the NSM neuron, but were not maintained past the experiment (and hence do not have strain names)

Cell culture, selection, and synchronization

Human embryonic kidney HEK293T cells and HeLa cells were obtained from the American Type Culture Collection and were cultured in DMEM in the presence of 10% fetal bovine serum (Sigma), 100µg/ml penicillin and streptomycin (Hyclone).

DNA transfections, siRNA knockdowns, immunoprecipitations

Proteins were expressed in HEK293T cells and immunoprecipitated as described (Kim et al. 2008, Starostina et al. 2007). HEK293T cells and HeLa cells were transfected with plasmids for human protein expression using Lipofectamine 3000 (Invitrogen) according to the manufacturer's instructions. For immunoprecipitation of human proteins, cells were collected 48 hrs after transfection and lysed in Triton X-100 (0.33% Triton X-100, 150 mM NaCl, 50 mM Tris pH 7.4, 1 mM EDTA, protease inhibitor cocktail (Roche). Cell lysates were centrifuged at 13,000 rpm for 25 min at 4°C and the supernatant was pre-cleared with sepharose 4B beads (Sigma Aldrich).

Proteins were immunoprecipitated using anti-FLAG M2 affinity agarose gel (Sigma Aldrich), and EZview™ Red Anti-HA Affinity Gel (Sigma Aldrich) beads respectively.

For immunofluorescence, HeLa cells grown on 8 well Lab-Tek II chamber slides (Nunc) and fixed for 30 min at room temperature with a formaldehyde fixation mixture of 3.7% formaldehyde, 80 mM HEPES (pH 6.9); 0.8 mM EGTA; and 1.6 mM MgSO4. Cells were washed three times with PBT (PBS with 0.1% Triton X-100 and 0.1% bovine serum albumin) and kept in PBT overnight as a blocking solution. Primary antibodies (mouse monoclonal anti-FLAG M2, 1:650 dilution; and rabbit monoclonal anti-HA, 1:1000) in PBT was incubated with the fixed cells for 2 hrs, and then washed with PBT.

Secondary antibodies (Dylite 488 anti-rabbit, 1:500 and rhodamine anti-mouse 1:500) were incubated in PBT for 30 min, washed and mounted for viewing in 1 mg/ml p-phenylenediamine (anti-fade agent) and 90% glycerol. Images of the same antibodies/Hoechst were taken with the same exposure times and processed identically using Adobe Photoshop software. Quantitation of nuclear and total immunofluorescence signal was performed with OpenLab software (version 5.0; Improvision).

References

Austin, M.U., Liau, W.S., Balamurugan, K., Ashokkumar, B., Said, H.M., and LaMunyon, C.W. (2010). Knockout of the folate transporter folt-1 causes germline and somatic defects in C. elegans. BMC Dev Biol *10*, 46. 10.1186/1471-213X-10-46.

Balamurugan, K., Ashokkumar, B., Moussaif, M., Sze, J.Y., and Said, H.M. (2007). Cloning and functional characterization of a folate transporter from the nematode Caenorhabditis elegans. American journal of physiology. Cell physiology *293*, C670-681. 10.1152/ajpcell.00516.2006.

Balashova, O.A., Visina, O., and Borodinsky, L.N. (2017). Folate receptor 1 is necessary for neural plate cell apical constriction during Xenopus neural tube formation. Development *144*, 1518-1530. 10.1242/dev.137315.

Chaudhari, S.N., Mukherjee, M., Vagasi, A.S., Bi, G., Rahman, M.M., Nguyen, C.Q., Paul, L., Selhub, J., and Kipreos, E.T. (2016). Bacterial Folates Provide an Exogenous Signal for C. elegans Germline Stem Cell Proliferation. Dev Cell *38*, 33-46. 10.1016/j.devcel.2016.06.013.

Copp, A.J., Stanier, P., and Greene, N.D. (2013). Neural tube defects: recent advances, unsolved questions, and controversies. The Lancet. Neurology *12*, 799-810. 10.1016/S1474-4422(13)70110-8.

Cserzo, M., Eisenhaber, F., Eisenhaber, B., and Simon, I. (2002). On filtering false positive transmembrane protein predictions. Protein Eng *15*, 745-752.

Frokjaer-Jensen, C., Davis, M.W., Ailion, M., and Jorgensen, E.M. (2012). Improved Mos1-mediated transgenesis in C. elegans. Nat Methods *9*, 117-118. 10.1038/nmeth.1865.

Frokjaer-Jensen, C., Jain, N., Hansen, L., Davis, M.W., Li, Y.B., Zhao, D., Rebora, K., Millet, J.R.M., Liu, X., Kim, S.K., et al. (2016). An Abundant Class of Non-coding DNA Can Prevent Stochastic Gene Silencing in the C. elegans Germline. Cell *166*, 343-357. 10.1016/j.cell.2016.05.072.

Gurel, G., Gustafson, M.A., Pepper, J.S., Horvitz, H.R., and Koelle, M.R. (2012). Receptors and other signaling proteins required for serotonin control of locomotion in Caenorhabditis elegans. Genetics *192*, 1359-1371. 10.1534/genetics.112.142125.

Hantute-Ghesquier, A., Haustrate, A., Prevarskaya, N., and Lehen'kyi, V. (2018). TRPM Family Channels in Cancer. Pharmaceuticals (Basel) *11*. 10.3390/ph11020058.

Hostettler, L., Grundy, L., Kaser-Pebernard, S., Wicky, C., Schafer, W.R., and Glauser, D.A. (2017). The Bright Fluorescent Protein mNeonGreen Facilitates Protein Expression Analysis In Vivo. G3 (Bethesda) *7*, 607-615. 10.1534/g3.116.038133.

Iwanir, S., Brown, A.S., Nagy, S., Najjar, D., Kazakov, A., Lee, K.S., Zaslaver, A., Levine, E., and Biron, D. (2016). Serotonin promotes exploitation in complex environments by accelerating decision-making. BMC biology *14*, 9. 10.1186/s12915-016-0232-y.

Petersen, T.N., Brunak, S., von Heijne, G., and Nielsen, H. (2011). SignalP 4.0: discriminating signal peptides from transmembrane regions. Nat Methods *8*, 785-786. 10.1038/nmeth.1701.

Rhoades, J.L., Nelson, J.C., Nwabudike, I., Yu, S.K., McLachlan, I.G., Madan, G.K., Abebe, E., Powers, J.R., Colon-Ramos, D.A., and Flavell, S.W. (2019). ASICs Mediate Food Responses in an Enteric Serotonergic Neuron that Controls Foraging Behaviors. Cell *176*, 85-+. 10.1016/j.cell.2018.11.023.

Shaye, D.D., and Greenwald, I. (2011). OrthoList: a compendium of C. elegans genes with human orthologs. PloS one *6*, e20085. 10.1371/journal.pone.0020085.

Spencer, W.C., McWhirter, R., Miller, T., Strasbourger, P., Thompson, O., Hillier, L.W., Waterston, R.H., and Miller, D.M., 3rd (2014). Isolation of specific neurons from C. elegans larvae for gene expression profiling. PLoS One *9*, e112102. 10.1371/journal.pone.0112102.

Stevenson, Z.C., Moerdyk-Schauwecker, M.J., Jamison, B., and Phillips, P.C. (2020). Rapid Self-Selecting and Clone-Free Integration of Transgenes into Engineered CRISPR Safe Harbor Locations inCaenorhabditis elegans. G3-Genes Genom Genet *10*, 3775-3782. 10.1534/g3.120.401400.

Suckling, C.J., Sweeney, J.R., and Wood, H.C. (1977). Dihydropteroate synthase: purification by affinity chromatography and mechanism of action. J Chem Soc Perkin 1 *4*, 439-442.

Suh, J., and Hutter, H. (2012). A survey of putative secreted and transmembrane proteins encoded in the C. elegans genome. BMC genomics *13*, 333. 10.1186/1471-2164-13-333.

Sun, A.Y., and Lambie, E.J. (1997). gon-2, a gene required for gonadogenesis in Caenorhabditis elegans. Genetics *147*, 1077-1089. 10.1093/genetics/147.3.1077.

Sze, J.Y., Victor, M., Loer, C., Shi, Y., and Ruvkun, G. (2000). Food and metabolic signalling defects in a Caenorhabditis elegans serotonin-synthesis mutant. Nature *403*, 560-564. 10.1038/35000609.

Zhao, R., Matherly, L.H., and Goldman, I.D. (2009). Membrane transporters and folate homeostasis: intestinal absorption and transport into systemic compartments and tissues. Expert Rev Mol Med *11*, e4. 10.1017/S1462399409000969.

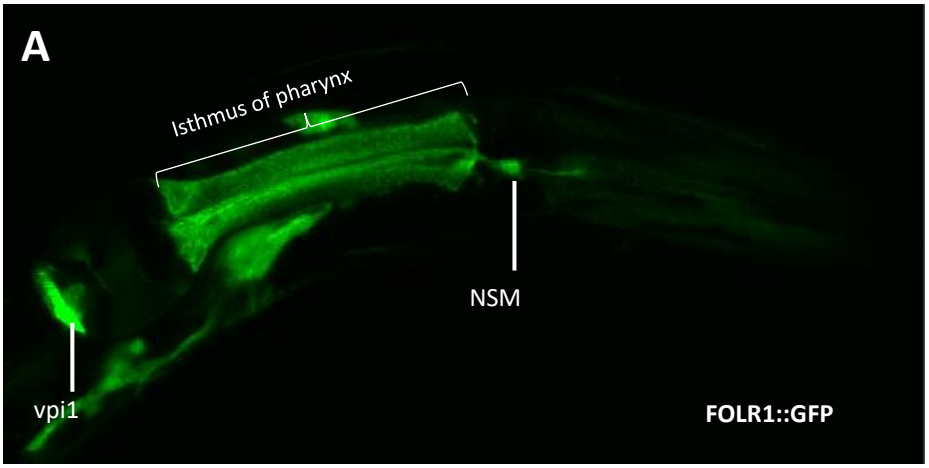
A
Isthmus of pharynx
NSM
vpi1
FOLR1::GFP

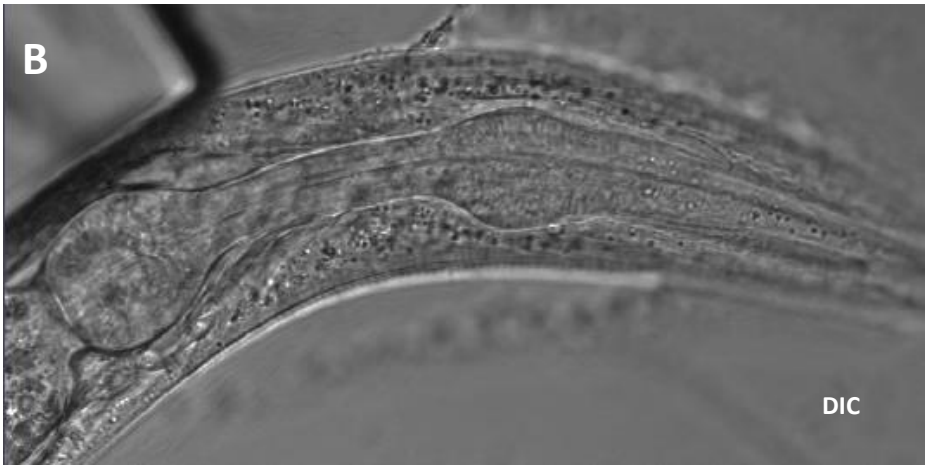
B
DIC

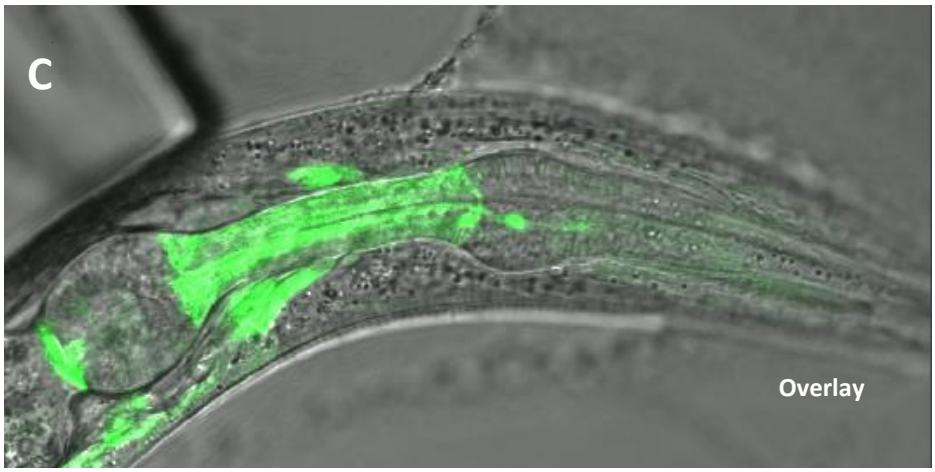
C
Overlay

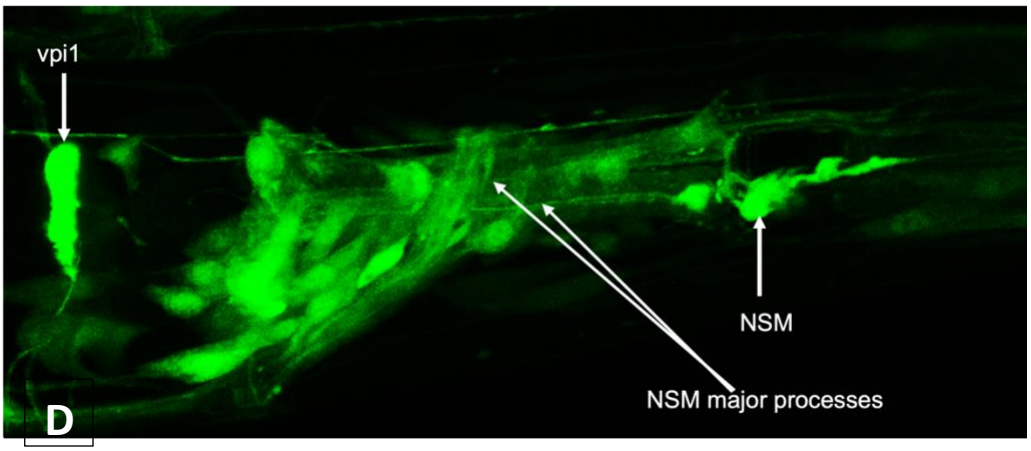

Figure. 4.1 FOLR-1::GFP driven by its own promoter expresses in the NSM neurons, the isthmus of the pharynx, and the pharyngeal-intestinal valve cells.

(A) epifluorescence image of Pfolr1::FOLR-1::GFP driven by its own promoter from an extrachromosomal array.

(B)DIC image of the worm

(C) Overlay between the epifluorescence and the DIC (D) confocal maximum intensity projection micrograph of the Pfolr1::FOLR-1::GFP driven by its own promoter.

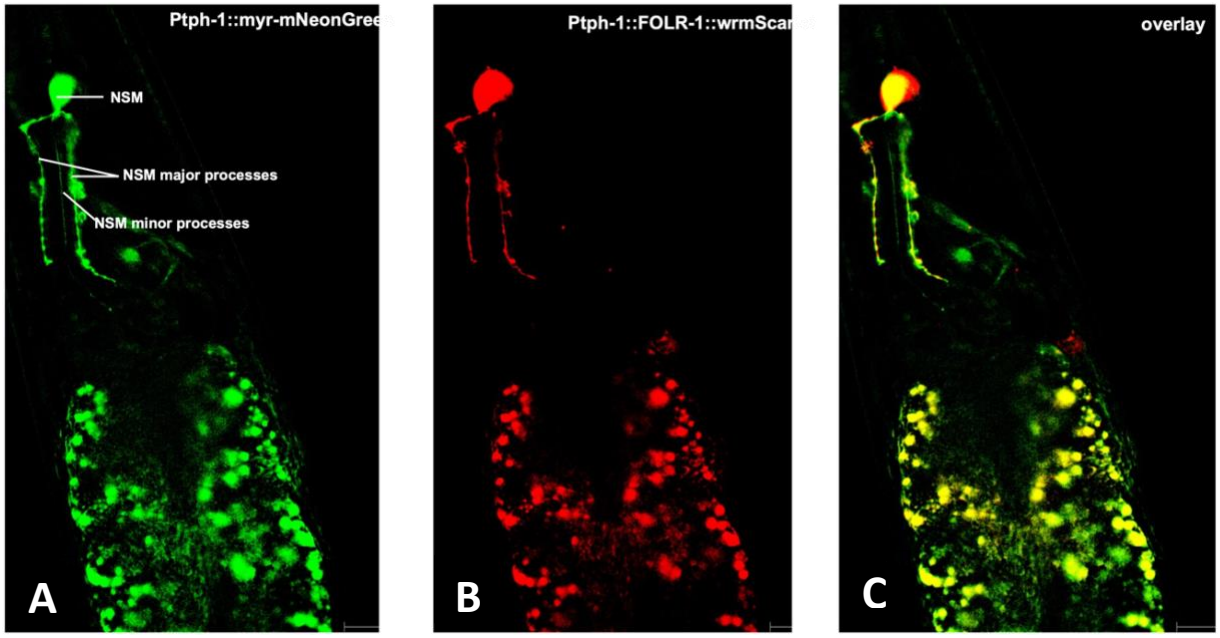

Figure. 4.2. pFOLR1 is specifically expressed in NSM neurons using Ptph promoter of *C. elegans*

(A) membrane-localized mNeonGreen and (B) FOLR-1::wrmScarlet specifically expressed in the NSM neurons. Analysis of these transgenic animals shows that FOLR-1::wrmScarlet is present in the NSM neuronal processes – extending about two-thirds of the length of the neuronal processes from the cell body (C) The overlay of both the fluorescence protein.

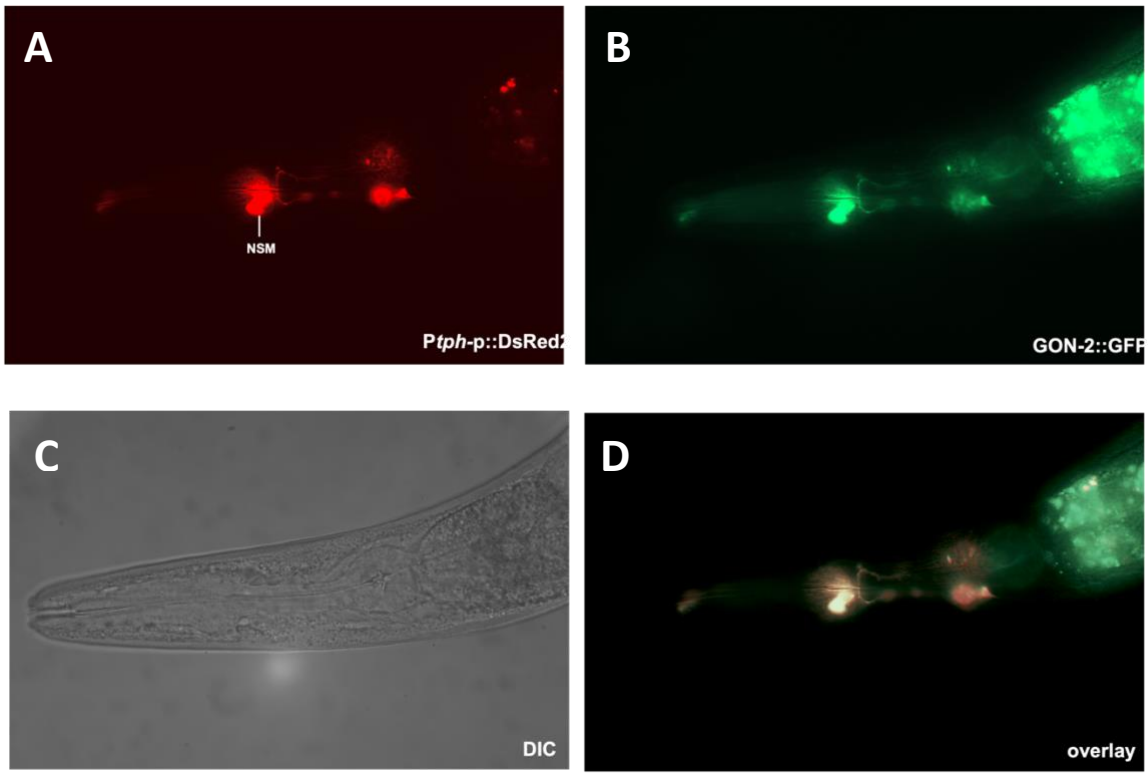

Figure. 4.3. GON-2 localizes to NSM and its major processes using its own promoter

(A) membrane-localized DsRed2 and (B) GON-2:: GFP expressed in the NSM neurons using their own promoters (C) DIC micrograph of the worm. (D) Overlay between GON-2:: GFP and the membrane-localized DsRed2 indicate that GON-2 localizes in the two major processes of the NSM neuron.

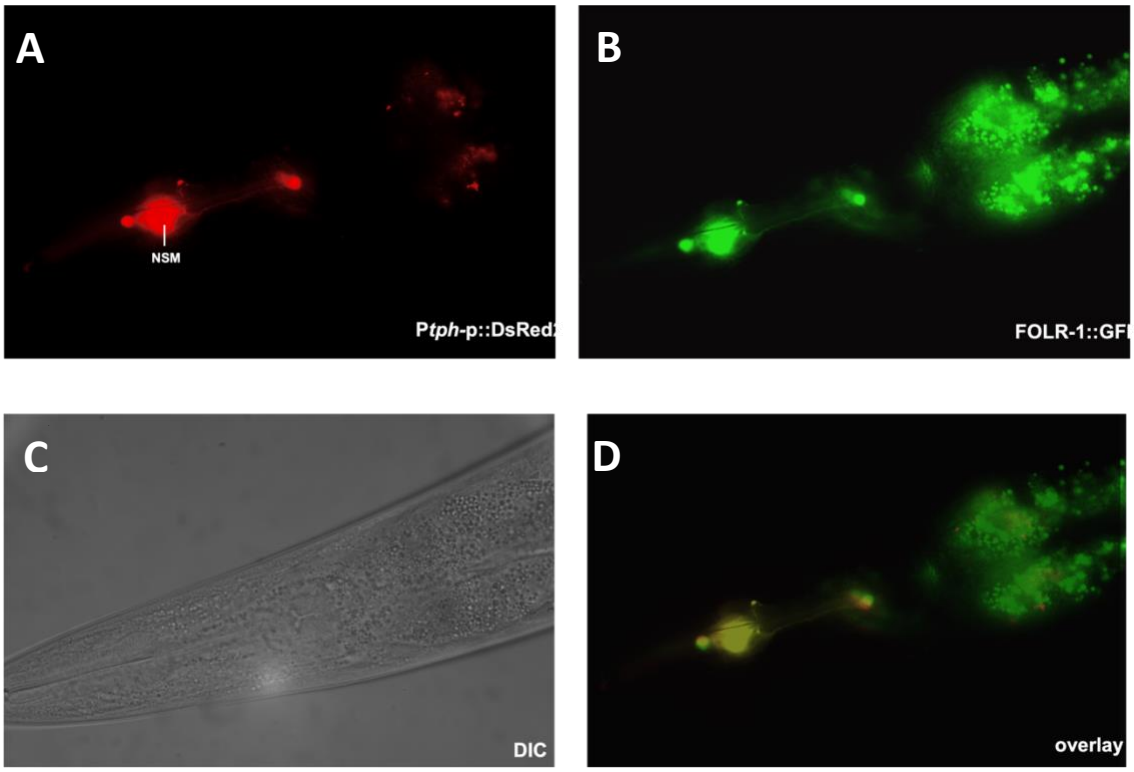

Figure. 4.4. FOLR-1 localizes to NSM and its major processes using its own promoter

(A) membrane-localized DsRed2 and (B) FOLR-1:: GFP expressed in the NSM neurons using their own promoters (C) DIC micrograph of the worm. (D) Overlay between FOLR-1:: GFP and the membrane-localized DsRed2 indicate that GON-2 localizes in the two major processes of the NSM neuron.

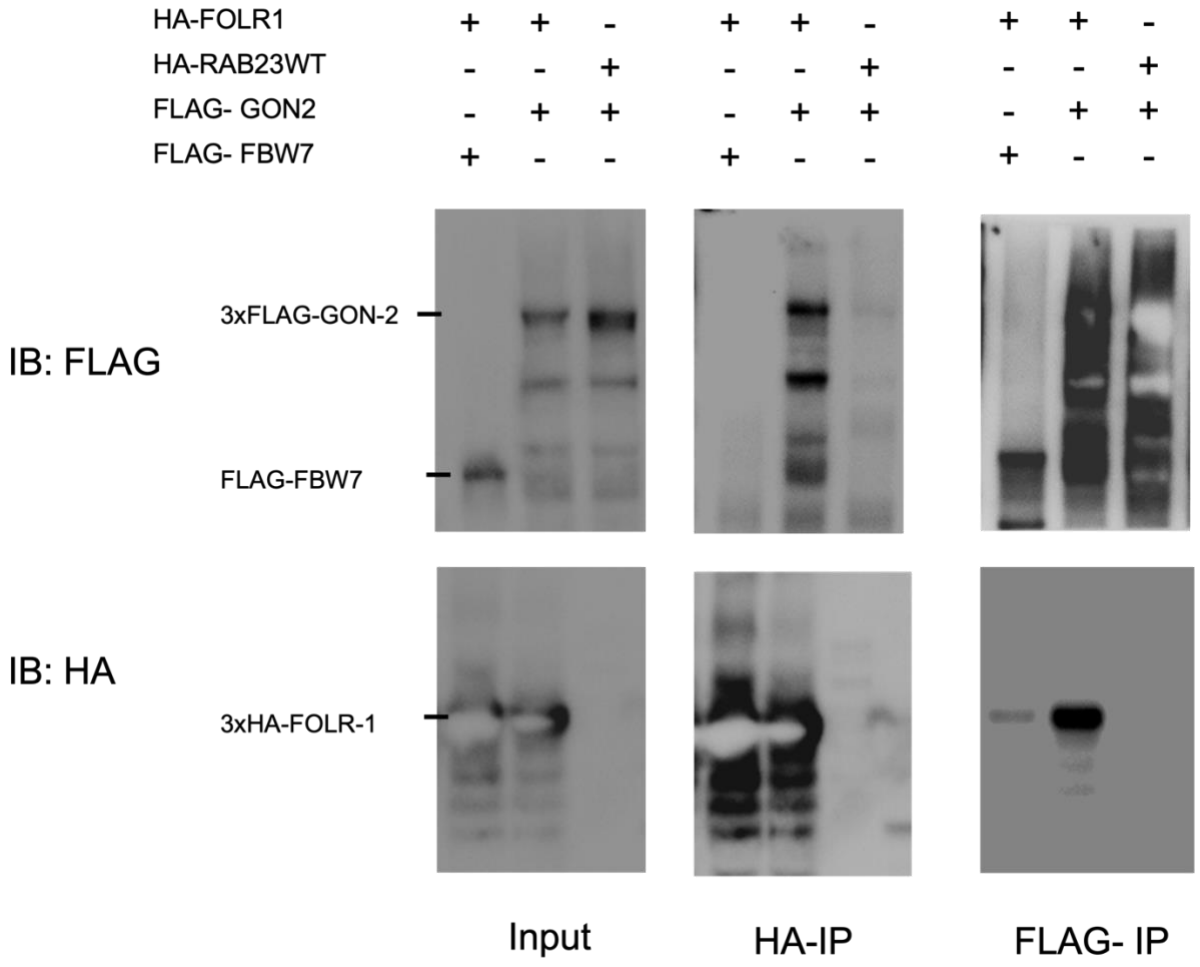

Figure. 4.5. FOLR-1 physically interacts with GON-2. Co-expressed 3xHA-FOLR-1 and 3xFLAG-GON-2 ectopically in human HEK293T and immunoprecipitated 3xHA-FOLR1 and HA-Rab23WT (control) to probed to determine co-immunoprecipitation of3xFLAG-GON2 and 3xFLAG-FBW7 to determine if the two proteins physically interact with each other. The experiment was also conducted in other direction (immunoprecipitated the FLAG proteins and probed for HA co-IPs). The white spots in between bands are due to the bleed-in that occur with excessive ECL reaction.

DISCUSSION AND CONCLUSION

CAND1/2 catalyzes the redistribution of SCF complexes to promote mitotic progression

SCFs (Skp1-Cul1-F-box proteins) are widely studied E3 ligases that mediate timely ubiquitylation and degradation of specific substrate proteins. SRs determine the substrate specificity of the SCF complex. There are 69 human SRs are identified (Wang et al., 2014). The variety of SRs allows the generation of many ubiquitin ligases that promote the ubiquitylation and degradation of many substrate proteins. This allows SCFs to control numerous key cellular processes, including cell cycle progression. It's the timely removal of cell cycle regulators by the SCF that allows several irreversible transitions between cell cycle phases. In Chapter 3 we show that the inactivation of CAND1 during mitosis in human cells results in the ectopic binding of a subset of SRs to the CUL1-RBX1 complex during mitosis, which negatively impacts mitotic progression. In normal (unperturbed) cell cycles, we show that CAND1/2 is required for the significant reorganization of SCF complexes that promote mitotic progression.

CAND1 is the SR exchange factor that is directly involved in the process of assembly and disassembly of active SCF complexes (Pierce et al., 2013; Reitsma et al., 2017). CAND1 interacts with the unneddylated form of CUL1 when it is not bound to the adaptor Skp1 (Goldenberg et al., 2004; Pierce *et al.*, 2013; Zheng et al., 2002). The neddylation of the CUL1-RBX1 can inhibit the CAND1 association with the CUL1-RBX1 module (Liu et al., 2002). But our experiments show that the association of CAND1 to CUL1-RBX1 during mitosis is not

regulated by the neddylation state of the CUL1-RBX1 complex, thereby suggesting this phenomenon implies a novel regulatory mechanism that requires further investigation.

Another observation we had when investigating the CAND1-CUL1 complexes, is that the mitotic complex is more stable than the S-phase complex. Our results show that CAND1 is bound to 50% of CUL1 (at least 90% of the unneddylated CUL1). SCF ligases has a milliseconds rate to initiate ubiquitylation, and when substrates aren't bound the SR gets auto ubiquitylated and degrades itself, hence having all SCF enzymes always assembled and active could create problems(Pierce *et al.*, 2013; Saha and Deshaies, 2008). Therefore, having CAND1 as an intermediate exchange factor causes a a delay between substrate binding to a SR and its assembly into an active SCF, thus increasing the specificity of the system. This is done by increasing the "maximal *koff* value" of a substrate(Liu et al., 2018; Pierce *et al.*, 2013). Based on the current understanding of how the SCF is regulated through CAND1, SR, and substrate binding, this increased association of CAND1 during mitosis suggests that CAND1 is involved in selective association of SR during mitosis. Yet how this specificity is regulated needs further investigation.

The current understanding is that substrate availability and its binding to SRs increases the stability of SCF complexes (Liu *et al.*, 2018). Studies on F-box protein has been expanding over the couple of decades since this was characterized and understanding the differences between F-box proteins are important as it brings the SCF complex complex ligases functional diversity. Recognizing substrates through phospho-degrons" is a common mechanism that is known to regulate SR–substrate pairing, where the substrate gets phosphorylated at a defined amino acid sequence known as the 'degron', which gets recognized by the SR(Yada et al., 2004). There are other methods of substrate recognition have also been characterized. e.g., ligand-based substrate recognition (where a molecule or a small molecule or a cofactor facilitates the substrate

recognition), localization-based recognition, etc. (Nguyen and Busino, 2020). Since substrates have been recognized in playing an important role in SCF regulation, understating their biochemical and biological roles will make it possible to understand the broad activity scope of E3 ligases.

Though SRs associate with cullins through a common adaptor SKP1, each SR shows variation in its efficiency in binding to Cul1 (Reitsma *et al.*, 2017). Reistma et al further describes that the absence of Cand1/2 (in asynchronous cells) significantly suppressed the exchange of SRs among SCF complexes in cell lysates, with the exception of FBXO5/Emi1, which is interestingly a substrate of SCF-FBXW11 (which is the SR that we found to physically interact with CAND1 during mitosis and whose loading onto SCF complexes in mitosis was promoted by CAND1).

Emi1 (early mitotic inhibitor 1) is an F-box protein that acts as a SR for SCF complexes, and independently as an important protein for cell cycle regulation. It functions through inhibition of the APC/C ubiquitin ligase activity in G1 phase to promote DNA replication, in S phase to prevent DNA re-replication, and in G2-M phase to ensure proper mitotic progression (Lara-Gonzalez et al., 2017). It has been reported to show mitotic defects during embryogenesis (Lee et al., 2006). Failure of β-TrCP2/FBXW11 and β-TrCP/BTRC to target the degradation of substrates like EMI1, PLK1 and PLK4, CDC25A, and WEE1 results in cell cycle arrest, mitotic spindle dysfunction, and centrosome duplication (Skaar et al., 2013). There is a report asserting that CAND1 overexpression significantly stabilized the SCF-β-TrCP/2 substrate PLK4, resulting in centrosome overduplication and mitotic defects (Korzeniewski et al., 2012). This observation seems to contrast with our observation of a similar phenotype when CAND1 is absent (rather than overexpressed). Based on our findings, we would expect that PLK4 was stabilized when CAND1/2

is knocked down, as CAND1/2 knockdown reduces the generation of SCF-FBXW11, and thus presumably reduces the degradation of PLK4.

These results encourage further studies to explore the SCF–CAND1 axis for cell cycle regulation, especially identifying the key substrates will provide major insights on how this regulation happens. Overall, this study will highlight the role of altered SCF components in cancer.

FOLR1 regulation of neuronal signaling in *C. elegans*

Emerging evidence in vertebrates suggests that non-canonical folate pathways (independent of one carbon metabolism) regulate neural tube closure and cancer through cell signaling. The majority of *C. elegans* signaling pathways are conserved in humans (Shaye and Greenwald, 2011). Multiple signaling pathways have been implicated in FOLR1-directed signaling in human cells (see Chapter 2). The multitude of proposed FOLR1 signaling pathways raises the possibility that several of these pathway activations may occur in response to the activation of different upstream signaling pathways. Our results in *C. elegans* suggest the possibility that Ca2+ entry mediates the intracellular signaling by FOLR-1. The regulation of Ca2+ entry has not been described as a potential signaling pathway in mammals, but it has the potential to operate upstream of signaling components in other intracellular signaling pathways.

GON-2 is a transient receptor potential-M (TRPM) channel that is orthologous to mammalian TRPM7, which is overexpressed in diverse cancers and promotes cancer progression (Hantute-Ghesquier et al., 2018). GON-2 is able to transport Ca^{2+} and Mg^{2+}, but has a ten-fold higher permeability for Ca^{2+} than Mg^{2+}(Xing et al., 2008). It would be interesting to determine if the interaction between FOLR-1 and GON-2 is conserved in human cells, and if this contributes to the promotion of cancer progression by FOLR-1. It has been reported that FOLR1 is involved

in signaling with the serine/threonine kinase ERK (MAP kinase). This ERK1/2 signaling pathway involves receptor tyrosine kinases that activate the small GTPase protein RAS, which then leads to the sequential phospho-activations of the serine/threonine kinases RAF, MEK, and ERK1/2 (Lavoie et al., 2020). Various tumors activate this pathway to increase cell division and migration (Lavoie *et al.*, 2020). There is evidence on both direct and indirect interactions between the Ca^{2+} and MAPK signaling pathway. (White and Sacks, 2010). Understanding how folates work with other membrane transporters in relaying signaling molecules, especially by Ca^{2+} will open avenues of research. Also this research will provide more insight over how folates involves in regulating Ca^{2+} homeostasis, as TRPM channels are known to involve in regulating Ca^{2+} homeostasis(Elizondo et al., 2010; Faouzi et al., 2017).

The U.S. is one of the few countries in the world that fortifies their food supply with folic acid. Notably, when the U.S. began fortifying grains with folic acid in 1996, there was a transient increase (that lasted for several years) in the rate of colon cancer (Mason et al., 2007). Folic acid fortification is currently thought to both accelerate the progression of certain cancers, and also prevent the genesis of certain cancers by ameliorating folate deficiency (which can increase cancer risk) (Kim, 2008; Liu et al., 2011; Ulrich, 2008). It is currently not definitively established in humans whether folates act in signaling independently of their role in one-carbon metabolism, although the evidence presented in Chapter 2 suggests that folate signaling through FOLR1 does occur. A role for folates in signaling would have potentially important health policy implications, e.g., in guidance on voluntary supplementation with high doses of folic acid. This would be a particular concern given that folic acid (a synthetic, non-natural folate) has a much higher affinity for FOLR1 than naturally-occurring folates (Leamon et al., 2009).

Reference

Elizondo, M.R., Budi, E.H., and Parichy, D.M. (2010). trpm7 regulation of in vivo cation homeostasis and kidney function involves stanniocalcin 1 and fgf23. Endocrinology *151*, 5700-5709. 10.1210/en.2010-0853.

Faouzi, M., Kilch, T., Horgen, F.D., Fleig, A., and Penner, R. (2017). The TRPM7 channel kinase regulates store-operated calcium entry. J Physiol *595*, 3165-3180. 10.1113/jp274006.

Goldenberg, S.J., Cascio, T.C., Shumway, S.D., Garbutt, K.C., Liu, J., Xiong, Y., and Zheng, N. (2004). Structure of the Cand1-Cul1-Roc1 complex reveals regulatory mechanisms for the assembly of the multisubunit cullin-dependent ubiquitin ligases. Cell *119*, 517-528. 10.1016/j.cell.2004.10.019.

Hantute-Ghesquier, A., Haustrate, A., Prevarskaya, N., and Lehen'kyi, V. (2018). TRPM Family Channels in Cancer. Pharmaceuticals-Base *11*. ARTN 58

10.3390/ph11020058.

Kim, Y.I. (2008). Folic acid supplementation and cancer risk: Point. Cancer Epidem Biomar *17*, 2220-2225. 10.1158/1055-9965.Epi-07-2557.

Korzeniewski, N., Hohenfellner, M., and Duensing, S. (2012). CAND1 promotes PLK4-mediated centriole overduplication and is frequently disrupted in prostate cancer. Neoplasia *14*, 799-806. 10.1593/neo.12580.

Lara-Gonzalez, P., Kim, T., and Desai, A. (2017). Taming the Beast: Control of APC/C(Cdc20)-Dependent Destruction. Cold Spring Harb Symp Quant Biol *82*, 111-121. 10.1101/sqb.2017.82.033712.

Lavoie, H., Gagnon, J., and Therrien, M. (2020). ERK signalling: a master regulator of cell behaviour, life and fate. Nat Rev Mol Cell Biol *21*, 607-632. 10.1038/s41580-020-0255-7.

Leamon, C.P., You, F., Santhapuram, H.K., Fan, M., and Vlahov, I.R. (2009). Properties influencing the relative binding affinity of pteroate derivatives and drug conjugates thereof to the folate receptor. Pharm Res *26*, 1315-1323. 10.1007/s11095-009-9840-3.

Lee, H., Lee, D.J., Oh, S.P., Park, H.D., Nam, H.H., Kim, J.M., and Lim, D.S. (2006). Mouse emi1 has an essential function in mitotic progression during early embryogenesis. Molecular and Cellular Biology *26*, 5373-5381. 10.1128/Mcb.00043-06.

Liu, J., Furukawa, M., Matsumoto, T., and Xiong, Y. (2002). NEDD8 modification of CUL1 dissociates p120(CAND1), an inhibitor of CUL1-SKP1 binding and SCF ligases. Mol Cell *10*, 1511-1518. 10.1016/s1097-2765(02)00783-9.

Liu, X., Reitsma, J.M., Mamrosh, J.L., Zhang, Y., Straube, R., and Deshaies, R.J. (2018). Cand1-Mediated Adaptive Exchange Mechanism Enables Variation in F-Box Protein Expression. Mol Cell *69*, 773-786 e776. 10.1016/j.molcel.2018.01.038.

Liu, Z., Ciappio, E.D., Crott, J.W., Brooks, R.S., Nesvet, J., Smith, D.E., Choi, S.W., and Mason, J.B. (2011). Combined inadequacies of multiple B vitamins amplify colonic Wnt signaling and promote intestinal tumorigenesis in BAT-LacZxApc1638N mice. FASEB J *25*, 3136-3145. 10.1096/fj.11-184143.

Mason, J.B., Dickstein, A., Jacques, P.F., Haggarty, P., Selhub, J., Dallal, G., and Rosenberg, I.H. (2007). A temporal association between folic acid fortification and an increase in colorectal cancer rates may be illuminating important biological principles: A hypothesis. Cancer Epidem Biomar *16*, 1325-1329. 10.1158/1055-9965.Epi-07-0329.

Nguyen, K.M., and Busino, L. (2020). The Biology of F-box Proteins: The SCF Family of E3 Ubiquitin Ligases. Adv Exp Med Biol *1217*, 111-122. 10.1007/978-981-15-1025-0_8.

Pierce, N.W., Lee, J.E., Liu, X., Sweredoski, M.J., Graham, R.L., Larimore, E.A., Rome, M., Zheng, N., Clurman, B.E., Hess, S., et al. (2013). Cand1 promotes assembly of new SCF complexes through dynamic exchange of F box proteins. Cell *153*, 206-215. 10.1016/j.cell.2013.02.024.

Reitsma, J.M., Liu, X., Reichermeier, K.M., Moradian, A., Sweredoski, M.J., Hess, S., and Deshaies, R.J. (2017). Composition and Regulation of the Cellular Repertoire of SCF Ubiquitin Ligases. Cell *171*, 1326-1339 e1314. 10.1016/j.cell.2017.10.016.

Saha, A., and Deshaies, R.J. (2008). Multimodal activation of the ubiquitin ligase SCF by Nedd8 conjugation. Mol Cell *32*, 21-31. 10.1016/j.molcel.2008.08.021.

Shaye, D.D., and Greenwald, I. (2011). OrthoList: a compendium of C. elegans genes with human orthologs. PLoS One *6*, e20085. 10.1371/journal.pone.0020085.

Skaar, J.R., Pagan, J.K., and Pagano, M. (2013). Mechanisms and function of substrate recruitment by F-box proteins. Nat Rev Mol Cell Biol *14*, 369-381. 10.1038/nrm3582.

Ulrich, C.M. (2008). Folate and cancer prevention--where to next? Counterpoint. Cancer Epidemiol Biomarkers Prev *17*, 2226-2230. 10.1158/1055-9965.EPI-07-2952.

Wang, Z., Liu, P., Inuzuka, H., and Wei, W. (2014). Roles of F-box proteins in cancer. Nat Rev Cancer *14*, 233-247. 10.1038/nrc3700.

White, C.D., and Sacks, D.B. (2010). Regulation of MAP Kinase Signaling by Calcium. Methods Mol Biol *661*, 151-165. 10.1007/978-1-60761-795-2_9.

Xing, J., Yan, X., Estevez, A., and Strange, K. (2008). Highly Ca2+-selective TRPM channels regulate IP3-dependent oscillatory Ca2+ signaling in the C. elegans intestine. J Gen Physiol *131*, 245-255. 10.1085/jgp.200709914.

Yada, M., Hatakeyama, S., Kamura, T., Nishiyama, M., Tsunematsu, R., Imaki, H., Ishida, N., Okumura, F., Nakayama, K., and Nakayama, K.I. (2004). Phosphorylation-dependent degradation of c-Myc is mediated by the F-box protein Fbw7. Embo Journal *23*, 2116-2125. 10.1038/sj.emboj.7600217.

Zheng, J., Yang, X., Harrell, J.M., Ryzhikov, S., Shim, E.H., Lykke-Andersen, K., Wei, N., Sun, H., Kobayashi, R., and Zhang, H. (2002). CAND1 binds to unneddylated CUL1 and regulates the formation of SCF ubiquitin E3 ligase complex. Mol Cell *10*, 1519-1526. 10.1016/s1097-2765(02)00784-0.